Blood transcriptomics reveal systemic eosinophilic and neutrophilic inflammation patterns in patients with nasal polyps

Wenqin Liu[1], Kanghua Wang[1], Haoyan Guan[2], Ling Ma[3], Yueming Cui[2], Chang Liu[1], Jianbo Shi[2], Yunping Fan[1], Yueqi Sun[1]

Rhinology 62: 6, 739 - 749, 2024
https://doi.org/10.4193/Rhin24.248

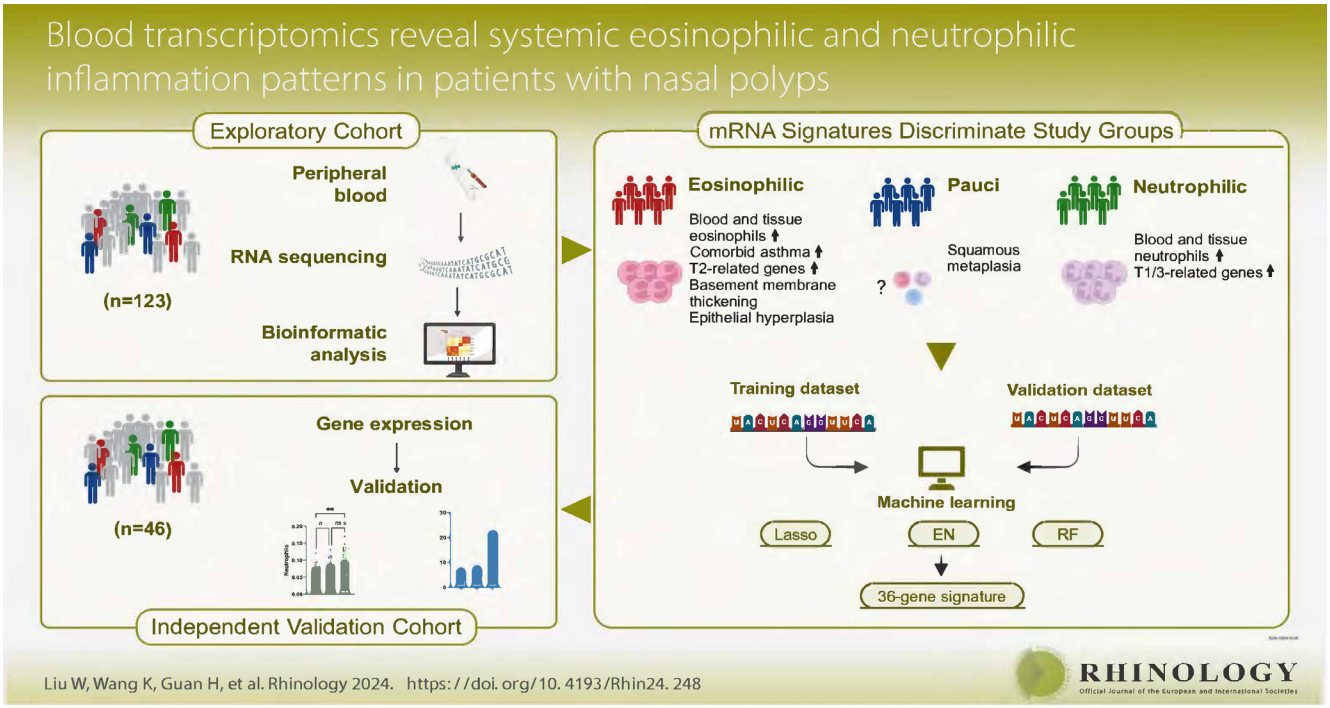

Abstract

Background: Chronic rhinosinusitis with nasal polyps (CRSwNP) is a chronic sinonasal disease characterized by heterogeneous inflammation. However, the presence of systemic inflammation heterogeneity in CRSwNP patients remains unknown. This study aims to profile transcriptomic alterations in the blood of CRSwNP patients and characterize the CRSwNP heterogeneity based on blood transcriptomic biomarkers.

Methodology: Patients with CRSwNP were prospectively recruited from three hospitals and chronologically divided into exploratory (n=123) and independent validation (n=46) cohorts. Transcriptomic profiles were generated by whole blood mRNA sequencing and subjected to patient clustering, differential expression, and pathway analysis. Differences in immune pattern and clinicopathologic features between clusters were assessed. A transcriptomic signature was defined and applied to an independent cohort to validate the findings.

Results: CRSwNP patients showed diverse blood transcriptomic profiles versus healthy controls, or when stratified by tissue and blood eosinophils and asthma comorbidity. Transcriptome-wide correlation analysis revealed a transcriptional signature associated with blood eosinophil levels, consisting of nine T2-related genes (CLC, SIGLEC8, ALOX15, IL5RA, PTGDR2, CCL23, CCR3, EPX and IL1RL1). Three distinct clusters with differing systemic eosinophilic and neutrophilic inflammation patterns and asthma comorbidity were identified based on transcriptomic profiling of T2 and T1/3-related blood biomarkers. A 36-gene signature was developed by machine learning and accurately predicted the three CRSwNP subtypes. Validation on an independent cohort confirmed the prediction robustness.

Conclusions: There is heterogeneous systemic inflammation associated with eosinophilic and neutrophilic patterns in patients with CRSwNP. Endotyping based on blood transcriptomic biomarkers might lead to more personalized treatment strategies for CRSwNP in the future.

Key words: rhinosinusitis, nasal polyp, transcriptome, endotype

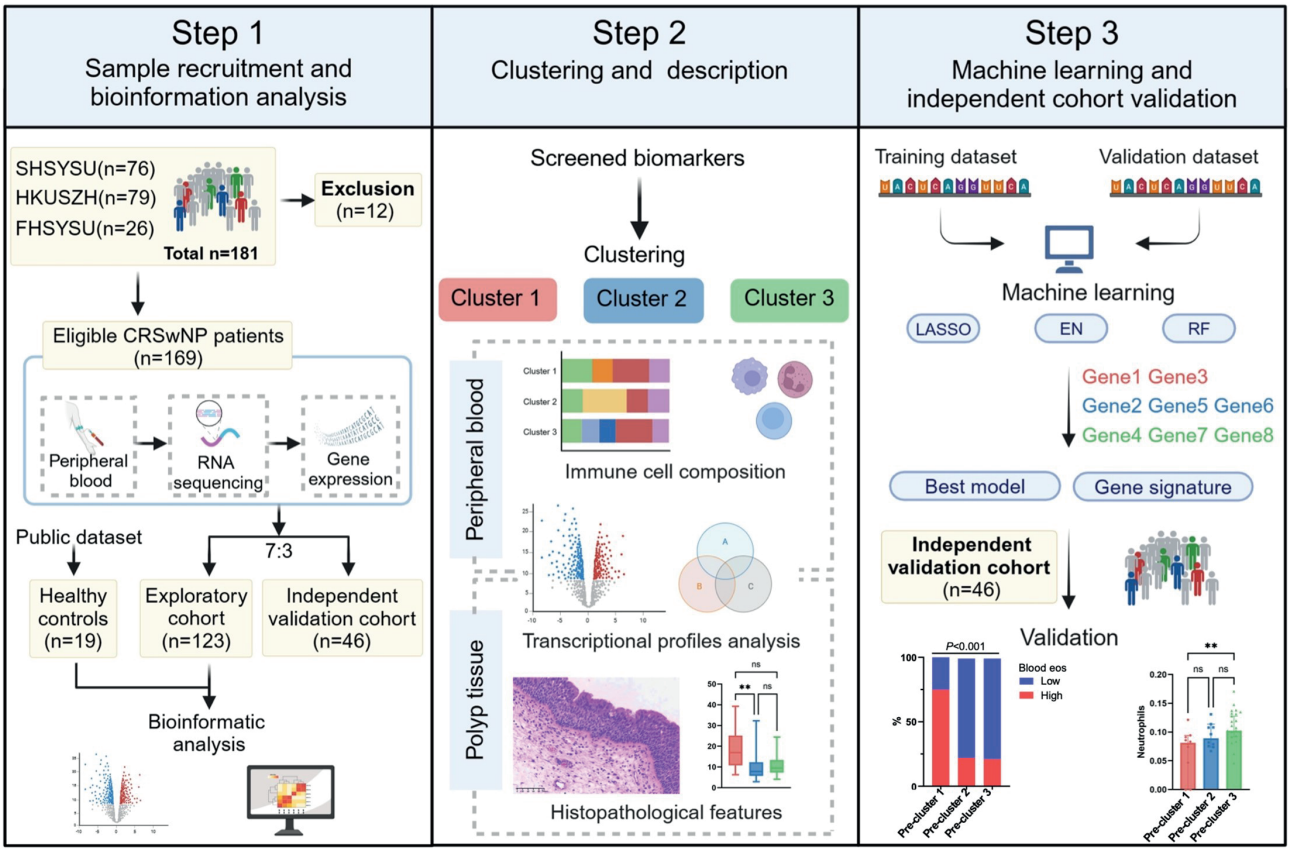

Figure 1. Study workflow.

Introduction

Chronic rhinosinusitis with nasal polyps (CRSwNP) is a chronic condition causing non-cancerous growths in the nasal and sinus mucosa, leading to symptoms like nasal obstruction and a reduced sense of smell, which significantly affect quality of life [1]. Current therapeutic approaches, including corticosteroids and endoscopic sinus surgery, offer relief but often fail to provide a long-term solution [1, 2], highlighting the need for deeper insights into the underlying pathophysiology of CRSwNP.

One of the critical aspects of understanding CRSwNP lies in acknowledging their inherent heterogeneity [3-5]. Historically, the study of CRSwNP has been dominated by a focus on local nasal inflammation [3, 4, 6]. However, this perspective has overlooked potential systemic factors contributing to the disease. In recent years, growing studies have categorized CRSwNP based on specific biomarkers in peripheral blood, revealing a complex landscape of inflammation in CRSwNP [7-10]. Despite these advances, current research often remains confined to local nasal tissue studies, neglecting the potential insights that could be gleaned from systemic analysis.

This study aimed to explore the systemic inflammation heterogeneity of CRSwNP by establishing a prospective, multicenter cohort and collecting peripheral blood samples for whole blood RNA sequencing. Inspired by successes in diseases like asthma [11, 12], chronic obstructive pulmonary disease [13], atopic dermatitis [14], and eosinophilic esophagitis [15], where blood transcriptomics identified distinct endotypes and informed targeted therapies, our research sought to classify CRSwNP by systemic transcriptomic profiles. This method might reveal new insights into the endotypic heterogeneity and support developing more personalized treatments for CRSwNP.

Materials and methods

Study design and participants

This was a multicenter prospective cohort study involving three tertiary hospitals, including the Seventh Affiliated Hospital of Sun Yat-Sen University (SHSYSU), the First Affiliated Hospital of Sun Yat-Sen University (FHSYSU), and the University of Hong Kong-Shenzhen Hospital (HKUSZH). The study was approved by the Ethics Committees of the three hospitals and conducted with written informed consent from every patient. Patients (≥16 years) with diffuse (bilateral) CRSwNP undergoing endoscopic sinus surgery were prospectively recruited. CRSwNP was diagnosed according to the international position papers [1, 2]. The study was part of the clinical trial registered at www.chictr.org.cn (ChiCTR2200059594). The study design and workflow are outlined in Figure 1. More information is provided in the Methods section of the Online Repository.

Sample acquisition

Peripheral blood and nasal polyp tissue samples were collected during sinus surgery. More information is provided in the Methods section of the Online Repository.

RNA sequencing and data analysis

The RNA libraries were constructed using the VAHTS Universal V6 RNA-seq Library Prep Kit with the manufacturer's instructions and sequenced using an Illumina NovaSeq 6000 platform. More information is provided in the Methods section of the Online Repository.

Statistical analysis

Data are expressed as median and interquartile range. P-values less than 0.05 were considered significant. More information is provided in the Methods section of the Online Repository.

Data availability

The accession number for the raw sequencing data from human samples in the study is GSA (Genome Sequence Archive) HRA006483 and HRA006324. More information is provided in the Methods section of the Online Repository.

Results

Characteristics of the study cohort

Between May 2021 and December 2022, a total of 181 (76 SHSYSU; 26 FHSYSU; 79 HKUSZH) CRSwNP participants with available peripheral blood samples that passed RNA quality control were enrolled and chronologically divided into a 70% exploratory cohort (n=128) and a 30% independent validation cohort (n = 53). RNA-seq data from samples with either a low read count or a pronounced batch effect due to improper sample processing were excluded, resulting in 169 CRSwNP patients (123 of the exploratory cohort and 46 of the validation cohort) as eligible samples for the per-protocol analysis. Demographic and clinical characteristics of the study subjects are shown in Table E1.

Characterization of blood transcriptomic profiles in patients with CRSwNP

We first assessed the overall differences in blood gene expression of CRSwNP patients from the exploratory cohort (n=123) versus sex- and age-matched healthy controls (n=19). Using an adjusted $P < 0.05$ with an absolute fold change > 2, a total of 5227 DEGs were identified, including 2575 upregulated and 2652 downregulated genes (Figure 2A, Table E2).

CRSwNP patients were then stratified into eCRSwNP (n=60) and neCRSwNP (n=63) subtypes based on tissue eosinophil counts (cutoff value: 10/HPF). As a result, a total of 5145 and 5273 DEGs were identified in eCRSwNP and neCRSwNP, respectively, compared to healthy controls (Figure 2B, Table E3-E4). We then compared the DEGs in each pairwise analysis and those that were shared between eCRSwNP and neCRSwNP. Strikingly, we identified a large number of DEGs in blood shared between eCRSwNP and neCRSwNP patients, including 2447 upregulated and 2490 downregulated genes, corresponding to 96% and 94% of the eCRSwNP and neCRSwNP DEGs, respectively (Figure 2C). In contrast, eCRSwNP only had 119 uniquely up-regulated and 89 uniquely down-regulated genes, whereas neCRSwNP had 130 uniquely up-regulated and 206 uniquely down-regulated genes (Figure 2C, full list in Table E5). We identified 929 (417 functions enriched in the common up-DEGs and 517 functions enriched in the common down-DEGs) significant functions enriched in the common DEGs for blood in patients with eCRSwNP/neCRSwNP, including functions associated with regulation of leukocyte differentiation, mononuclear cell differentiation and regulation of T cell activation (Top 5 functions were shown in Figure 2D, full list in Table E6). These evaluations identified gene profiles in blood that mark difference from healthy controls to CRSwNP patients and illustrated a surprisingly high degree of concordance between the blood gene expression between patients with eCRSwNP and neCRSwNP.

Blood transcriptomic differences in CRSwNP patients stratified by tissue and blood eosinophil levels and asthma comorbidity

We then examined the DEGs in blood transcriptomic profiles of CRSwNP patients stratified by a tissue eosinophil cutoff level of 10/HPF, namely eCRSwNP (n=60) versus neCRSwNP (n=63) (Table E1). A total of 168 genes were identified, including 145 upregulated and 23 downregulated genes (Figure E2A and Table E7). Notably, there were 11 T2-related genes, such as PTGDR2, CLC, IL5RA, SIGLEC8, ALOX15, and CCL23, were found to be significantly upregulated in patients with eCRSwNP versus neCRSwNP.

We further divided the patients into those with high (n=69) and low (n=54) blood eosinophils by a blood eosinophil cutoff value of 300/μl (Table E1). A total of 247 genes were identified including 193 upregulated and 54 downregulated genes (Figure E2B and Table E8). There were 16 T2-related genes including PTGDR2, SIGLEC8, ALOX15, IL5RA, STAC, CCL23, EPX and CLC, were identified among the upregulated genes in the patients with high versus low blood eosinophils. Further analysis using Panther Classification System (http://panth erdb.org/) identified Gene Ontology Biological Processes (GOBP) that might be associated to CRSwNP with high blood eosinophils, revealing that cellular processes, biological regulation, responses to stimuli, and metabolic processes were the predominant biological processes (Figure E2C). Several functional pathways were found to be enriched in CRSwNP patients with high blood eosinophils, such as embryonic organ development, and positive regulation of MAPK cascade (Figure E2C).

To investigate whether the blood transcriptional profile in

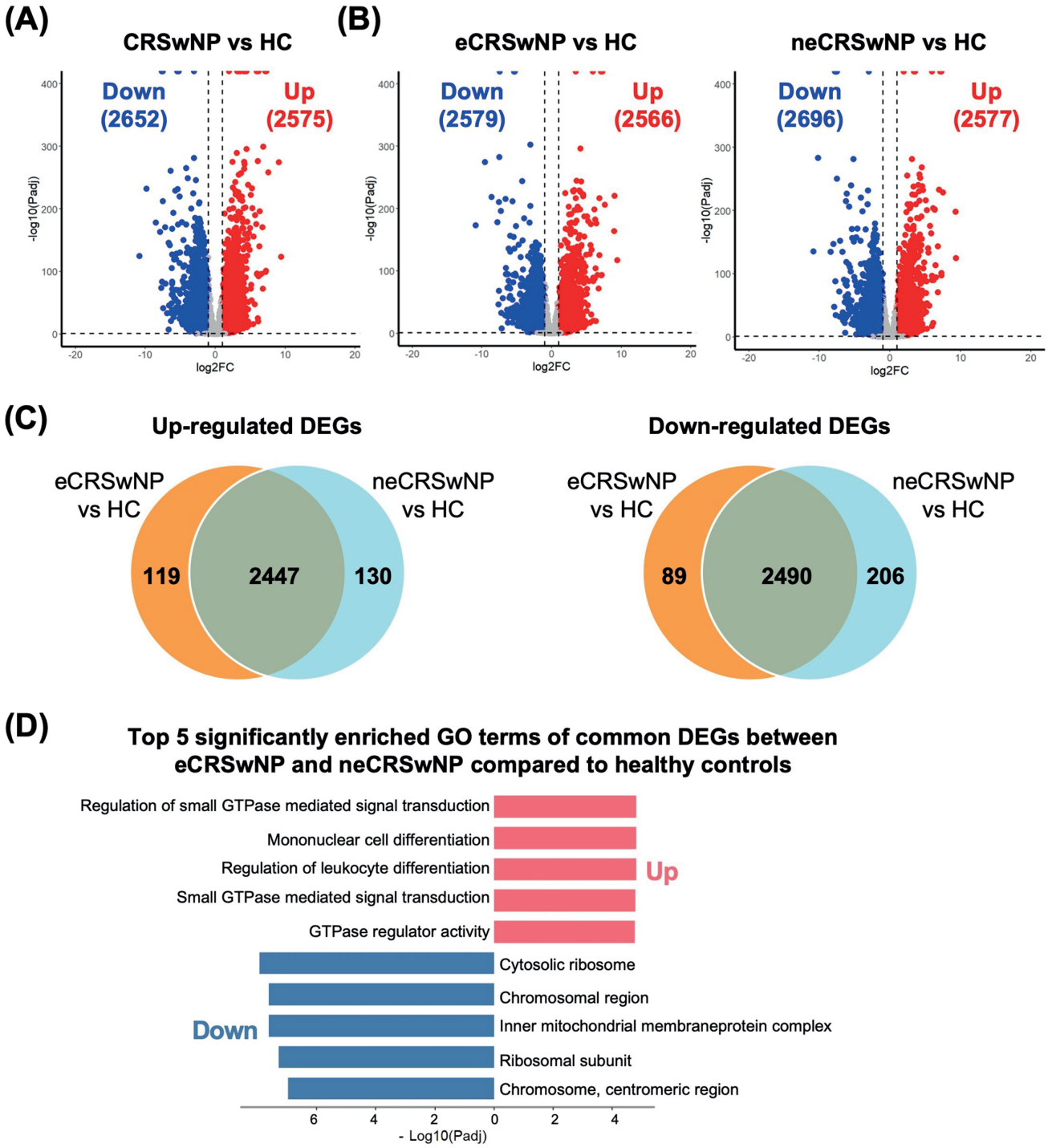

Figure 2. Differential expression analysis of blood transcriptome between patients with CRSwNP and healthy controls. Volcano plots showing DEGs (defined as adjusted p-value < 0.05 and fold change > 2) in blood of CRSwNP (n=123) (A), as well as eCRSwNP (n=60) and neCRSwNP (n=63) (B), versus age- and sex-matched healthy controls (n=19). (C) Venn diagram of up- and downregulated DEGs in eCRSwNP and neCRSwNP (including shared and distinct DEGs). (D) The top five significantly enriched GO terms for common DEGs between eCRSwNP and neCRSwNP compared to healthy controls.

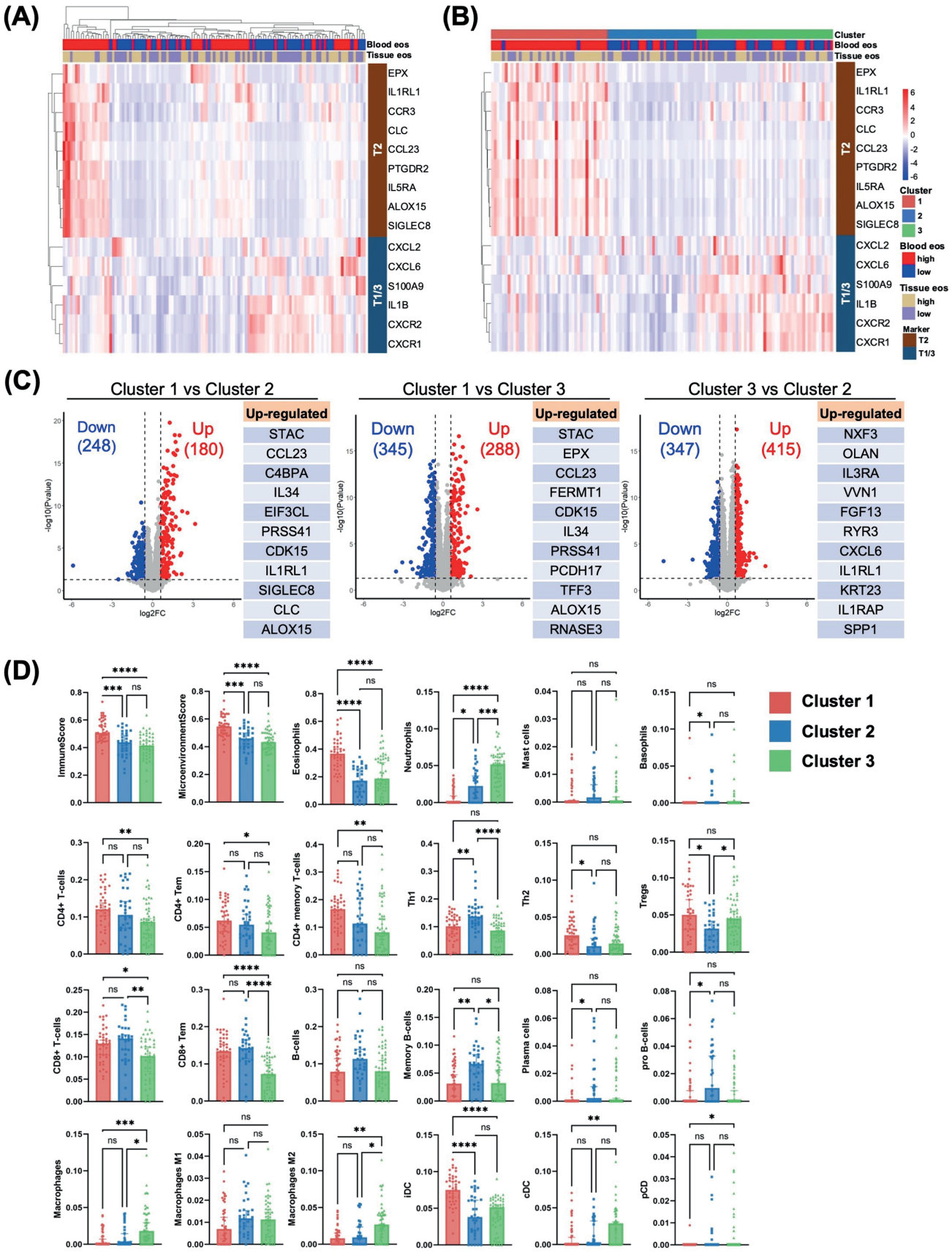

Figure 3. Clustering analysis of CRSwNP patients based on blood biomarkers. (A) Heatmap illustrating the unsupervised hierarchical clustering of the cohort based on the screened T2-related biomarkers and selected T1/3-related biomarkers, with rows representing genes and columns representing

CRSwNP patients was associated with asthma comorbidity, we subdivided the patients with CRSwNP into two subgroups on the basis of with (n=26) or without concomitant asthma (n=97). We found 202 DEGs including 135 upregulated and 67 downregulated genes (Figure E3A and Table E9). Notably, 9 T2-related genes including STAC, SIGLEC8, IL-4, CCL23, CLC, ALOX15, PTGDR2, IL-5RA, and IL1RL1, were identified among the upregulated genes in the patients with versus without asthma. GO analysis showed several functional pathways such as chemotaxis and collagen-containing extracellular matrix were enriched in CRSwNP patients with asthma (Figure E3B and Table E9).

Classification of CRSwNP patients based on blood biomarkers

We next investigated whether transcriptomic profiling of whole blood can partition CRSwNP patients to distinct blood transcriptomic subgroups. We first performed an unsupervised hierarchical clustering analysis based on the expression of the top 300 hypervariable genes. As a result, an optimal number of 3 clusters was obtained (Figure E4A). However, these 3 clusters were neither associated with the expressions of T1, T2 and T3 biomarkers, nor tissue or blood eosinophil patterns (Figure E4B).

CRSwNP have been well stratified broadly into two endotypes: T2 and non-T2 (or T1/3)[1, 16, 17]. Here, we hypothesized that these endotypes can also be reflected in the blood transcriptome of patients with CRSwNP. We then used the nine selected eosinophil-related genes (Figure E5) as T2 biomarkers, together with a gene-set of CXCL2, CXCL6, S100A9, IL1B, CXCR2 and CXCR1 as T1/3 biomarkers, to perform clustering analysis. Overall, the results showed that the cases with high expression of T2 biomarkers appeared clustered to the left, whereas high expression of T1/3 biomarkers were clustered to the right (Figure 3A). Based on the second-order branching of the dendrogram of the columns, three major CRSwNP clusters were identified. We therefore designated these clusters as cluster 1 (n=42, 34.2%), 2 (n=32, 26.0%) and 3 (n=49, 39.8%) (Figure 3B, Table E1). Principal component analysis confirmed that this clustering approach yield satisfactory separation of patient subgroups (Figure E6). Interestingly, there was heterogeneity in blood and tissue eosinophil patterns among the three clusters. However, cluster 1 obviously had higher percentages of high blood and tissue eosinophils, as well as comorbid asthma, than cluster 2 and 3 (Figure 3B, Table E1). There were no significant differences between the three clusters in age, gender, current smoker, comorbid allergic rhinitis, Lund-Kennedy endoscopic score, Lund-Mackay CT score, TNSS and SNOT-22 score between the three clusters (Table E1). We then compared the blood transcriptomic profiles between the three clusters. There were 428 (180 upregulated and 248 downregulated), 633 (288 upregulated and 345 downregulated), and 762 (415 upregulated and 347 downregulated) DEGs ($P < 0.05$ with an absolute fold change > 1.5) between cluster 1 and 2, cluster 1 and 3, and cluster 3 and 2, respectively (Figure 3C, full list of DEGs in Table E12-E14). We further explored blood immune cell composition within each cluster based on the xCell algorithm. The results showed that cluster 1 had higher ImmuneScore, MicroenvironmentScore, eosinophils, CD4 T cells and their memory subsets, Th2 cells, and iDC scores versus cluster 2 and 3 (Figure 3D). In contrast, cluster 3 had higher neutrophils, macrophages and their M2 subtypes, cDC and pDC scores than cluster 1 and 2 (Figure 3D).

Histopathological and transcriptomic features of CRSwNP subtypes classified by blood biomarkers

We next explored the histopathological features of the three CRSwNP clusters (n=19, 21 and 20 for cluster 1, 2 and 3, respectively). The results showed that CRSwNP of cluster 1 had significantly higher tissue eosinophils versus that of cluster 2 and 3, whereas cluster 3 exhibited more neutrophil infiltration compared to cluster 1 and 2 (Figure 4A). In addition, cluster 1 polyps displayed more pronounced features of epithelial remodeling, such as basement membrane thickening and epithelial hyperplasia compared with those of cluster 2 and 3 (Figure 4B). Interestingly, cluster 2 polyps exhibited higher degree of squamous metaplasia versus cluster 3. However, we did not observe obvious histopathological feature in cluster 3 polyps (Figure 4B). We further characterized the tissue transcriptomic profiles of the three CRSwNP clusters by performing bulk RNA-seq analysis (n=13, 10 and 12 for cluster 1, 2 and 3, respectively). The results showed that there were 2174 (1199 upregulated and 975 downregulated), 2544 (1426 upregulated and 1118 downregulated), and 735 (383 upregulated and 352 downregulated) DEGs ($P < 0.05$ with an absolute fold change > 1.5) between cluster 1 and 2, cluster 1 and 3, and cluster 3 and 2, respectively (Figure 4C, full list of DEGs in Table E15-E17). Notably, cluster 1 polyps

legend Figure 3 continued.

individual patient samples, grouped by cluster assignment and annotated for blood and tissue eosinophil levels. (B) This heatmap depicts the same patients and biomarkers as in Figure 3A, but now the cases with high expression of T2-biomarkers are sorted on the left as cluster 1, and the cases with high expression of T1/3-biomarkers sorted on the right as cluster 3. Cases with low expression of T2/1/3-biomarkers are sorted on the middle as cluster 2. (C) Volcano plots of differential gene expression analysis of blood transcriptome between the three clusters, indicating the number of significantly upregulated and downregulated genes, with key up-regulated genes listed on the right side. (D) Bar graphs showing the relative composition of immune cells within the clusters as inferred from blood transcriptional profiling using the xCell tool.

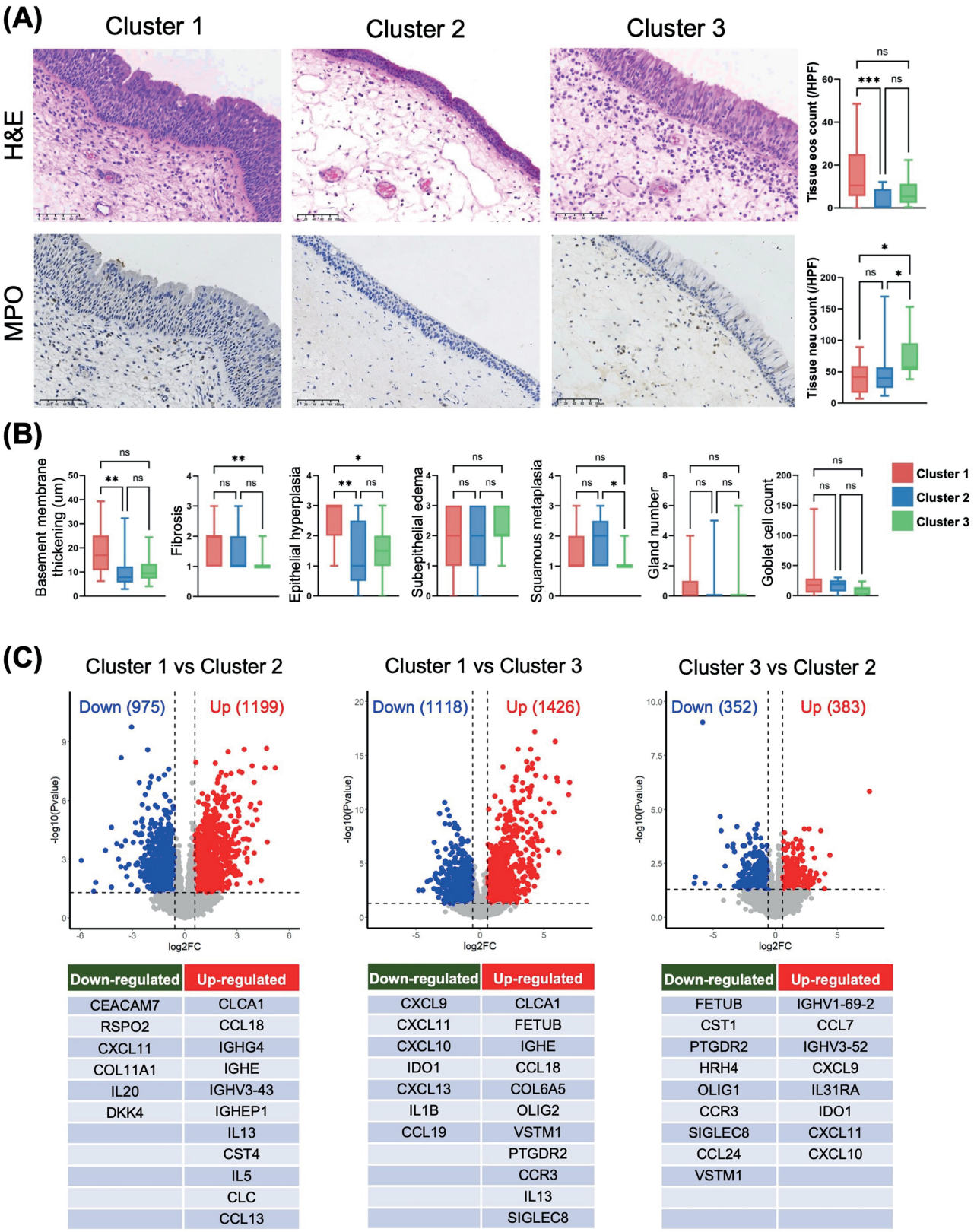

Down-regulated	Up-regulated
CEACAM7	CLCA1
RSPO2	CCL18
CXCL11	IGHG4
COL11A1	IGHE
IL20	IGHV3-43
DKK4	IGHEP1
	IL13
	CST4
	IL5
	CLC
	CCL13

Down-regulated	Up-regulated
CXCL9	CLCA1
CXCL11	FETUB
CXCL10	IGHE
IDO1	CCL18
CXCL13	COL6A5
IL1B	OLIG2
CCL19	VSTM1
	PTGDR2
	CCR3
	IL13
	SIGLEC8

Down-regulated	Up-regulated
FETUB	IGHV1-69-2
CST1	CCL7
PTGDR2	IGHV3-52
HRH4	CXCL9
OLIG1	IL31RA
CCR3	IDO1
SIGLEC8	CXCL11
CCL24	CXCL10
VSTM1	

Figure 4. Histopathological and transcriptomic analysis of the three CRSwNP clusters. (A) Representative H&E and immunohistochemical staining of MPO, as well as the quantification of eosinophil and neutrophil (MPO+) counts, in polyp tissues of the three clusters are shown. (B) Comparisons in basement membrane thickening, fibrosis, epithelial hyperplasia, subepithelial edema, squamous metaplasia, gland number and goblet cells, between the three clusters by histopathologic analysis. (C) Volcano plots of differential gene expression analysis of polyp tissue transcriptome between the three clusters, indicating the number of significantly upregulated and downregulated genes, with key genes listed on the bottom.

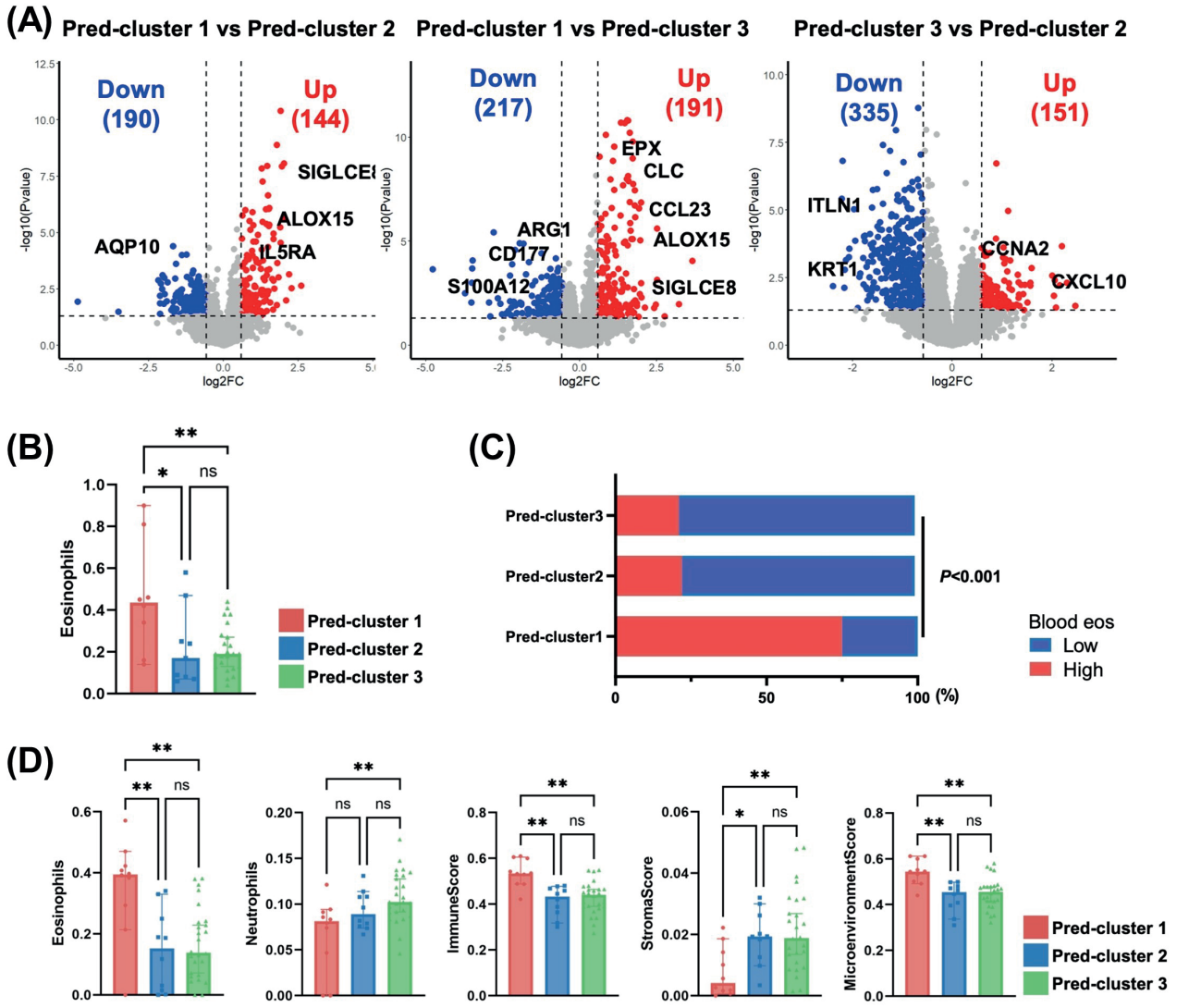

Figure 5. Biomarker identification for distinguishing the three blood-based CRSwNP clusters by machine learning and validation of an independent cohort. (A) Volcano plots of differential gene expression analysis of blood transcriptome between the three predicted clusters, with notable upregulated and downregulated genes. (B-C) Blood eosinophil counts (B) and percentages (C) of the patients with high blood eosinophils (≥300/μl) between the three predicted clusters. (D) Bar graphs showing the relative composition of eosinophils and neutrophils, as well as ImmuneScore, StromaScore, and MicroenvironmentScore, within the three predicted clusters as inferred from blood transcriptional profiling using the xCell tool.

expressed more T2-related genes, such as CLCA1, CCL18, IGHG4, IGHE, PTGDR2, CCR3, IL13, IL5, CLC, SIGLEC8, and CCL13 versus polyp tissues of cluster 2 and 3. By contrast, cluster 3 polyps had higher expression of T1/3-related genes including CXCL9, CXCL11, CXCL10, IDO1, and IL1B compared to the cluster 1 and 2 polyps (Figure 4C, Table E15-E17). Interestingly, cluster 2 polyps also expressed more T2-related genes, such as CST1, PTGDR2, HRH4, CCR3, SIGLEC8, and CCL24, than cluster 3 polyps (Figure 4C, Table E17).

Transcriptomic signatures for distinguishing the blood-based CRSwNP subtypes

We next sought to identify a set of biomarkers susceptible to discriminate between the three blood-based CRSwNP clusters by using machine learning approach (Figure E7A-B). As shown in Figure E7C, the LASSO_min-based model comprised 36 gene biomarkers, including 6 cluster-1-specific biomarkers (ALOX15, DERL1, FBP1, FEXO7, PDIA4 and PLEKHA2) with the highest score in CRSwNP cluster 1, 12 cluster-2-specific biomarkers (CIZ1, DEGS1, DPM2, HBA2, HLA-DRB1, KRT23, LPCAT2, SHARPIN, SPON2, SRXN1, TCF7 and UBE2D1) with the highest score in CRSwNP cluster 2, and 18 cluster-3-specific biomarkers (ESYT2, HBG2, HLA-DRB1, HLA-DRB5, KCNJ15, MAN2A2, OSCAR, PF4, PPBP, PTGDS, RNF187, S100A12, SHARPIN, SLC25A39, SLPI, SRA1, TMEM91, and YBX3) with the highest score in CRSwNP cluster 3 (full list of coefficients for each gene in Table E18). For predicting

each blood-based CRSwNP cluster, the LASSO_min-based model reached an AUC of 0.95 for cluster 1, 0.86 for cluster 2, and 0.88 for cluster 3 (Figure E7B).

Independent validation

We finally validated the LASSO_min-based model on an independent validation cohort (n=46). Three clusters were predicted by the LASSO_min-based model (here referred to as pred-cluster) using the 36-gene signature. Comparison of blood transcriptional profiles between the three pred-clusters resulted in a total of 334 (144 upregulated and 190 downregulated), 408 (191 upregulated and 217 downregulated), and 486 (151 upregulated and 335 downregulated) DEGs between pred-cluster 1 versus pred-cluster 2, pred-cluster 1 versus pred-cluster 3, and pred-cluster 3 versus pred-cluster 2, respectively (Figure 5A, full list of DEGs in Table E19-E21). As expected, pred-cluster 1 expressed higher levels of many T2-related genes, such as SIGLEC8, ALOX15, IL5RA, EPX, CLC in blood, compared to pred-cluster 2 and 3 (Figure 5A, Table E19-E21). In addition, pred-cluster 3 had more T1/3-related transcripts including S100A12, CD177, CCNA2, and CXCL10, than pred-cluster 1 and 2 (Figure 5A, Table E20-E21). Moreover, pred-cluster 1 had a significantly higher mean blood eosinophil counts as well as percentages of the patients with high blood eosinophils compared to pred-cluster 2 and 3 (Figure 5B-C). xCell algorithm analysis further showed that pred-cluster 1 had the highest score of eosinophils, as well as ImmuneScore and MicroenvironmentScore, whereas pred-cluster 3 exhibited higher neutrophil scores than pred-cluster 1 (Figure 5D). Interestingly, StromaScore was the lowest in pred-cluster 1.

Discussion

To the best of our knowledge, this is the first study to characterize the systemic inflammation heterogeneity through whole blood transcriptome profiling in a large prospective cohort of patients with CRSwNP. We found that CRSwNP patients had diverse blood transcriptomic profiles versus healthy controls. When stratified by eosinophil levels or asthma comorbidity, a couple of T2-related genes were identified among the upregulated genes in the patients with high tissue or blood eosinophils or concomitant asthma. In addition, transcriptome-wide correlation analysis revealed a transcriptional signature associated with blood eosinophil levels, consisting of nine T2-related genes (CLC, SIGLEC8, ALOX15, IL5RA, PTGDR2, CCL23, CCR3, EPX and IL1RL1). Furthermore, we identified three distinct clusters with differing systemic eosinophilic and neutrophilic inflammation patterns and asthma comorbidity based on transcriptomic profiling of T2 and T1/3-related blood biomarkers. Moreover, a 36-gene signature was developed by a LASSO-based machine learning algorithm and shown to accurately predicted the three CRSwNP subtypes. Validation on an independent cohort confirmed the prediction robustness, showing distinct blood immune profiles among the predicted subtypes.

In addition to eosinophils and IgE [7], several inflammation mediators in blood, such as periostin [7, 18], ECP [19], soluble CD40L [20] and CSF1R [21], have been identified as biomarkers associated with clinical severity, inflammatory endotype, and treatment response, suggesting the systemic nature of inflammation in at least a subset of, if not all, CRSwNP patients. In the present study, our findings contribute to this narrative by identifying a wide array of blood DEGs that not only differ from healthy individuals but also exhibit variability among CRSwNP patients themselves. This variability underscores the systemic inflammation present and the heterogeneity within CRSwNP pathogenesis, aligning with the evolving recognition of airway diseases such as asthma [22] and chronic obstructive pulmonary disease [23, 24] as a systemically influenced disorder. In addition, conventional subgroup comparisons demonstrated that the majority of blood DEGs between eCRSwNP and neCRSwNP were shared when compared to healthy controls. These overlapping DEGs are enriched in leukocyte and mononuclear cell differentiation and T cell activation pathways, highlighting the fundamental role of both innate and adaptive immune responses play underlying the development of CRSwNP. Moreover, many of the uniquely up-regulated DEGs in eCRSwNP were eosinophil related such as CCL23, IL5RA and CLC, whereas several genes of the uniquely up-regulated DEGs in neCRSwNP were Th17 response related including PRKCD, FPR2, AOAH and PADI4, both findings in keeping with current concepts.

The use of blood transcriptomic profiling, as demonstrated in studies on atopic dermatitis (AD) [14], asthma [11, 12], and other inflammatory conditions [25, 26], has highlighted the heterogeneous systemic inflammation present in these diseases. For instance, in AD, transcriptomic profiling has uncovered two candidate endotypes characterized by distinct inflammatory expression signatures, one with a pronounced eosinophil and IL-5-related pattern and the other with a significantly lower degree of transcriptomic dysregulation [14]. In the present study, our analysis identified three CRSwNP clusters characterized by unique inflammatory profiles in blood transcriptome. Cluster 1, high expression of T2-related genes and an increased presence of eosinophils both in blood and tissue, was associated with a higher prevalence of comorbid asthma. This suggests a systemic T2 inflammation endotype in these patients. This finding is consistent with existing literature that associates T2-high inflammation with both eosinophilic disorders and asthma, suggesting a shared pathophysiological mechanism across these conditions [27-29]. Conversely, cluster 3, which demonstrated an upregulation of T1/3-related genes and an increase in neutrophil counts, presented a nuanced picture. Although this cluster had a lower association with asthma than cluster 1, it nonetheless appeared a higher rate of asthma comorbidity compared to cluster 2. This

observation indicates a potential systemic T1/3 inflammation phenotype in patients with CRSwNP and hints at the complex interplay between T1/3 inflammatory responses and asthma, possibly suggesting a distinct asthma phenotype associated with non-eosinophilic inflammation [30, 31], which merits further investigation. Cluster 2, lacking significant expression of T1/2/3 genes in blood, might represent a localized chronic inflammation limited to the nasal mucosa. By dissecting the blood transcriptomic profiles of CRSwNP patients, our findings contribute to the understanding of the mechanisms underlying this heterogeneous disease and support the development of individualized therapeutic approaches. For example, patients in cluster 1 might benefit more from targeted T2 antagonists, given their systemic T2 inflammation and higher asthma comorbidity. In contrast, patients in cluster 3, with their unique systemic T1/3 inflammation, might require different therapeutic approaches, possibly targeting neutrophilic inflammation or T1/3-specific pathways. For patients in cluster 2, the lack of systemic inflammation markers suggests that the inflammation is primarily confined to the nasal mucosa. Therefore, endoscopic sinus surgery could be considered an appropriate therapeutic measure.

Practical constraints including limited resources, time, and ethical considerations, contributed to the existing cohort sizes. Although these limitations are typical of clinical research, they highlight the necessity for future studies with larger sample sizes to substantiate and expand upon our findings.

Conclusion

This study provides the first strong evidence of heterogeneous systemic inflammation associated with eosinophilic and neutrophilic patterns in patients with CRSwNP. Larger studies are needed to determine the utility of blood biomarkers derived from this study. Follow-up biological studies might add new insights into disease mechanisms and more personalized treatment strategies for CRSwNP in the future.

Authorship contribution

WL, KW, HG, LM, YC, and CL participated in tissue sample collection. WL, KW, HG, and YC performed RNA-Seq experiments. WL and YS analyzed data. KW, HG, LM, YC, CL and YF participated in data discussions. WL, JS and YS designed the study and prepared the manuscript.

Conflict of interest

All authors declare no financial or commercial conflicts of interest.

Funding

This work was supported by grants from the National Natural Science Foundation of China (82371114 and 82171105), the Research start-up fund of part-time PI, SAHSYSU (ZSQYJZPI202009), Shenzhen Fundamental Research Program (JCYJ20220530144805011), Guangdong Basic and Applied Basic Research Foundation (2023A1515012497 and 2024A1515013003), Science and Technology Project of Panyu District, Guangzhou (2021-Z04-004).

References

1. Fokkens WJ, Lund VJ, Hopkins C, et al. European Position Paper on Rhinosinusitis and Nasal Polyps 2020. Rhinology. 2020;58(Suppl S29):1-464.
2. Orlandi RR, Kingdom TT, Smith TL, et al. International consensus statement on allergy and rhinology: rhinosinusitis 2021. Int Forum Allergy Rhinol. 2021;11(3):213-739.
3. Kato A, Peters AT, Stevens WW, Schleimer RP, Tan BK, Kern RC. Endotypes of chronic rhinosinusitis: relationships to disease phenotypes, pathogenesis, clinical findings, and treatment approaches. Allergy. 2022;77(3):812-826.
4. Chapurin N, Wu J, Labby AB, Chandra RK, Chowdhury NI, Turner JH. Current insight into treatment of chronic rhinosinusitis: phenotypes, endotypes, and implications for targeted therapeutics. J Allergy Clin Immunol. 2022;150(1):22-32.
5. Schleimer RP. Immunopathogenesis of chronic rhinosinusitis and nasal polyposis. Annu Rev Pathol. 2017;12:331-357.
6. Ko YG, Kim MH, Park JY, et al. Chronic rhinosinusitis endotypes associate with distinct local cytokine milieus that shape the distribution of innate lymphoid cells. Allergy. 2022;77(7):2246-2250.
7. Jonstam K, Westman M, Holtappels G, Holweg CTJ, Bachert C. Serum periostin, IgE, and SE-IgE can be used as biomarkers to identify moderate to severe chronic rhinosinusitis with nasal polyps. J Allergy Clin Immunol. 2017;140(6):1705-1708 e3.
8. Drake VE, Rafaels N, Kim J. Peripheral blood eosinophilia correlates with hyperplastic nasal polyp growth. Int Forum Allergy Rhinol. 2016;6(9):926-934.
9. Zhong B, Yuan T, Du J, et al. The role of preoperative blood eosinophil counts in distinguishing chronic rhinosinusitis with nasal polyps phenotypes. Int Forum Allergy Rhinol. 2021;11(1):16-23.
10. Zielinska-Blizniewska H, Paprocka-Zjawiona M, Merecz-Sadowska A, Zajdel R, Blizniewska-Kowalska K, Malinowska K. Serum IL-5, POSTN and IL-33 levels in chronic rhinosinusitis with nasal polyposis correlate with clinical severity. BMC Immunol. 2022;23(1):33.
11. Bigler J, Boedigheimer M, Schofield JPR, et al. A severe asthma disease signature from gene expression profiling of peripheral blood from U-BIOPRED cohorts. Am J Respir Crit Care Med. 2017;195(10):1311-1320.
12. Zeng X, Qing J, Li CM, et al. Blood transcriptomic signature in type-2 biomarker-low severe asthma and asthma control. J Allergy Clin Immunol. 2023;152(4):876-886.
13. Moll M, Boueiz A, Ghosh AJ, et al. Development of a blood-based transcriptional risk score for chronic obstructive pulmonary disease. Am J Respir Crit Care Med. 2022;205(2):161-170.
14. Mobus L, Rodriguez E, Harder I, et al. Blood transcriptome profiling identifies 2 candidate endotypes of atopic dermatitis. J Allergy Clin Immunol. 2022;150(2):385-395.
15. Erwin EA, Jaramillo LM, Smith B, et al. Sex differences in blood transcriptional profiles and clinical phenotypes in pediatric patients with eosinophilic esophagitis. J Allergy Clin Immunol Pract. 2021;9(9):3350-3358 e8.
16. Bachert C, Marple B, Schlosser RJ, et al. Adult chronic rhinosinusitis. Nat Rev Dis Primers. 2020;6(1):86.
17. Bachert C, Zhang N, Hellings PW, Bousquet J. Endotype-driven care pathways in patients with chronic rhinosinusitis. J

Allergy Clin Immunol. 2018;141(5):1543-1551.
18. Asano T, Kanemitsu Y, Takemura M, et al. Serum periostin as a biomarker for comorbid chronic rhinosinusitis in patients with asthma. Ann Am Thorac Soc. 2017;14(5):667-675.
19. Tsai PC, Lee TJ, Chang PH, Fu CH. Role of serum eosinophil cationic protein in distinct endotypes of chronic rhinosinusitis. Rhinology. 2024;62(1):111-118.
20. Liu Z, Fan Y, Zhou A, Liu J, Jiao Q. Assessment of serum soluble CD40 ligand levels in patients with chronic rhinosinusitis. World Allergy Organ J. 2024;17(3):100880.
21. Niu Y, Cao S, Luo M, Ning J, Wen N, Wu H. Serum proteomics identify CSF1R as a novel biomarker for postoperative recurrence in chronic rhinosinusitis with nasal polyps. World Allergy Organ J. 2024;17(3):100878.
22. Tattersall MC, Jarjour NN, Busse PJ. Systemic inflammation in asthma: what are the risks and impacts outside the airway? J Allergy Clin Immunol Pract. 2024. 12(4):849-862.
23. King PT. Inflammation in chronic obstructive pulmonary disease and its role in cardiovascular disease and lung cancer. Clin Transl Med. 2015;4(1):68.
24. Obling N, Backer V, Hurst JR, Bodtger U. Nasal and systemic inflammation in Chronic Obstructive Pulmonary Disease (COPD). Respir Med. 2022;195:106774.
25. Yang JO, Zinter MS, Pellegrini M, et al. Whole blood transcriptomics identifies subclasses of pediatric septic shock. Crit Care. 2023;27(1):486.
26. Beretta L, Barturen G, Vigone B, et al. Genome-wide whole blood transcriptome profiling in a large European cohort of systemic sclerosis patients. Ann Rheum Dis. 2020;79(9):1218-1226.
27. Maison N, Omony J, Illi S, et al. T2-high asthma phenotypes across lifespan. Eur Respir J. 2022;60(3):2102288.
28. Coverstone AM, Seibold MA, Peters MC. Diagnosis and management of T2-high asthma. J Allergy Clin Immunol Pract. 2020;8(2):442-450.
29. Yancey SW, Keene ON, Albers FC, et al. Biomarkers for severe eosinophilic asthma. J Allergy Clin Immunol. 2017;140(6):1509-1518.
30. Wu D, Li L, Zhang M, Wang J, Wei Y. Two inflammatory phenotypes of nasal polyps and comorbid asthma. Ann Allergy Asthma Immunol. 2017;118(3):318-325.
31. Wu D, Bleier BS, Li L, et al. Clinical Phenotypes of nasal polyps and comorbid asthma based on cluster analysis of disease history. J Allergy Clin Immunol Pract. 2018;6(4):1297-1305 e1.

Yueqi Sun, MD, PhD
Department of Otolaryngology
the Seventh Affiliated Hospital of Sun Yat-sen University
No.628, Zhenyuan Road
Guangming District
Shenzhen
Guangdong 518107
China

E-mail: aqi1733@163.com or sunyq7@mail.sysu.edu.cn

Yunping Fan, MD, PhD
Department of Otolaryngology
the Seventh Affiliated Hospital of Sun Yat-sen University
No.628, Zhenyuan Road
Guangming District
Shenzhen
Guangdong 518107
China

E-mail: zhfanyp@163.com

Jianbo Shi, MD, PhD
Department of Otolaryngology
the First Affiliated Hospital of Sun Yat-sen University
58 Zhongshan Road II
Guangzhou
Guangdong, 510080
China

E-mail: tsjbent@163.com or shijb@mail.sysu.edu.cn

Wenqin Liu[1], Kanghua Wang[1], Haoyan Guan[2], Ling Ma[3], Yueming Cui[2], Chang Liu[1], Jianbo Shi[2,*], Yunping Fan[1,*], Yueqi Sun[1,*]

[1] Department of Otolaryngology, the Seventh Affiliated Hospital of Sun Yat-sen University, Shenzhen, China
[2] Department of Otolaryngology, the First Affiliated Hospital of Sun Yat-sen University, Guangzhou, China
[3] Department of Otorhinolaryngology, the University of Hong Kong-Shenzhen Hospital, Shenzhen, China

* These authors contributed equally to design and supervise this study

Rhinology 62: 6, 739 - 749, 2024
https://doi.org/10.4193/Rhin24.248

Received for publication:
June 9, 2024
Accepted: September 7, 2024

Associate Editor:
Michael Soyka

This manuscript contains online supplementary material

SUPPLEMENTARY MATERIAL

Study design and participants

This was a multicenter prospective cohort study involving three tertiary hospitals, including the Seventh Affiliated Hospital of Sun Yat-Sen University (SHSYSU), the First Affiliated Hospital of Sun Yat-Sen University (FHSYSU), and the University of Hong Kong-Shenzhen Hospital (HKUSZH). The study was approved by the Ethics Committees of the three hospitals, according to the Helsinki Declaration. Written informed consent was obtained from all participants (n=181). After removing participants that failed RNA sample quality control, the remaining participants were chronologically split into an exploratory cohort (n=123) and an independent validation cohort (n=46). The study was part of the clinical trial registered at www.chictr.org.cn (ChiCTR2200059594). The study design and workflow are outlined in Figure 1.

Patients (≥16 years) with diffuse (bilateral) CRSwNP (scored 1-4 points bilaterally based on the nasal polyp size score assessed by nasal endoscopy [1]) undergoing endoscopic sinus surgery were prospectively recruited for this study. CRSwNP was diagnosed according to the international position papers [2, 3]. Patients with the following items were excluded: 1) Patients who had an upper/lower respiratory tract infection, or received systemic or intranasal glucocorticoid or antibiotics treatment within 4 weeks before the surgery; 2) patients with unilateral CRSwNP, fungal rhinosinusitis, cystic fibrosis, antrochoanal polyps, recurrent lower airway infections, or sinonasal tumors. Atopy, allergic rhinitis, and asthma were not mandatory exclusion criteria. None of the participants had aspirin-exacerbated respiratory diseases or atopic dermatitis.

Demographics and comorbidities were collected before surgery. Atopic status was evaluated by using assays for specific IgE (HOB Biotech Group, Suzhou, China) against local common inhalant allergens. Specific IgE concentrations above 0.35 IU/mL were considered positive. The blood eosinophil numbers in total white blood cells were detected by blood routine test. The diagnosis of allergic rhinitis (AR) was made based on the concordance between an atopic status and typical allergic symptoms according to the Allergic Rhinitis and its Impact on Asthma guideline [4]. The diagnosis of asthma was performed by a specialist physician and was established according to the Global Initiative for Asthma 2006 guideline [5]. Current smoker was defined as smoking at least one cigarette per day (tobacco 1 g/day) and lasting for at least 6 months [6]. Symptoms were scored by total nasal symptom score (TNSS) method as previously described [7]. Endoscopic findings were scored according to the Lund-Kennedy method [8]. Computed tomography (CT) scans were graded based on the Lund-Mackay scoring system [9]. Subjective assessment was performed using the Sino-Nasal Outcome Test-22 (SNOT-22).

Sample acquisition and processing

Peripheral blood and nasal polyp tissue samples were collected during endoscopic sinus surgery. Peripheral blood samples were collected in PAXgene RNA tubes (BD Biosciences, San Jose, CA), kept overnight at room temperature up to 4 h, and then stored at - 80 °C for batched analysis. Total RNA was isolated using the PAXgene Blood RNA kit (PreAnalytiX, Hombrechtikon, Switzerland) including on-column DNase treatment (QIAGEN, Valencia, CA) and stored for further processing. A 2100 Bioanalyzer (Agilent Technologies, Santa Clara, CA) was used to assess RNA integrity, by which samples with an RNA concentration > 25 μg/μl and RNA integrity number [10] (RIN) > 6 were further processed for gene expression analysis.

For tissue transcriptome analysis, fresh polyp tissues were stored at - 80 °C upon collection. Then total RNA was extracted as we previously reported [11]. Quality control on concentration and integrity of the isolated RNA was performed as mentioned above.

Histopathologic evaluation and tissue eosinophil and neutrophil quantifications

Histopathologic evaluation and quantifications of tissue eosinophils were performed as we previously described [7, 12]. Briefly, polyp tissues were fixed in 10% formalin, and embedded in paraffin. Samples were cut into 4-μm thick sections and routinely stained with hematoxylin-eosin (H&E). The sections were observed under a microscope (Leica DM4 B; Leica, Wetzlar, Germany) by two independent observers who were blind to the clinical data. The top 5 densest, nonoverlapping cellular infiltrate fields of the subepithelial layer were chosen under low-power field (×100) in each section. Then eosinophils were counted in the focus of each area under HPF (×400, 0.072 mm2/frame, HPF). Eosinophil count was recorded in each focus field at 400-power and reported as absolute number per HPF. Then the following histopathological parameters of the tissues were observed in the selected regions at 200-power: epithelial hyperplasia, squamous metaplasia, subepithelial edema, fibrosis, gland number. The following histopathological parameters of the tissues were observed in the selected regions at 400-power: basement membrane thickening, goblet cell hyperplasia.

For tissue neutrophil quantifications, immunohistochemical staining for myeloperoxidase (MPO) was performed as we previously described [7]. Briefly, sections were deparaffinized in xylene and rehydrated in ethanol. Antigen retrieval was achieved through treating the sections with citrate buffer in a pressure cooker. After blocking the endogenous peroxidase in 3% hydrogen peroxide and with 1% bovine serum albumin, the sections were incubated with anti-human MPO monoclonal antibodies (MAB3174, R&D Systems, Minneapolis, MN, USA) at 4°C overnight at a dilution of 1:600 according to the manufacturer's

instructions. A Dako Detection Kit (Dako) was used to detect and visualize the bound primary antibodies. All sections were counterstained with Harris' hematoxylin. Then the MPO-positive cells were quantified as eosinophil quantification described above. The top five densest visual fields of the subepithelial layer were chosen at 100-power in each section. Then neutrophils were counted in the focus of each area under 400-power magnification (×400, 0.072 mm2/frame, HPF). The average number of neutrophils per HPF was calculated.

RNA sequencing and data processing

The libraries were constructed using the VAHTS Universal V6 RNA-seq Library Prep Kit with the manufacturer's instructions. The libraries were sequenced using an Illumina NovaSeq 6000 platform, generating 150 bp paired-end reads. Each sample generated approximately 50M raw reads. The raw reads, in fastq format, were processed using fastp to remove low-quality reads and obtain clean reads. Subsequently, about 48M clean reads for each sample were retained for further analysis. HISAT2 was then used to map the clean reads to the reference genome. The software and versions used are listed in Table E22. The transcriptome sequencing and analysis were conducted by OE Biotech Co., Ltd. (Shanghai, China).

Blood transcriptomic dataset of healthy control from public database

To investigate the gene expression characteristics in peripheral blood of patients with CRSwNP, we analyzed two public gene expression datasets, both concentrating on peripheral blood, to collect sequencing data from healthy controls. The two datasets, namely GSE207751 and GSE205465, were retrieved from the Gene Expression Omnibus database (GEO accessible at: https://www.ncbi.nlm.nih.gov/geo/) using R package GEOquery (version 2.68.0). We merged the data from healthy controls across the two datasets to conduct a differential analysis between patients with CRSwNP from our exploratory cohort and the matched healthy controls. To mitigate potential gender and age biases, we performed the analysis using healthy controls that were matched for age and gender.

Differential analysis

Given the multi-center nature of our study and the large number of samples, we aimed to investigate potential batch effects in our sequencing results. To accomplish this, we generated principal component analysis (PCA) plots to visualize data variation before and after batch effect correction. We observed that the distribution of different groups remained relatively uniform, both before and after correction (Figure E1). Consequently, for simplicity, we opted to use the data prior to correction for subsequent analyses.

Differential gene expression analysis was conducted using the R package DESeq2 (version 1.40.2) in the R (version 4.3.1) statistical computing environment to compare gene expression profiles across different groups. To filter out low-expression genes, we excluded those with total counts across all samples less than 1.5 times the number of samples. This step was crucial for ensuring the robustness and reliability of our analysis. Genes with a fold change (FC) > 1.5 and p-value < 0.05 or Genes with a fold change (FC) > 2 and adjusted p-value < 0.05 were considered differentially expressed genes (DEGs).

Then we created heat map and Volcano plot to visualize expression patterns of DEGs, and we created Venn diagram to visualize similar expression characteristics of DEGs in comparison between different groups using R package pheatmap (version 1.0.12), ggplot2 (version 3.4.4), VennDiagram (version 1.7.3). To explore the functional characteristics of DEGs, Kyoto Encyclopedia of Genes and Genomes (KEGG) pathway and Gene Ontology (GO)[2] annotation enrichment analyses were performed using the R package clusterProfiler (version 4.8.3)[13] or using the website(https://pantherdb.org/). Bubble plots representing either the top ten significant or top ten in the quantity of significant genes in GO and KEGG pathways were generated using the R package ggplot2.

Screening of eosinophil-related biomarkers from blood transcriptome

For subgroup identification, we initially selected a set of the top 300 genes with the highest expression variances. We then computed the Euclidean distance matrix for these hypervariable genes and performed hierarchical clustering using the complete linkage method, as shown in Figure E4A. This process classified the exploratory cohort patients into three distinct clusters. To determine if the classification based on hypervariable genes correlated with specific inflammatory endotypes, we further compared the expression of T2/1/3-related genes between the three clusters (Figure E4B). The results revealed no discernible differences in T2/1/3-related gene expression or in tissue and blood eosinophil patterns among the three clusters (Figure E4B), indicating that the clustering does not accurately reflect the inflammatory endotypes of the disease. We hypothesized that excessive noise and non-specific inflammation signals in peripheral blood may have compromised the clustering effectiveness. To improve the clustering, we chose to adopt a more focused approach by screening for biomarkers that distinctly represent various inflammatory endotypes.

We then sought to identify biomarkers indicative of T2 inflammation by examining peripheral blood eosinophil levels, motivated by prior research that positions eosinophils as markers for T2-driven inflammation [14]. This approach is further supported by our findings (Figure E2B-C), which show significant upregulation of eosinophil-associated genes in individuals with high eosinophil counts (≥ 300/μL). To select the biomarkers, we next

performed a transcriptome-wide correlation analysis of gene expression with blood eosinophil counts in CRSwNP patients. We conducted a correlation analysis between transcripts per million reads (TPM) and peripheral blood eosinophil counts after converting gene counts to TPM values using the corrplot R package (version 0.92). After correction for multiple testing, we found that among the top 200 genes with the highest correlation, there were nine eosinophil-related genes, including CLC, SIGLEC8, ALOX15, IL5RA, PTGDR2, CCL23, CCR3, EPX and IL1RL1 (Figure E5A, full list in Table E10).

We then used random forest algorithm to screen the most important eosinophil-related biomarkers from top 300 correlated genes. To normalize the data and reduce the effect of differing scales, we quantified the expression levels of these genes using the log2(TPM+1) transformation. The genes were ranked by their importance in the model, determined by the IncNodePurity value (Figure E5B). As a result, CLC, CCL23, SIGLEC8, ALOX15 and IL5RA were among the top 30 significant genes with the highest relative importance (Figure E5B, full list in Table E11).

We then identified genes among the top 200 correlated and the top 250 important genes that were previously reported in the literature [15-22] to be linked with T2 inflammation.

We also analyzed correlation of TPM values of the nine overlapping eosinophil-related biomarkers with blood eosinophil counts using GraphPad Prism 9.5 software. The results showed that all nine blood biomarkers were significantly correlated with blood eosinophil levels (Figure E5C), and had higher transcript levels in the patients with high eosinophils than those with low eosinophils (Figure E5D). This method led to the identification of nine genes as potential biomarkers for T2 inflammation.

Hierarchical clustering: subgroup identification.

To prevent excessive noise and non-specific inflammatory expression in peripheral blood from compromising the effectiveness of our clustering, we adopted a more focused approach for hierarchical clustering. We selected the nine screened T2-related genes, together with a set of T1/T3-related genes (CXCL2, CXCL6, S100A9, IL1B, CXCR2 and CXCR1), as identified in previous studies [23-26], to serve as biomarkers instead of using entire transcriptional profiles. This targeted methodology effectively differentiated inflammatory endotypes in peripheral blood of CRSwNP patients. Using hierarchical clustering analysis, we were able to categorize CRSwNP patients into distinct subgroups based on these biomarkers. To visualize the data, we produced PCA plots (Figure E6), where each sample was iteratively assigned to the most similar cluster, using the Lance-Williams dissimilarity formula and the complete linkage method to compute cluster distances and identify similarities. For gene expression hierarchical clustering, we used Pearson's correlation coefficient to measure similarity, effectively grouping transcripts by their expression patterns across all samples. We then clustered participant samples by the homogeneity of their expression profiles, employing Euclidean distance as the primary similarity metric [27-30].

Estimation of immune cell infiltrations in peripheral blood

xCell is a robust algorithm designed to estimate the infiltration levels of a diverse array of 64 cell types within immune and stromal categories through deconvolution [31]. This range encompasses stromal cells, stem cells, and both innate and adaptive immune cells. We applied this algorithm to calculate immune cell infiltration scores in the peripheral blood of each patient, using normalized data. The xCell-derived scores were then analyzed for differences between clusters using GraphPad Prism 9.5. This analysis was facilitated by the xCell online portal available at https://comphealth.ucsf.edu/app/xcell.

Classification of CRSwNP subtypes using blood transcriptomic signatures

All gene data were standardized to z-scores after TPM transformation. The normalized data were then divided into training (70%) and testing (30%) sets. The training set (n=87) and validation set (n=36) were used to develop a model that discriminates among CRSwNP patients and identifies signature expressions that significantly determine subgroup membership. We utilized regularization-based methods, LASSO (Least Absolute Shrinkage and Selection Operator) and EN (Elastic Net), as well as a non-regularization method, RF (Random Forest), to construct models. The best-performing model was selected based on its predictive accuracy and was trained to differentiate between clusters. After training, the model was tested on a validation dataset to predict cluster membership. This prediction involved assigning each sample to the cluster for which it had the highest calculated probability. The model's predictions were then used to infer the inflammatory endotypes of the samples within the clusters. To evaluate the model's performance, its predictions were compared with the actual endotypes in the validation dataset, assessing its accuracy and reliability. Receiver Operating Characteristic curves [32] were generated for each model, and the Area Under the Curve [2] was calculated to quantitatively assess the performance of the multi-class classification models. AUC values for each cluster were analyzed to identify the optimal model. The final multi-class classification model was constructed using a composite signature, created by combining selected signatures for each cluster with their corresponding coefficients in a weighted summation, to calculate predictive scores for different outcomes. As a result, we found that the performance between elastic net and LASSO algorithms were comparable with AUCs ranging from 0.85 to 0.90, whereas the random forest algorithms had the lowest AUC of 0.78 (Figure E7A). Since the model developed with LASSO via the lambda.min criterion (LASSO_min-based model) had the highest AUC of 0.90 (Figure

E7A), we therefore chose this algorithm as the optimal model to subsequent analysis.

Independent cohort validation

To further assess the accuracy and reliability of our optimal model in identifying inflammatory patterns, we prospectively recruited a validation cohort of CRSwNP patients at the University of Hong Kong Shenzhen Hospital and the Seventh Affiliated Hospital of Sun Yat-sen University from June to November 2022, adhering to institutional guidelines and obtaining informed consent. This cohort included 46 CRSwNP subjects. We collected demographic and clinical data for each subject and stored whole blood samples in RNAlater for RNA sequencing, using established methods. Three clusters were predicted by the LASSO_min-based model (here referred to as pred-cluster) using the 36-gene signature. Blood transcriptional profiles, as well as clinical parameters were compared between the three pred-clusters.

Statistical analysis

Due to the observational nature of this study and the absence of prior results, formal sample size calculations were not conducted. Data were presented as median values with interquartile ranges. We did not impute missing data. Differences between clusters were evaluated using the two-tailed Wilcoxon test for quantitative data and the chi-square test for qualitative data. For categorical variables, we applied either the chi-square test or Fisher's exact test as appropriate. Spearman correlation was used to assess correlations. P-values below 0.05 were considered statistically significant.

Data availability

The raw sequencing data from human samples reported in this study are accessible in the Genome Sequence Archive (GSA) under accession numbers HRA006483 and HRA006324. Source data are available for further reference.

References

1. Hong H, Chen F, Sun Y, et al. Nasal IL-25 predicts the response to oral corticosteroids in chronic rhinosinusitis with nasal polyps. J Allergy Clin Immunol. 2018;141(5):1890-2.
2. Fokkens WJ, Lund VJ, Hopkins C, et al. European Position Paper on Rhinosinusitis and Nasal Polyps 2020. Rhinology. 2020;58(Suppl S29):1-464.
3. Orlandi RR, Kingdom TT, Smith TL, et al. International consensus statement on allergy and rhinology: rhinosinusitis 2021. Int Forum Allergy Rhinol. 2021;11(3):213-739.
4. Bousquet J, Khaltaev N, Cruz AA, et al. Allergic Rhinitis and its Impact on Asthma (ARIA) 2008 update (in collaboration with the World Health Organization, GA(2)LEN and AllerGen). Allergy. 2008;63 Suppl 86:8-160.
5. Bateman ED, Hurd SS, Barnes PJ, et al. Global strategy for asthma management and prevention: GINA executive summary. Eur Respir J. 2008;31(1):143-78.
6. He H, Pan L, Cui Z, et al. Smoking Prevalence, Patterns, and Cessation Among Adults in Hebei Province, Central China: Implications From China National Health Survey (CNHS). Front Public Health. 2020;8:177.
7. Cui Y, Wang K, Shi J, Sun Y. Endotyping difficult-to-treat chronic rhinosinusitis with nasal polyps by structured histopathology. Int Arch Allergy Immunol. 2023;184(10):1036-46.
8. Psaltis AJ, Li G, Vaezeafshar R, Cho KS, Hwang PH. Modification of the Lund-Kennedy endoscopic scoring system improves its reliability and correlation with patient-reported outcome measures. Laryngoscope. 2014;124(10):2216-23.
9. Lund VJ, Kennedy DW. Quantification for staging sinusitis. The Staging and Therapy Group. Ann Otol Rhinol Laryngol Suppl. 1995;167:17-21.
10. Chapurin N, Wu J, Labby AB, Chandra RK, Chowdhury NI, Turner JH. Current insight into treatment of chronic rhinosinusitis: Phenotypes, endotypes, and implications for targeted therapeutics. J Allergy Clin Immunol. 2022;150(1):22-32.
11. Hong HY, Chen FH, Sun YQ, et al. Local IL-25 contributes to Th2-biased inflammatory profiles in nasal polyps. Allergy. 2018;73(2):459-69.
12. Ma L, Deng Y, Wang K, Shi J, Sun Y. Relationship between eosinophilic and neutrophilic inflammation in Chinese chronic rhinosinusitis with nasal polyps. Int Arch Allergy Immunol. 2023;184(6):576-86.
13. Yu G, Wang LG, Han Y, He QY. clusterProfiler: an R package for comparing biological themes among gene clusters. Omics. 2012;16(5):284-7.
14. Bachert C, Zhang N, Hellings PW, Bousquet J. Endotype-driven care pathways in patients with chronic rhinosinusitis. J Allergy Clin Immunol. 2018;141(5):1543-51.
15. Cardenas A, Sordillo JE, Rifas-Shiman SL, et al. The nasal methylome as a biomarker of asthma and airway inflammation in children. Nat Commun. 2019;10(1):3095.
16. Dunn JLM, Shoda T, Caldwell JM, et al. Esophageal type 2 cytokine expression heterogeneity in eosinophilic esophagitis in a multisite cohort. J Allergy Clin Immunol. 2020;145(6):1629-40.e4.
17. García-Sánchez A, Estravís M, Martin MJ, et al. PTGDR2 Expression in Peripheral Blood as a Potential Biomarker in Adult Patients with Asthma. J Pers Med. 2021;11(9).
18. Jiang Y, Gruzieva O, Wang T, et al. Transcriptomics of atopy and atopic asthma in white blood cells from children and adolescents. Eur Respir J. 2019;53(5).
19. Khalfaoui L, Symon FA, Couillard S, et al. Airway remodelling rather than cellular infiltration characterizes both type2 cytokine biomarker-high and -low severe asthma. Allergy. 2022;77(10):2974-86.
20. Okano M, Hirahara K, Kiuchi M, et al. Interleukin-33-activated neuropeptide CGRP-producing memory Th2 cells cooperate with somatosensory neurons to induce conjunctival itch. Immunity. 2022;55(12):2352-68.e7.
21. Wang W, Xu Y, Wang L, et al. Single-cell profiling identifies mechanisms of inflammatory heterogeneity in chronic rhinosinusitis. Nat Immunol. 2022;23(10):1484-94.
22. Yuan J, Liu Y, Yu J, et al. Gene knockdown of CCR3 reduces eosinophilic inflammation and the Th2 immune response by inhibiting the PI3K/AKT pathway in allergic rhinitis mice. Sci Rep. 2022;12(1):5411.
23. Gittler JK, Shemer A, Suárez-Fariñas M, et al. Progressive activation of T(H)2/T(H)22 cytokines and selective epidermal proteins characterizes acute and chronic atopic dermatitis. J Allergy Clin Immunol. 2012;130(6):1344-54.
24. Jovic S, Linge HM, Shikhagaie MM, et al. The neutrophil-recruiting chemokine GCP-2/CXCL6 is expressed in cystic fibrosis airways and retains its functional properties after binding to extracellular DNA. Mucosal Immunol. 2016;9(1):112-23.
25. Mattos MS, Ferrero MR, Kraemer L, et al. CXCR1 and CXCR2 Inhibition by Ladarixin Improves Neutrophil-Dependent Airway Inflammation in Mice. Front Immunol. 2020;11:566953.
26. Wang C, Zhou W, Su G, Hu J, Yang P. Progranulin Suppressed

Autoimmune Uveitis and Autoimmune Neuroinflammation by Inhibiting Th1/Th17 Cells and Promoting Treg Cells and M2 Macrophages. Neurol Neuroimmunol Neuroinflamm. 2022;9(2).
27. Mejias A, Dimo B, Suarez NM, et al. Whole blood gene expression profiles to assess pathogenesis and disease severity in infants with respiratory syncytial virus infection. PLoS Med. 2013;10(11):e1001549.
28. Berry MP, Graham CM, McNab FW, et al. An interferon-inducible neutrophil-driven blood transcriptional signature in human tuberculosis. Nature. 2010;466(7309):973-7.
29. Wittkowski KM, Song T. Nonparametric methods for molecular biology. Methods Mol Biol. 2010;620:105-53.
30. Wittkowski KM, Lee E, Nussbaum R, Chamian FN, Krueger JG. Combining several ordinal measures in clinical studies. Stat Med. 2004;23(10):1579-92.
31. Aran D, Hu Z, Butte AJ. xCell: digitally portraying the tissue cellular heterogeneity landscape. Genome Biol. 2017;18(1):220.
32. Zielinska-Blizniewska H, Paprocka-Zjawiona M, Merecz-Sadowska A, Zajdel R, Blizniewska-Kowalska K, Malinowska K. Serum IL-5, POSTN and IL-33 levels in chronic rhinosinusitis with nasal polyposis correlate with clinical severity. BMC Immunol. 2022;23(1):33.

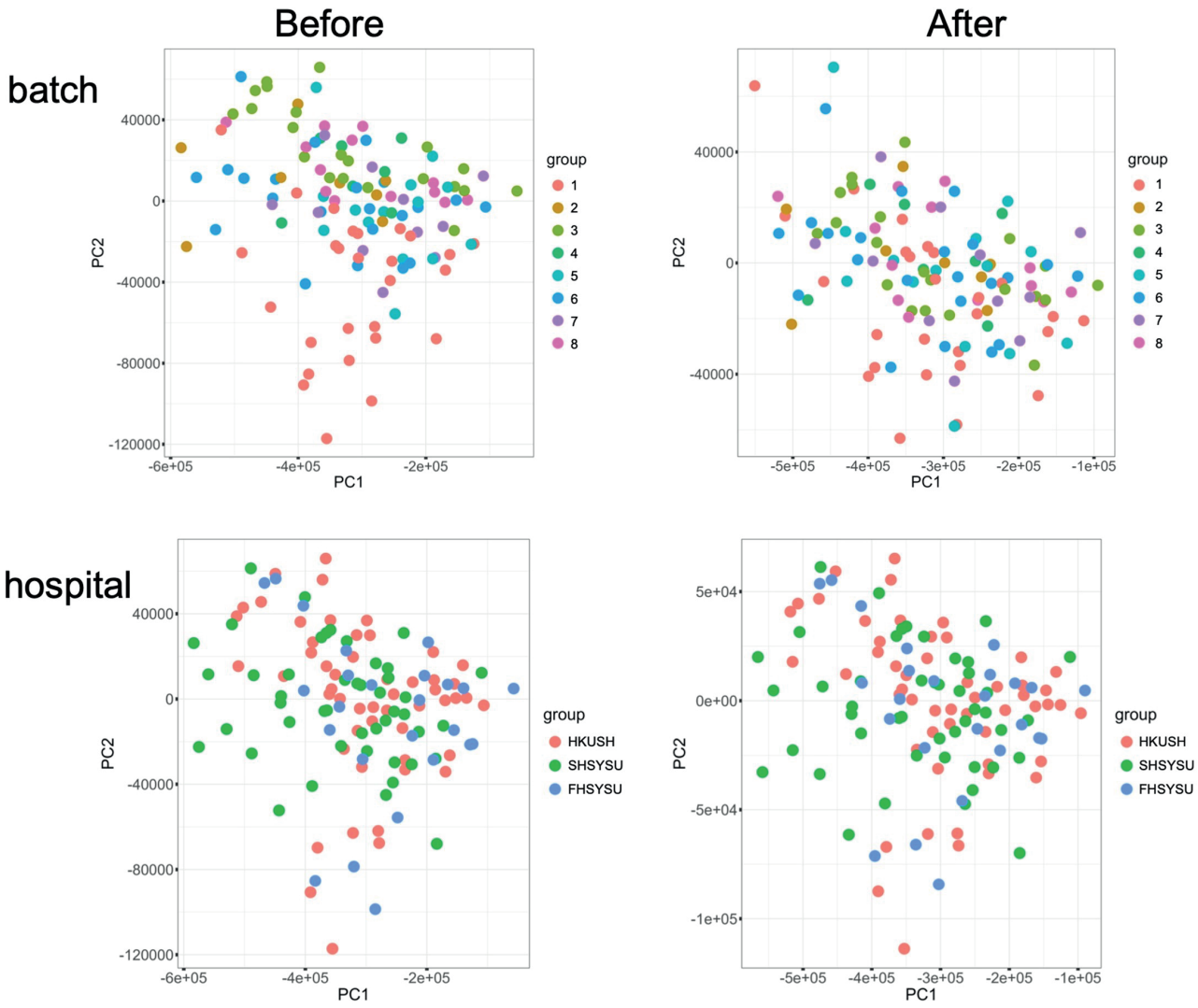

Figure E1. Principal component analysis (PCA) plot before and after batch effect and hospital adjustment.

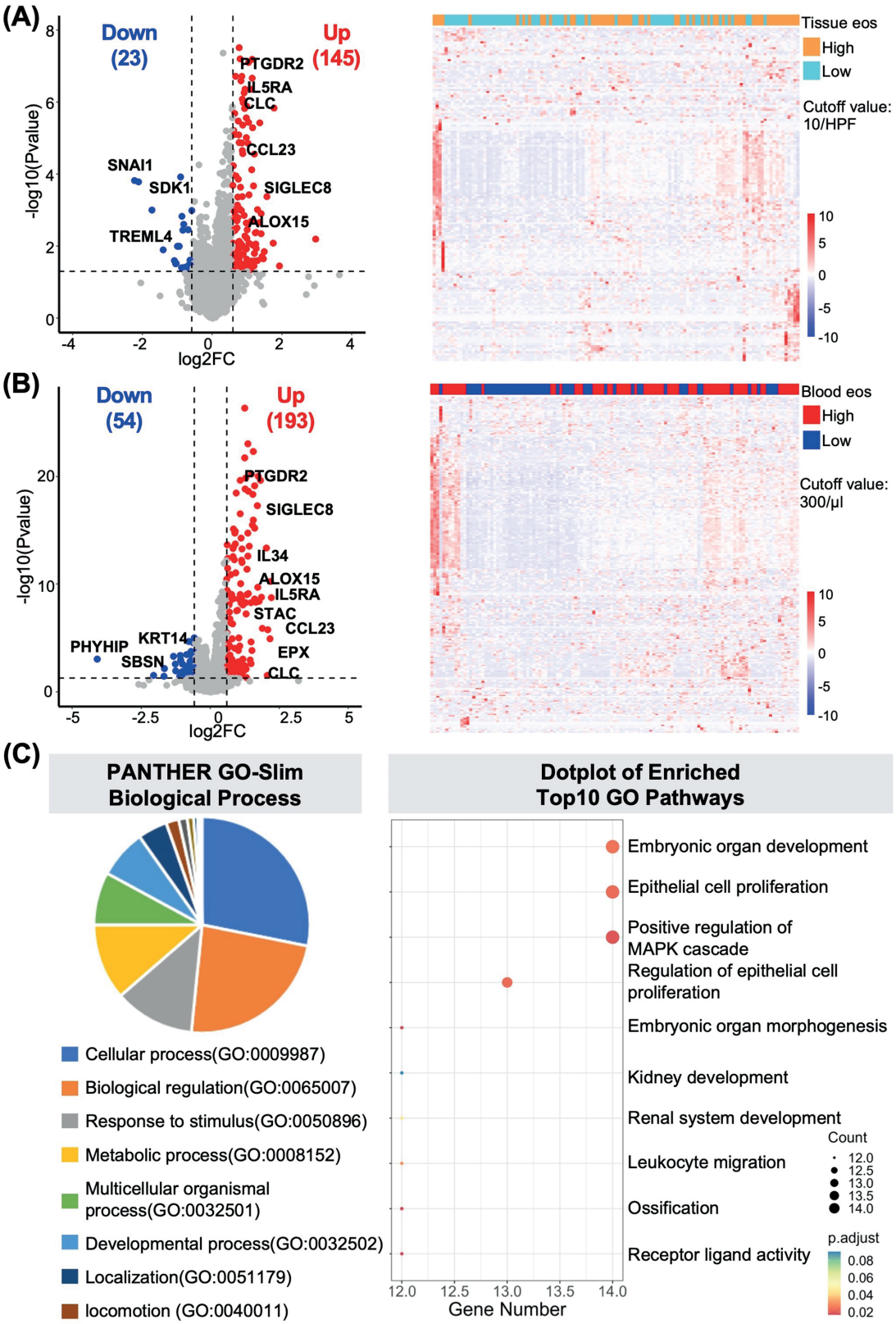

Figure E2. Differential expression analysis of blood transcriptome in CRSwNP patients stratified by tissue or blood eosinophil levels. Volcano plots and heatmaps show the differential gene expressions with notable upregulated and downregulated genes in CRSwNP patients with high versus low tissue (A) and blood (B) eosinophil levels. (C) The pie chart displays the distribution of gene functions according to PANTHER GO-Slim biological processes, and the dot plot visualizes the top 10 enriched GO pathways based on the gene count within each pathway in CRSwNP patients with high blood eosinophil levels.

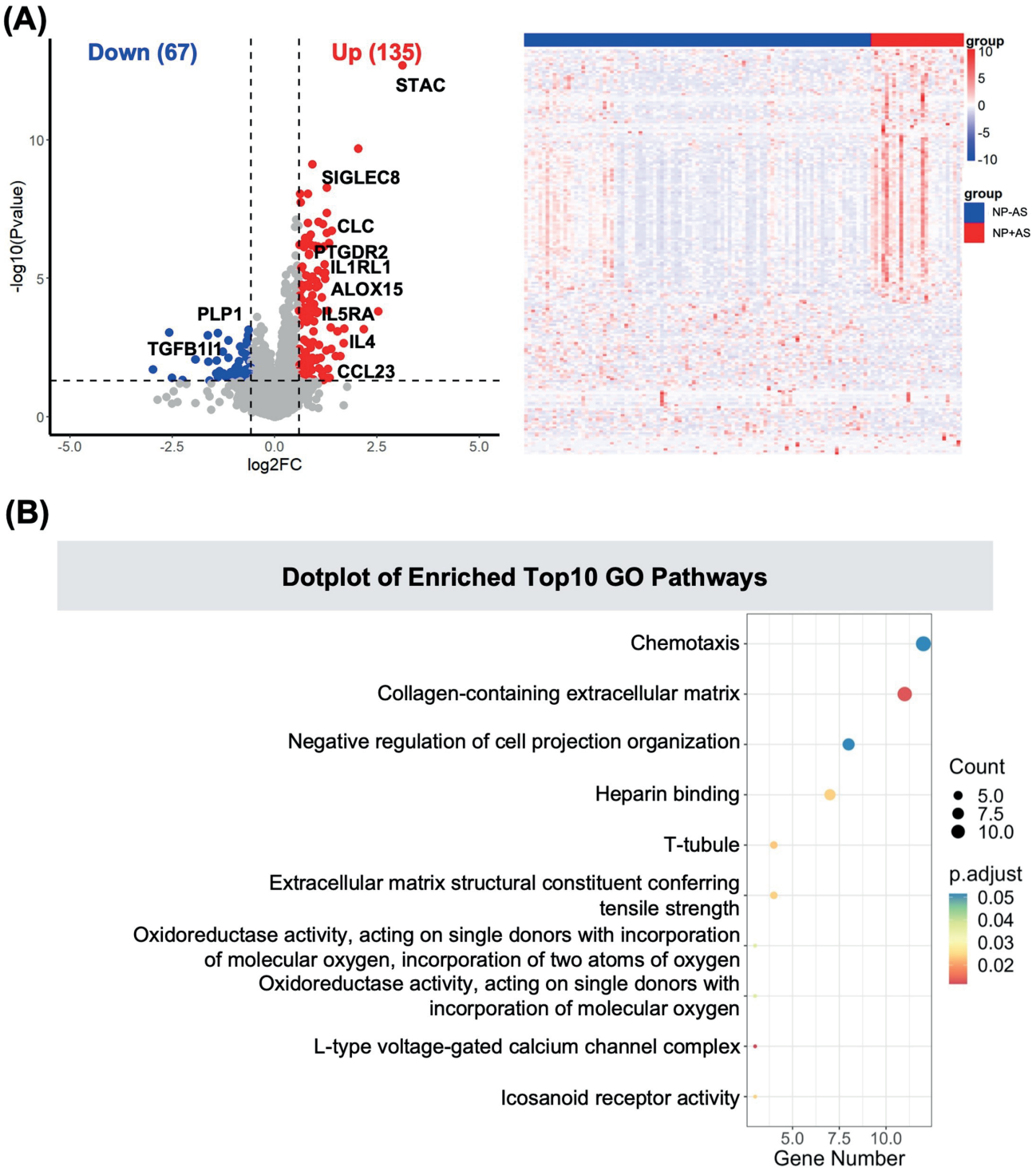

Figure E3. Blood transcriptomic differences between CRSwNP patients with and without asthma. (A) Volcano plot and heatmap show the differential gene expressions with notable upregulated and downregulated genes in CRSwNP patients with (n=26) versus without asthma (n=97). (B) Dot plot visualizes the top 10 enriched GO pathways within each pathway in CRSwNP patients with comorbid asthma.

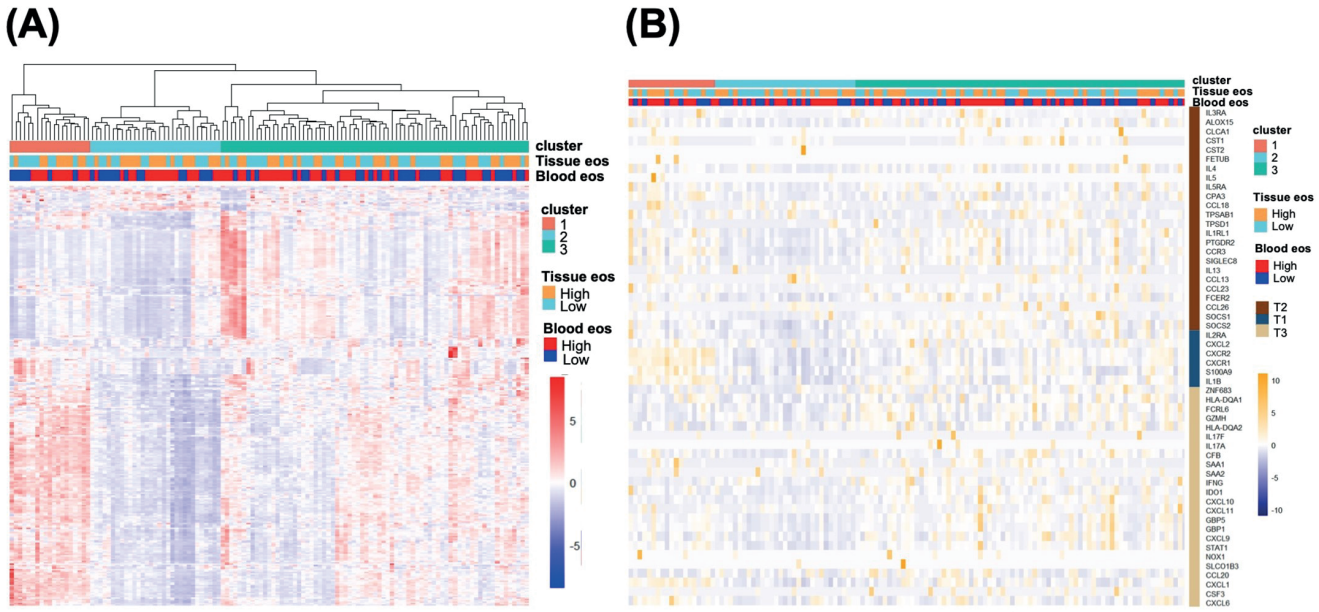

Figure E4. (A) Unsupervised hierarchical clustering analysis with top 300 hypervariable genes. (B) T2/1/3-biomarkers and tissue and blood eosinophil patterns between the patient clusters identified in (A).

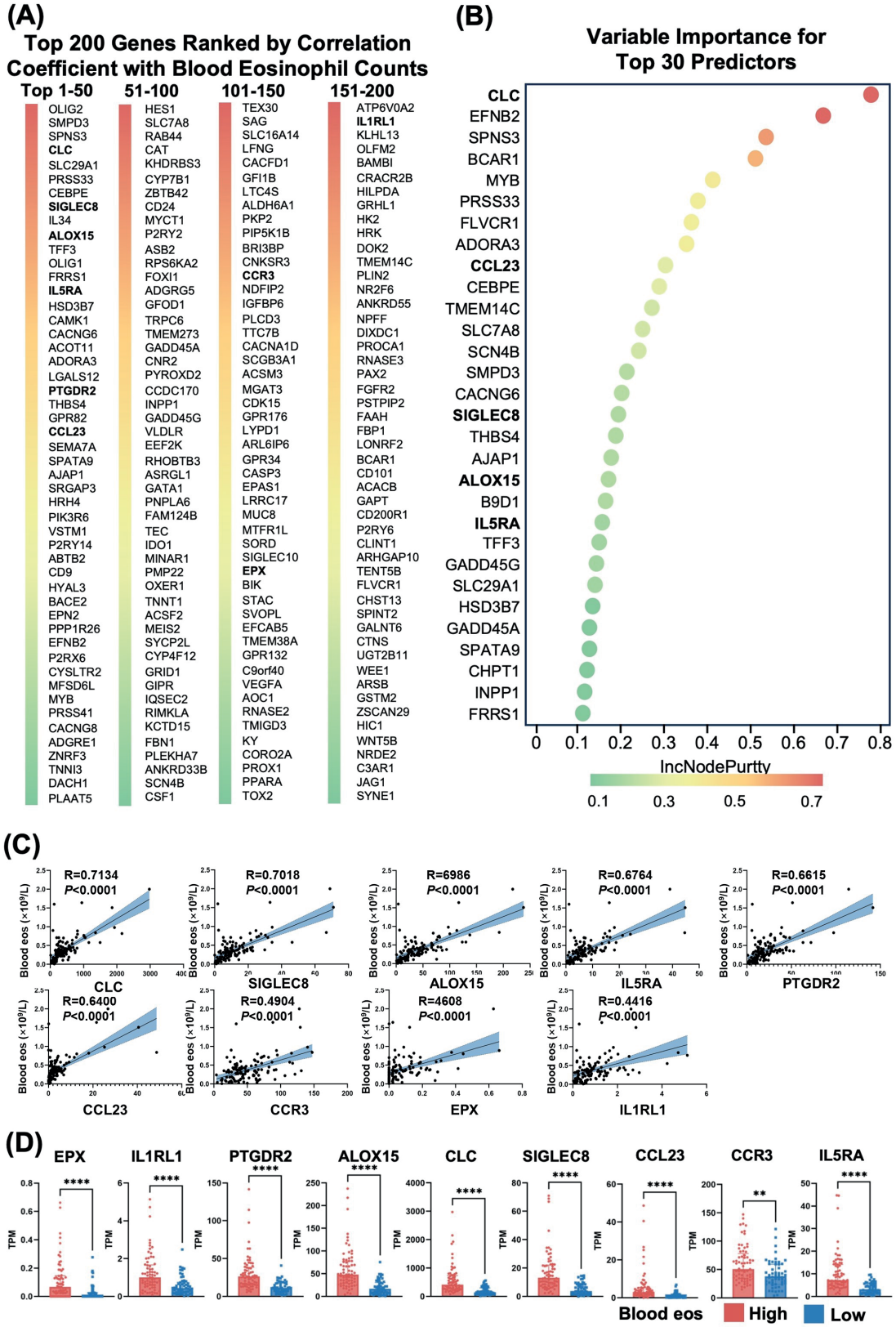

Figure E5. Transcriptomics-based screening of molecular signatures associated with high blood eosinophils in CRSwNP patients. (A) Analysis of correlations between blood transcriptome and blood eosinophil counts. Top 200 genes ranked by correlation coefficient are shown. (B) The critical eosinophil-related biomarkers were screened by using random forest algorithm. The top 30 significant genes are shown. IncNodePurity ranks the genes in accordance with their relative importance. (C) Correlations between the expression levels of the 9 identified biomarkers and blood eosinophil counts. (D) Significant differences in expression levels of the 9 identified biomarkers in CRSwNP patients with high versus low blood eosinophil counts.

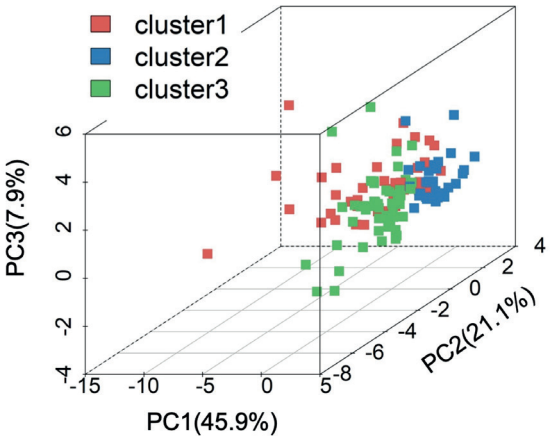

Figure E6. Principal Component Analysis (PCA) of clustering analysis displaying the segregation of the patient samples into distinct clusters.

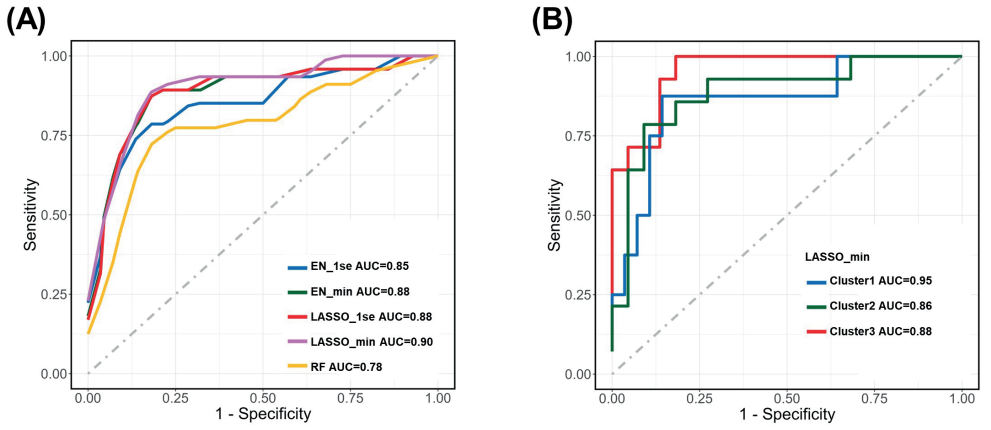

(C)

Cluster-1-specific biomarkers
ALOX15
DERL1
FBP1
FEXO7
PDIA4
PLEKHA2

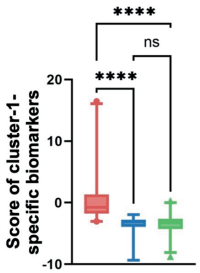

Cluster-2-specific biomarkers	
CIZ1	LPCAT2
DEGS1	SHARPIN
DPM2	SPON2
HBA2	SRXN1
HLA-DRB1	TCF7
KRT23	UBE2D1

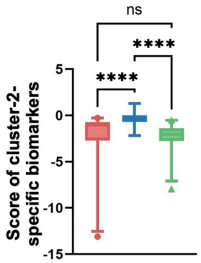

Cluster-3-specific biomarkers		
ESYT2	OSCAR	SHARPIN
HBG2	PF4	SLC25A39
HLA-DRB1	PPBP	SLPI
HLA-DRB5	PTGDS	SRA1
KCNJ15	RNF187	TMEM91
MAN2A2	S100A12	YBX3

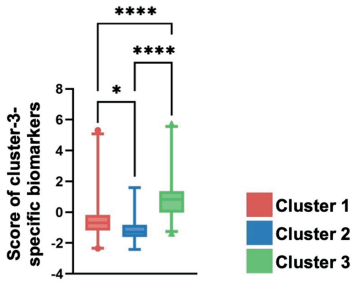

Figure E7. (A) ROC curves of different algorithms for identifying the best model to distinguish the three blood-based CRSwNP clusters. (B) ROC curves of the LASSO_min-based model for predicting the three clusters. The model established was then validated on an independent validation cohort of 46 patients with CRSwNP. Three clusters were predicted by the LASSO_min-based model using the cluster-specific biomarkers (the 36-gene set). (C) Lists of cluster-specific biomarkers identified, and the distribution of different scores predicted by the LASSO algorithm between the distinct clusters.

Table E1. Clinical characteristics.

		Age, median (IQR)	Male, n (%)	Current smoker, n (%)	Allergic rhinitis, n (%)	Asthma, n (%)	L-K endoscopic score, median (IQR)	L-M CT score, median (IQR)	TNSS, median (IQR)	SNOT-22, median (IQR)
CRSwNP(n=181)		38.00(17.00)	124(68.51)	29(16.02)	71(39.23)	31(17.13)	8.00(3.00)	17.00(9.00)	7.00(3.00)	31.50(25.00)
Exploratory cohort (n=123)		40.00(17.00)	95(70.37)	22(16.30)	56(45.53)	26(19.26)	9.00(3.00)	17.00(8.00)	8.00(3.00)	32.00(26.50)
Independent validation cohort (n=46)		33.00(21.75)	29(63.04)	7(15.22)	15(32.61)	5(10.87)	8.00(4.00)	17.00(9.75)	6.50(3.00)	29.50(16.75)
Tissue eos	eCRSwNP (n=60)	39.00(14.50)	41(68.33)	8(12.26)	**32(53.33)**	16(26.66)	9.00(3.00)	17.50(7.25)	7.00(3.00)	32.00(28.00)
	neCRSwNP (n=63)	40.00(18.00)	45(71.43)	12(19.05)	**21(33.33)**	10(15.87)	9.00(3.00)	17.50(7.25)	7.00(3.00)	32.00(28.00)
Blood eos	CRSwNP blood-eos-hi (n=69)	39.00(13.00)	50(72.46)	12(18.84)	35(50.72)	**19(27.54)**	8.00(3.50)	17.00(8.25)	7.00(3.00)	30.00(25.00)
	CRSwNP blood-eos-lo (n=54)	40.00(19.50)	36(66.67)	7(12.96)	18(33.33)	**7(12.96)**	10.00(2.00)	18.00(7.00)	7.50(2.75)	34.00(27.00)
Clustering analysis	Cluster 1 (n=42)	41.36(10.09)	26(61.90)	5(11.90)	24(57.14)	**17(40.48) ^**	8.00(3.00)	18.00(9.00)	8.00(3.00)	34.50(29.25)
	Cluster 2 (n=32)	40.56(13.46)	26(81.25)	6(18.75)	13(40.63)	**2(6.25) ^**	8.00(4.00)	17.00(9.75)	7.00(3.25)	28.00(31.00)
	Cluster 3 (n=49)	40.90(13.50)	34(69.39)	9(18.37)	16(32.65)	**7(14.29) ^**	10.00(2.00)	18.00(7.00)	8.00(3.00)	31.50(25.75)
Histopathologic analysis (n=60)		40.00(16.25)	44(73.33)	10(16.67)	27(45.00)	15(25.00)	9.00(2.00)	18.00(8.00)	7.00(2.00)	32.00(25.25)
Tissue transcriptome Analysis (n=35)		39.00(19.00)	21(60.00)	6(17.14)	10(28.57)	8(22.86)	10.00(3.00)	20.00(6.00)	8.00(3.00)	21.00(28.00)

Results in boldface indicate a p value of less than 0.05; * indicates a p value of less than 0.01; ^ indicates a p value of less than 0.001. IQR, interquartile range; L-K, Lund Kennedy; L-M, Lund Mackay; CT, computed tomography; HPF, high power field; TNSS, total nasal symptom score; SNOT-22, The 22-item sino-nasal outcome test.

Table E2. Top50 upregulated and downregulated DEGs in blood of patients with CRSwNP versus healthy controls.

Gene	Log2FoldChange	P-value	Regulated	Gene	Log2FoldChange	P-value	Regulated
PVRIG	9.39124717	4.29E-126	up	HNRNPH2	-10.87671234	2.84E-127	down
CD68	9.08584831	8.88E-278	up	CHMP3	-9.860624732	1.19E-235	down
ARL6IP4	7.545779312	6.17E-262	up	GIMAP5	-8.529996555	1.99E-181	down
IFI30	7.293305493	0	up	RPS10	-7.914101079	7.22E-166	down
NPIPB3	7.222855166	1.74E-103	up	NEIL3	-7.763435911	6.61E-76	down
TLR9	7.207699455	1.92E-101	up	ATP5F1E	-7.66620259	0	down
NDST2	7.112107703	0	up	ACSS3	-7.640005483	6.83E-86	down
MBD6	6.831920927	2.64E-303	up	DISC1	-7.534926972	1.35E-215	down
TRIM74	6.779319866	8.20E-75	up	PHF11	-7.495040725	0	down
LIME1	6.748468673	7.09E-174	up	ABHD12B	-7.469358103	5.18E-43	down
GTF2H4	6.547747064	3.36E-98	up	AP3S2	-7.180531164	1.24E-173	down
MRPL38	6.371857125	2.19E-199	up	A2M	-7.11466724	1.21E-82	down
SRXN1	6.276193641	3.55E-143	up	LDHAL6A	-6.898421369	7.90E-35	down
CTRL	6.189052024	6.14E-95	up	SLC12A1	-6.700746592	2.77E-08	down
LENG8	6.17731326	0	up	ZNF117	-6.666883664	6.49E-149	down
SNX32	6.146048379	1.36E-21	up	CACNB2	-6.610615619	1.01E-47	down
GABARAP	6.091600981	3.68E-280	up	CC2D2A	-6.521289778	1.07E-144	down
HBG1	6.066606794	1.11E-26	up	PRPH2	-6.46815002	1.27E-35	down
PDXP	5.979521308	1.92E-99	up	SCNM1	-6.397752423	2.79E-264	down
NR1D1	5.948258115	1.28E-97	up	CYP3A5	-6.342578577	1.57E-22	down
SRCAP	5.911815479	0	up	BCAP29	-6.288598764	8.60E-51	down
FLT3LG	5.853082673	9.41E-179	up	RFTN2	-6.254185681	1.11E-37	down
LY6G5B	5.654508711	7.61E-193	up	WWTR1	-6.236334218	7.77E-108	down
HBA1	5.625424236	2.69E-49	up	FMC1	-6.21739873	2.47E-65	down
TMEM35B	5.482169585	1.56E-158	up	CD302	-6.198710874	4.99E-130	down
SPATA21	5.375839	1.48E-17	up	SLC25A6	-6.197633734	6.09E-74	down
GET4	5.295735543	4.16E-204	up	APOBEC2	-6.196828545	1.05E-40	down
PRR12	5.209981374	5.51E-236	up	RNASEK	-6.185685054	1.28E-82	down
LCN10	5.203697451	1.39E-55	up	ASB3	-6.183271128	1.84E-171	down
IGLL5	5.110755765	9.23E-81	up	SPRY3	-6.167436036	3.35E-86	down
AGAP5	5.089654891	5.63E-75	up	SOX6	-6.056128613	2.78E-64	down
BCKDHA	5.068030484	1.44E-225	up	ZBED1	-6.035977522	4.74E-197	down
LAT	4.946544356	2.78E-172	up	RPL36A	-5.984923086	2.30E-72	down
SPNS1	4.921514247	1.72E-137	up	LAMB1	-5.971335602	1.80E-28	down
PLPPR3	4.849256329	3.17E-16	up	POU5F2	-5.890627926	9.42E-60	down
RAB1B	4.813639901	4.86E-164	up	TBC1D7	-5.885441553	6.47E-122	down
SHE	4.788205782	4.59E-17	up	PLCE1	-5.730318075	7.73E-40	down
DNLZ	4.748766646	2.29E-53	up	VAMP7	-5.715989074	4.18E-58	down
SCAF1	4.681257258	7.27E-242	up	ANKRD36C	-5.710253834	1.74E-232	down
ABHD16A	4.677114894	3.67E-144	up	ARHGEF26	-5.671294041	1.20E-35	down
NPIPB13	4.671925466	2.29E-41	up	SPATA1	-5.62352596	9.98E-73	down
PGAM2	4.663165518	5.26E-22	up	SKA3	-5.619396111	3.14E-55	down
AGPAT1	4.631329022	9.64E-156	up	HEMGN	-5.604265793	2.90E-122	down
CRIP1	4.589071182	2.97E-182	up	GYPA	-5.593533431	1.26E-44	down
OGFOD2	4.546622146	8.56E-128	up	MYH10	-5.548457812	4.18E-131	down
TRAPPC5	4.544379351	1.17E-145	up	TRIM69	-5.447693082	0	down
ZACN	4.503228346	1.58E-12	up	CHKB	-5.436712724	5.97E-41	down
RAVER1	4.48018817	3.52E-299	up	SNRPN	-5.411695425	5.36E-235	down
MIF	4.466125361	4.80E-107	up	POMK	-5.337648051	7.71E-178	down
REXO1	4.445975939	0	up	KIF14	-5.274335139	6.75E-53	down

Table E3. Top50 upregulated and downregulated DEGs in blood of patients with eCRSwNP versus healthy controls.

Gene	Log2FoldChange	P-value	Regulated	Gene	Log2FoldChange	P-value	Regulated
PVRIG	9.416581947	2.60E-120	up	HNRNPH2	-10.89789238	2.11E-176	down
CD68	9.038360466	3.41E-224	up	CHMP3	-9.590173288	1.11E-278	down
ATP6V0C	8.947140524	7.15E-167	up	GIMAP5	-8.639586471	5.17E-222	down
ARL6IP4	7.620925974	8.39E-210	up	RPS10	-7.815801752	1.06E-181	down
IFI30	7.298925083	0	up	NEIL3	-7.628850502	1.52E-48	down
NPIPB3	7.16902134	2.50E-96	up	DISC1	-7.561932435	4.35E-214	down
TLR9	7.131868803	1.34E-95	up	ACSS3	-7.555686663	1.17E-70	down
NDST2	7.097450662	0	up	ATP5F1E	-7.514625143	9.48E-287	down
LIME1	6.873824763	3.74E-128	up	PHF11	-7.464398156	0	down
MBD6	6.8679474	1.70E-220	up	AP3S2	-7.303466185	8.35E-200	down
TRIM74	6.746105376	5.68E-74	up	ABHD12B	-7.248303127	2.43E-34	down
GTF2H4	6.562190667	1.82E-96	up	SLC12A1	-7.206106936	6.92E-09	down
MRPL38	6.381092761	2.11E-179	up	A2M	-7.020194319	2.86E-58	down
SNX32	6.321687803	5.02E-21	up	LDHAL6A	-6.687304908	6.48E-31	down
SRXN1	6.296356889	5.24E-107	up	SCNM1	-6.603181984	3.01E-219	down
LENG8	6.251940476	6.06E-186	up	ZNF117	-6.596800964	2.19E-107	down
CTRL	6.193591023	1.12E-90	up	CC2D2A	-6.54901878	1.55E-97	down
GABARAP	6.11674453	4.63E-202	up	SLC25A6	-6.436427796	5.40E-98	down
PDXP	5.985502649	1.23E-91	up	CACNB2	-6.42848487	9.19E-40	down
HBG1	5.964323927	1.11E-21	up	RNASEK	-6.346905374	1.08E-75	down
NR1D1	5.952127337	2.14E-86	up	PRPH2	-6.307544971	2.66E-28	down
SRCAP	5.877150775	0	up	CD302	-6.304442203	1.80E-97	down
FLT3LG	5.749455965	6.31E-137	up	CYP3A5	-6.286629084	1.14E-18	down
HBA1	5.681013256	4.14E-32	up	BCAP29	-6.256574715	1.64E-36	down
LY6G5B	5.629239067	2.39E-178	up	ASB3	-6.205522889	6.31E-139	down
TMEM35B	5.544789513	2.33E-144	up	SPRY3	-6.189241991	7.42E-87	down
SPATA21	5.523083899	1.84E-18	up	APOBEC2	-6.168474316	6.86E-38	down
GET4	5.459884858	3.25E-130	up	WWTR1	-6.147254084	2.54E-77	down
LRCH4	5.349058722	3.18E-86	up	FMC1	-6.04665113	5.81E-59	down
PRR12	5.252428876	2.94E-183	up	RPL36A	-5.979798737	1.54E-74	down
LCN10	5.158123104	5.28E-47	up	TBC1D7	-5.950074309	6.48E-134	down
BCKDHA	5.074214896	4.83E-191	up	ZBED1	-5.939592495	2.04E-159	down
AGAP5	5.041510272	1.55E-73	up	POU5F2	-5.937669348	5.11E-62	down
IGLL5	5.012492063	1.25E-65	up	RFTN2	-5.890112834	1.32E-31	down
FTH1	4.998448911	1.02E-37	up	SOX6	-5.840034694	2.77E-41	down
SHE	4.987487407	2.19E-17	up	SPATA1	-5.620431773	4.76E-56	down
PLPPR3	4.960564272	2.75E-16	up	ANKRD36C	-5.619417695	1.99E-215	down
MINK1	4.960046624	9.63E-129	up	LAMB1	-5.602451674	6.04E-19	down
ABHD16A	4.884936926	2.16E-90	up	HEMGN	-5.532880121	2.65E-84	down
RAB1B	4.871233518	5.88E-91	up	MYH10	-5.525994649	4.72E-96	down
LAT	4.834383083	7.02E-110	up	ARHGEF26	-5.492319838	6.48E-27	down
PGAM2	4.785996604	4.10E-22	up	VAMP7	-5.451342311	3.88E-43	down
AGPAT1	4.759638564	1.66E-101	up	SNRPN	-5.447280846	1.13E-157	down
DNLZ	4.741169735	2.05E-51	up	TRIM69	-5.394610115	0	down
SMPD3	4.724114728	8.57E-52	up	PLCE1	-5.389179339	2.98E-29	down
CRIP1	4.696406882	3.40E-158	up	GYPA	-5.356567876	3.52E-27	down
SCAF1	4.688605765	1.15E-190	up	SKA3	-5.337704273	7.52E-32	down
OGFOD2	4.684372988	2.08E-89	up	POMK	-5.328350991	7.32E-139	down
MIF	4.658938915	5.05E-64	up	CHKB	-5.30290396	1.23E-36	down
ZACN	4.621947093	2.56E-11	up	AMPH	-5.287813001	6.13E-36	down

Table E4. Top50 upregulated and downregulated DEGs in blood of patients with neCRSwNP versus healthy controls.

Gene	Log2FoldChange	P-value	Regulated	Gene	Log2FoldChange	P-value	Regulated
PVRIG	9.367798295	1.82E-127	up	HNRNPH2	-10.84787368	4.12E-138	down
CD68	9.300080848	3.43E-201	up	CHMP3	-10.16576885	7.48E-287	down
ARL6IP4	7.545446417	8.67E-232	up	GIMAP5	-8.425602477	7.34E-138	down
IFI30	7.29618253	0	up	RPS10	-8.009894703	4.65E-150	down
NPIPB3	7.274239117	8.48E-104	up	NEIL3	-7.907340921	5.72E-50	down
TLR9	7.273943522	4.67E-100	up	ATP5F1E	-7.816515258	0	down
NDST2	7.11295969	0	up	ACSS3	-7.71327147	1.36E-90	down
MBD6	6.957275656	3.03E-236	up	ABHD12B	-7.700313903	1.49E-36	down
TRIM74	6.809797013	7.86E-73	up	PHF11	-7.514213805	0	down
LIME1	6.796037072	1.35E-146	up	DISC1	-7.504487497	6.39E-254	down
GTF2H4	6.532908073	6.33E-97	up	A2M	-7.196091411	3.77E-74	down
SRXN1	6.438113905	2.27E-116	up	LDHAL6A	-7.119599858	9.96E-34	down
MRPL38	6.363029967	3.03E-205	up	AP3S2	-7.060429938	2.82E-155	down
LENG8	6.329665261	1.16E-204	up	CACNB2	-6.795664266	3.36E-35	down
CTRL	6.186967846	2.05E-92	up	ZNF117	-6.73701406	2.94E-137	down
GABARAP	6.151444908	3.62E-207	up	RFTN2	-6.697725071	5.06E-41	down
HBG1	6.10587121	1.11E-23	up	PRPH2	-6.629414869	1.27E-27	down
SRCAP	5.980636874	0	up	CC2D2A	-6.487053132	5.07E-93	down
PDXP	5.97729369	2.44E-99	up	LAMB1	-6.411469075	1.64E-33	down
NR1D1	5.972959593	1.79E-92	up	FMC1	-6.388862081	4.25E-57	down
SNX32	5.965502593	7.32E-19	up	CYP3A5	-6.384531382	6.48E-24	down
FLT3LG	5.82307322	7.36E-167	up	SLC12A1	-6.327256681	6.67E-08	down
LY6G5B	5.661776057	3.20E-179	up	WWTR1	-6.315934055	3.71E-86	down
HBA1	5.584529217	2.04E-51	up	BCAP29	-6.308423013	1.53E-31	down
TMEM35B	5.471083638	1.31E-136	up	SOX6	-6.293108411	6.04E-66	down
GET4	5.422804119	2.51E-143	up	SCNM1	-6.2177744	2.98E-218	down
LCN10	5.257999853	3.00E-55	up	APOBEC2	-6.214077433	4.20E-37	down
PRR12	5.255475186	4.66E-204	up	ASB3	-6.158003751	1.53E-121	down
SPATA21	5.2311282	3.73E-14	up	PLCE1	-6.146469967	3.07E-34	down
IGLL5	5.200231569	1.95E-90	up	ZBED1	-6.122936168	2.15E-230	down
AGAP5	5.135231857	1.24E-71	up	SPRY3	-6.115886758	2.74E-91	down
FTH1	5.128150105	3.16E-41	up	CD302	-6.097493144	6.92E-84	down
BCKDHA	5.08557616	2.73E-219	up	RNASEK	-6.034553568	8.50E-68	down
RAB1B	4.919277687	7.17E-99	up	VAMP7	-6.023368958	2.31E-66	down
ABHD16A	4.862489867	3.85E-93	up	SLC25A6	-5.995753732	2.41E-56	down
LAT	4.83520292	1.90E-120	up	RPL36A	-5.976544479	1.13E-69	down
DNLZ	4.770561167	2.87E-48	up	SKA3	-5.942619945	1.07E-52	down
AGPAT1	4.755592163	2.23E-111	up	GYPA	-5.854501194	8.94E-47	down
NPIPB13	4.741116536	2.00E-38	up	POU5F2	-5.852099047	4.20E-61	down
PLPPR3	4.74086861	7.05E-14	up	ARHGEF26	-5.843801699	1.22E-37	down
SCAF1	4.703509681	8.15E-236	up	TBC1D7	-5.822945715	1.14E-117	down
SPNS1	4.687909395	1.01E-94	up	ANKRD36C	-5.793950263	1.39E-209	down
OGFOD2	4.658290105	2.60E-90	up	HEMGN	-5.674239534	2.03E-113	down
CDC42EP2	4.591940265	1.37E-54	up	SPATA1	-5.615139605	1.21E-60	down
ATP6V0C	4.585107895	2.70E-22	up	SUMO4	-5.586285165	1.64E-50	down
SHE	4.579156822	6.57E-15	up	MYH10	-5.564297386	4.37E-106	down
MIF	4.576064292	1.25E-75	up	KIF14	-5.559570355	7.51E-48	down
PGAM2	4.544570828	6.97E-20	up	CHKB	-5.549834657	1.22E-43	down
RAVER1	4.543199823	3.78E-242	up	TRIM69	-5.493449402	2.45E-243	down
TRAPPC5	4.53507638	2.67E-158	up	KY	-5.461668177	2.07E-59	down

Table E5. Part of unique and common DEGs in eCRSwNP or neCRSwNP versus healthy controls.

Common up	eCRSwNP vs HC-unique-up	neCRSwNP vs HC-unique-up	Common down	eCRSwNP vs HC-unique-down	neCRSwNP vs HC-unique-down
U2AF2	CREB3L3	GLYR1	ATP5F1E	LGALS1	SERBP1
ATP2A3	GSTM1	MED29	PHF11	OSBPL10	FAM107B
SRCAP	CCL23	NADSYN1	RSRC1	MAFB	SET
RNF166	IL5RA	RPRD1B	CHMP3	SOBP	NSL1
NDST2	FAM166A	DELE1	PRKRIP1	TAF4B	GPBP1
IFI30	SPNS3	KDM5C	DISC1	MRPS34	THUMPD1
TMEM259	FGFR2	GIT2	TRIM69	NPHP1	METTL14
REXO1	C4BPA	KIAA0513	CSPP1	ZNF229	CLN5
STXBP2	TENT5B	PPP2R1A	ZBED1	CUL4A	POGLUT1
ARHGEF1	OLIG2	RASGRP2	EDEM2	ADAP2	PHAX
PRRC2A	SLIT3	ZHX2	SCNM1	CTBP2	ZNF227
ATXN2L	CACNG6	POFUT1	NEK1	FXN	NRDE2
RAVER1	SERPINE3	ARMC6	ANKRD36C	DHRS7B	CEP120
PKN1	SYCP2L	PLEKHG3	NFIA	ANKRD29	PRMT9
MBD6	CLC	SCAF4	SEC62	TBL1X	TPP2
SCAF1	TRIM64B	MAP4K2	P2RY8	KIR2DL1	UBXN7
STIMATE	CYP7B1	BTN2A2	SNRPN	RBPMS2	ARID5B
ARL6IP4	LGALS12	DCTN1	BBX	RAP1GAP	ARMC1
LDB1	SLC29A1	ZNF746	CWF19L2	CDK19	CCDC90B
ATF6B	P2RX6	SRGAP2	RSF1	CSNK1G3	TIMMDC1
BCKDHA	LYPD1	PFAS	TAF1D	ARL6	FASTKD2
CAMTA2	LIF	THEMIS2	GALK2	HPCAL1	CAPN7
KXD1	SDC1	DENND5A	FBXW7	AK5	TNIK
PRKCSH	TMIGD3	DPH2	ZNF573	PTGES	LYRM2
ZNF410	SLC34A1	EXTL3	POMK	TMEM165	ZNF431
PNPLA6	CASQ1	PREX1	SCFD1	CTH	HSF2
GABARAP	ICAM4	SLC15A3	PHF14	RPUSD2	PRIM2
MAPK8IP3	ZBTB42	LAPTM5	THOC2	MYO5C	MFSD4B
MRPL38	TMEM273	HYAL2	AP3S2	SHISA2	JMY
LENG8	CDK15	PLCB3	POLR2M	LAMTOR1	GPATCH11
PRR12	APC2	AGPAT2	MAP3K13	ABHD14A	NBN
CD68	MMP8	DNMBP	ZNF557	GSAP	TMEM14B
CCAR2	HYAL3	CCDC86	ATRX	DLEU7	EIF1AX
CRIP1	RBP5	OAZ2	NUCKS1	GTF2E2	HDAC8
CNOT3	COL15A1	LPAR5	RPS10	ZNF418	COMMD1
CDK11A	ADAMTS14	ZNF516	FOXP1	EAPP	MTERF1
CALM3	CMTM5	STX3	N4BP2L2	SASH1	GFOD1
LY6G5B	IQCN	SLC43A3	MTDH	NFIC	KBTBD6
DCAF15	GRID1	NCSTN	TRIM13	CTSG	FAHD1
ABR	OAZ3	BCKDK	DDX21	ANOS1	STOML2
FCHSD1	HDC	FCGRT	HNRNPH2	FPR3	TTLL5
TBC1D10A	IGF2	POLM	GIMAP5	NOP10	ANKH
RABGEF1	PMP22	AOAH	AKAP9	AIF1	EPHA4
FLT3LG	GOLGA8H	TRMT61A	ZNF117	ATOH8	ELOB
KRTCAP2	GPR176	PRKCD	PRPF40A	GSTA4	NDUFS3
INPPL1	OLFML2B	ZNF335	RFC1	RAC1	GOLIM4
UBQLN4	SYNGR3	COPG1	TRDMT1	TXNRD3	DBF4
RAB24	GDF10	ECE1	RDX	ELF2	CNPY4
ARL8A	TNFRSF18	SLC12A6	ATXN3	SFSWAP	ICA1
TRAPPC5	LAG3	C11orf24	RSBN1	VPREB3	INO80D

Table E6. Top50 functions enriched in the common upregulated or downregulated DEGs

Description (Overlap-Up)	P.adjust	Description (Overlap-Down)	P.adjust
regulation of small GTPase mediated signal transduction	1.53269E-05	mitotic cell cycle phase transition	1.7823E-05
mononuclear cell differentiation	1.53269E-05	respiratory electron transport chain	1.7823E-05
regulation of leukocyte differentiation	1.53269E-05	mitochondrial respiratory chain complex assembly	1.7823E-05
small GTPase mediated signal transduction	1.62369E-05	cytoplasmic translation	1.7823E-05
regulation of lymphocyte differentiation	0.000191609	chromosome segregation	1.7823E-05
phagocytosis	0.000208359	aerobic electron transport chain	1.7823E-05
Ras protein signal transduction	0.00042009	centrosome cycle	1.7823E-05
regulation of T cell activation	0.000459684	regulation of cell cycle phase transition	3.057E-05
regulation of T cell differentiation	0.000473114	ATP synthesis coupled electron transport	3.057E-05
regulation of Ras protein signal transduction	0.000590993	mitochondrial ATP synthesis coupled electron transport	3.057E-05
regulation of hemopoiesis	0.000956326	nuclear chromosome segregation	3.60598E-05
leukocyte cell-cell adhesion	0.001066786	regulation of mitotic cell cycle phase transition	3.69705E-05
regulation of cell-cell adhesion	0.001093619	proton motive force-driven ATP synthesis	4.32535E-05
T cell differentiation	0.001392381	nuclear division	5.56522E-05
positive regulation of cell development	0.00256439	NADH dehydrogenase complex assembly	5.56522E-05
positive regulation of leukocyte differentiation	0.002835052	mitochondrial respiratory chain complex I assembly	5.56522E-05
positive regulation of hemopoiesis	0.002835052	rRNA processing	5.56522E-05
positive regulation of lymphocyte activation	0.003092451	oxidative phosphorylation	5.56522E-05
lymphocyte differentiation	0.003092451	microtubule-based transport	5.56522E-05
leukocyte migration	0.003092451	DNA replication	5.56522E-05
positive regulation of T cell activation	0.004305903	microtubule organizing center organization	5.79907E-05
positive regulation of cell activation	0.005163215	electron transport chain	5.86647E-05
protein insertion into ER membrane	0.005471551	purine ribonucleoside triphosphate biosynthetic process	6.06308E-05
positive regulation of leukocyte cell-cell adhesion	0.006597132	purine nucleoside triphosphate biosynthetic process	7.33176E-05
T cell proliferation	0.007144964	organelle fission	8.25129E-05
regulation of autophagy	0.007210373	ATP biosynthetic process	0.000140889
regulation of leukocyte cell-cell adhesion	0.007210373	mitochondrial electron transport, NADH to ubiquinone	0.000150369
positive regulation of lymphocyte differentiation	0.007210373	rRNA metabolic process	0.000150369
glycerolipid metabolic process	0.00730528	ribonucleoside triphosphate biosynthetic process	0.000181206
leukocyte proliferation	0.00730528	kinetochore organization	0.000181206
regulation of protein-containing complex assembly	0.00836294	nucleoside triphosphate biosynthetic process	0.000286222
leukocyte homeostasis	0.008453502	cilium organization	0.000286222
canonical NF-kappaB signal transduction	0.008560229	RNA splicing	0.000286222
positive regulation of leukocyte activation	0.008665596	proton motive force-driven mitochondrial ATP synthesis	0.00028967
positive regulation of JNK cascade	0.008989713	purine ribonucleoside triphosphate metabolic process	0.00033906
glycerolipid biosynthetic process	0.008989713	DNA recombination	0.00033906
regulation of pattern recognition receptor signaling pathway	0.008989713	cilium assembly	0.00033906
positive regulation of T cell differentiation	0.008989713	cellular respiration	0.000361836
positive regulation of cell-cell adhesion	0.009038891	ribosomal small subunit biogenesis	0.000454421
positive regulation of cell adhesion	0.012237866	ribosome biogenesis	0.000454421
regulation of leukocyte proliferation	0.012631294	double-strand break repair via homologous recombination	0.000454421
cellular component disassembly	0.012631294	double-strand break repair	0.000478712
monocyte differentiation	0.013306035	reproductive system development	0.000587266
phospholipid metabolic process	0.013809265	cytoskeleton-dependent intracellular transport	0.000670925
positive regulation of proteolysis	0.016033453	sister chromatid segregation	0.000670925
regulation of endocytosis	0.017014584	purine nucleoside triphosphate metabolic process	0.000676593
response to interleukin-4	0.017014584	mitotic nuclear division	0.000676593
regulation of canonical NF-kappaB signal transduction	0.017053053	reproductive structure development	0.000676593
lymphocyte homeostasis	0.019229811	transport along microtubule	0.000681754
actin filament organization	0.020025399	recombinational repair	0.00069403

Table E7. Top50 upregulated and downregulated DEGs in blood of patients with eCRSwNP versus neCRSwNP

Gene	Log2FoldChange	P value	Regulated	Gene	Log2FoldChange	P value	Regulated
SBSN	2.964538403	0.006291912	up	SLX1B	-2.231024018	0.000148481	down
KRT14	1.921180428	0.03536506	up	RNF17	-2.110917349	0.000164239	down
STAC	1.769364186	1.47E-06	up	TREML4	-1.733109944	0.000984434	down
PKP1	1.748719778	0.008101265	up	SLC44A5	-1.4060943	0.0126237	down
FGFR3	1.559525261	0.000416408	up	HIPK4	-1.092499072	0.024821249	down
HR	1.484166477	0.014182897	up	DCHS2	-1.04674148	0.030568054	down
CTHRC1	1.465511085	0.022020592	up	BNIP5	-1.036584463	0.029962667	down
ADAMTS12	1.426602912	0.01945588	up	LOC112268260	-1.003189558	0.010097309	down
ANTXR1	1.39695683	0.004453298	up	OR4F16	-0.953097623	0.010081839	down
AHNAK2	1.391496309	0.001224842	up	SDK1	-0.91549987	0.000118609	down
CCL23	1.354295037	3.69E-06	up	LEFTY2	-0.890047229	0.039646448	down
UGT2B11	1.348904621	0.002208725	up	TBC1D3K	-0.872552213	0.001486532	down
ISLR	1.29917977	0.02499843	up	CLCN1	-0.844256412	0.003527867	down
ALDH3B2	1.290401653	0.000949419	up	GRK7	-0.826953134	0.002485538	down
CLDN1	1.252146381	0.011441447	up	NPC1L1	-0.793063019	0.038452331	down
TBC1D3I	1.25145713	0.004160152	up	TBC1D3	-0.739575941	0.037667999	down
EGFR	1.246899798	0.008591962	up	NXPE2	-0.728239151	0.049561945	down
UBE2QL1	1.228974815	0.004272866	up	SERINC2	-0.692426118	0.003435874	down
CREB3L3	1.210134396	2.77E-05	up	ERFE	-0.672683505	0.032901932	down
TBC1D3H	1.210002423	0.025557571	up	LKAAEAR1	-0.670320194	0.032076396	down
TNNI3	1.209417297	0.01572989	up	CD300LD	-0.643890015	0.024467817	down
APOC1	1.195656181	0.035075037	up	ANOS1	-0.623052387	0.033712121	down
KRT8	1.182502359	0.000212975	up	SNAI1	-0.590959994	0.001011919	down
LONRF2	1.156580705	5.04E-06	up				
AMOTL2	1.150707283	0.00908452	up				
HRK	1.143874431	2.12E-07	up				
PRSS33	1.142129901	6.32E-08	up				
TFF3	1.125586919	7.59E-05	up				
MYH14	1.123447704	0.025934706	up				
VIP	1.118433374	0.039121368	up				
PROX1	1.11332087	0.002033778	up				
KRT17	1.107664605	0.043988908	up				
OLIG2	1.107417546	4.36E-07	up				
KRT15	1.082838206	0.040486461	up				
GREP1	1.060541033	0.02947834	up				
COL23A1	1.052487509	0.000371739	up				
GRIK4	1.049920303	0.008128624	up				
PMP22	1.04285723	7.88E-08	up				
IL34	1.042502037	3.58E-06	up				
DMKN	1.028000418	1.41E-05	up				
OSMR	1.017130038	0.032733126	up				
KIRREL1	1.008334714	0.029894745	up				
SMTNL1	1.00766323	0.040408084	up				
HOXA7	0.994364876	0.003482219	up				
SLIT3	0.989260361	0.005926037	up				
SIGLEC8	0.985043483	1.28E-06	up				
ARHGEF16	0.981296832	0.023136992	up				
GRID1	0.9797981	0.00228509	up				
CACNG6	0.97432538	2.76E-06	up				
TMEM54	0.972015964	0.011748555	up				

Table E8. Top50 upregulated and downregulated DEGs in whole peripheral blood of patients with CRSwNP with high blood eosinophils versus those with low blood eosinophil.

Gene	Log2FoldChange	P-value	Regulated	Gene	Log2FoldChange	P-value	Regulated
STAC	2.203673887	1.79E-09	up	PHYHIP	-4.113048497	0.000851868	down
LYPD1	2.183714597	5.42E-11	up	SBSN	-2.068124432	0.029136473	down
TNNI3	2.167539715	1.13E-05	up	KRT14	-1.68351784	0.035353142	down
UGT2B11	2.081513171	1.62E-06	up	PRSS50	-1.675855012	0.006894267	down
RASD2	2.069837118	0.028232987	up	GNG5P2	-1.334111727	0.000511932	down
CCL23	2.022419098	4.39E-14	up	MEDAG	-1.282381946	0.002542771	down
EPX	1.874339517	1.28E-06	up	SLC6A3	-1.254519594	0.011261293	down
GRID1	1.854684855	1.52E-09	up	VWA1	-1.111629789	0.033437045	down
IL34	1.823622054	2.23E-20	up	AMPH	-1.102211754	0.000419169	down
SYCP2L	1.762280785	3.63E-09	up	OLAH	-1.087942132	0.001104688	down
PRSS33	1.727801644	9.37E-21	up	EDNRB	-1.023788209	0.013024586	down
TFF3	1.722303164	1.94E-10	up	TEKT2	-1.007544418	0.002561894	down
OLIG2	1.704922462	4.90E-18	up	LEFTY2	-0.952470998	0.02677023	down
CREB3L3	1.647290466	4.65E-09	up	OIT3	-0.938848636	0.018375762	down
CDK15	1.606637501	2.37E-09	up	DRD3	-0.881230693	0.006453643	down
SIGLEC8	1.604815481	6.77E-20	up	SORBS2	-0.862545699	0.004082233	down
PRSS41	1.604052246	5.79E-16	up	SDK1	-0.86064346	0.000335505	down
CACNG6	1.553065935	1.11E-16	up	BTBD17	-0.859984583	0.018963365	down
SMPD3	1.552696795	4.62E-23	up	NTRK3	-0.840121513	0.048483035	down
ALOX15	1.538533882	4.30E-19	up	ANOS1	-0.815093737	0.004957118	down
PLAAT5	1.52094044	2.94E-16	up	VNN1	-0.789816461	2.07E-05	down
PAX2	1.501312424	0.000139477	up	CD300LD	-0.774522465	0.006729073	down
CLC	1.487092798	5.77E-21	up	CAPN11	-0.755619647	0.046362934	down
FOXI1	1.475362985	2.21E-05	up	A3GALT2	-0.74986669	0.002599356	down
GPR176	1.474885982	4.89E-09	up	HBG2	-0.746729467	0.010795991	down
PCDH17	1.470888081	0.002393493	up	SLC1A3	-0.741323223	0.001352293	down
UROC1	1.444218036	0.001097816	up	GIMAP5	-0.737653617	0.037218864	down
CYP7B1	1.408578667	2.91E-14	up	DNAI3	-0.723888957	0.03380858	down
TRPC6	1.378283723	7.45E-10	up	NOMO3	-0.70890046	0.001392944	down
IL5RA	1.37274771	2.19E-19	up	GALNT14	-0.704050089	0.000173981	down
CACNG8	1.363005642	1.68E-15	up	RETN	-0.69322912	0.006720779	down
SLC29A1	1.361867417	8.60E-24	up	HROB	-0.690543309	0.000418692	down
PMP22	1.355895618	2.43E-13	up	GSDMA	-0.689836277	0.017093945	down
AJAP1	1.321152186	9.17E-10	up	HCAR1	-0.685313807	0.043206861	down
SPATA9	1.317730806	4.08E-12	up	CDKL2	-0.662987467	0.00979478	down
MAGED4B	1.301382139	0.047485559	up	HP	-0.662157873	0.002270713	down
MEIS2	1.294673182	5.48E-08	up	ZNF334	-0.662091237	0.027437192	down
METTL21C	1.290253279	0.00725593	up	RBPMS2	-0.657358546	0.006187048	down
HRK	1.280002213	5.00E-09	up	MMP9	-0.65591262	0.000469485	down
ADORA3	1.279501247	1.38E-20	up	OSBPL6	-0.6358606	0.001538798	down
UBE2QL1	1.264160844	0.003886345	up	LEP	-0.633461196	0.018519773	down
PTGDR2	1.254097094	1.35E-19	up	TPST1	-0.62704747	0.000250291	down
CEBPE	1.246412903	1.75E-22	up	EFCAB1	-0.623230903	0.041421833	down
SPNS3	1.245291404	4.22E-27	up	ALOX5AP	-0.621613066	2.68E-05	down
SAG	1.233046217	0.003514198	up	KREMEN2	-0.615883351	0.018242649	down
CLDN1	1.187002174	0.012219211	up	CCL2	-0.615422332	0.042326641	down
FGFR2	1.181084748	8.45E-09	up	ORM1	-0.61362554	0.014538859	down
ADAMTS7	1.173908885	0.000845324	up	SERINC2	-0.609408506	0.011038271	down
IDO1	1.148511104	9.40E-13	up	SH3RF2	-0.604195221	0.009394635	down
HRH4	1.144467812	5.21E-14	up	RGS8	-0.593542291	0.031207079	down

Table E9. Top50 upregulated and downregulated DEGs and functions enriched in blood of CRSwNP patients with asthma versus without asthma.

Gene	Log2Fold-Change	P-value	Regulated	Gene	Log2Fold-Change	P-value	Regulated	Description	P.adjust
STAC	2.203673887	1.79E-09	up	PHYHIP	-4.113048497	0.000851868	down	negative regulation of cell projection organization	0.051536763
LYPD1	2.183714597	5.42E-11	up	SBSN	-2.068124432	0.029136473	down	chemotaxis	0.051536763
TNNI3	2.167539715	1.13E-05	up	KRT14	-1.68351784	0.035353142	down	taxis	0.051536763
UGT2B11	2.081513171	1.62E-06	up	PRSS50	-1.675855012	0.006894267	down	adenylate cyclase-modulating G protein-coupled receptor signaling pathway	0.099340866
RASD2	2.069837118	0.028232987	up	GNG5P2	-1.334111727	0.000511932	down	regulation of amyloid-beta clearance	0.099340866
CCL23	2.022419098	4.39E-14	up	MEDAG	-1.282381946	0.002542771	down	positive regulation of MAPK cascade	0.099340866
EPX	1.874339517	1.28E-06	up	SLC6A3	-1.254519594	0.011261293	down	negative regulation of neuron projection development	0.099340866
GRID1	1.854684855	1.52E-09	up	VWA1	-1.111629789	0.033437045	down	epithelial cell proliferation	0.099340866
IL34	1.823622054	2.23E-20	up	AMPH	-1.102211754	0.000419169	down	L-type voltage-gated calcium channel complex	0.011711358
SYCP2L	1.762280785	3.63E-09	up	OLAH	-1.087942132	0.001104688	down	collagen-containing extracellular matrix	0.012862949
PRSS33	1.727801644	9.37E-21	up	EDNRB	-1.023788209	0.013024586	down	T-tubule	0.023458703
TFF3	1.722303164	1.94E-10	up	TEKT2	-1.007544418	0.002561894	down	postsynaptic membrane	0.100180546
OLIG2	1.704922462	4.90E-18	up	LEFTY2	-0.952470998	0.02677023	down	collagen trimer	0.100180546
CREB3L3	1.647290466	4.65E-09	up	OIT3	-0.938848636	0.018375762	down	synaptic membrane	0.142030123
CDK15	1.606637501	2.37E-09	up	DRD3	-0.881230693	0.006453643	down	glutamatergic synapse	0.142030123
SIGLEC8	1.604815481	6.77E-20	up	SORBS2	-0.862545699	0.004082233	down	voltage-gated calcium channel complex	0.142030123
PRSS41	1.604052246	5.79E-16	up	SDK1	-0.86064346	0.000335505	down	very-low-density lipoprotein particle	0.144065525
CACNG6	1.553065935	1.11E-16	up	BTBD17	-0.859984583	0.018963365	down	triglyceride-rich plasma lipoprotein particle	0.144065525
SMPD3	1.552696795	4.62E-23	up	NTRK3	-0.840121513	0.048483035	down	complex of collagen trimers	0.144065525
ALOX15	1.538533882	4.30E-19	up	ANOS1	-0.815093737	0.004957118	down	postsynaptic specialization membrane	0.144065525
PLAAT5	1.52094044	2.94E-16	up	VNN1	-0.789816461	2.07E-05	down	endocytic vesicle lumen	0.15234996
PAX2	1.501312424	0.000139477	up	CD300LD	-0.774522465	0.006729073	down	icosanoid receptor activity	0.024151619
CLC	1.487092798	5.77E-21	up	CAPN11	-0.755619647	0.046362934	down	heparin binding	0.024151619
FOXI1	1.475362985	2.21E-05	up	A3GALT2	-0.74986669	0.002599356	down	extracellular matrix structural constituent conferring tensile strength	0.024151619
GPR176	1.474885982	4.89E-09	up	HBG2	-0.746729467	0.010795991	down	oxidoreductase activity, acting on single donors with incorporation of molecular oxygen, incorporation of two atoms of oxygen	0.037412064
PCDH17	1.470888081	0.002393493	up	SLC1A3	-0.741323223	0.001352293	down	oxidoreductase activity, acting on single donors with incorporation of molecular oxygen	0.037412064
UROC1	1.444218036	0.001097816	up	GIMAP5	-0.737653617	0.037218864	down	glycosaminoglycan binding	0.063482803
CYP7B1	1.408578667	2.91E-14	up	DNAI3	-0.723888957	0.03380858	down	calcium channel activity	0.073465234
TRPC6	1.378283723	7.45E-10	up	NOMO3	-0.70890046	0.001392944	down	prostaglandin receptor activity	0.073465234
IL5RA	1.37274771	2.19E-19	up	GALNT14	-0.704050089	0.000173981	down	prostanoid receptor activity	0.079458811
CACNG8	1.363005642	1.68E-15	up	RETN	-0.69322912	0.006720779	down	sulfur compound binding	0.082214538
SLC29A1	1.361867417	8.60E-24	up	HROB	-0.690543309	0.000418692	down	calcium ion transmembrane transporter activity	0.086952651
PMP22	1.355895618	2.43E-13	up	GSDMA	-0.689836277	0.017093945	down	calcium channel regulator activity	0.087101743
AJAP1	1.321152186	9.17E-10	up	HCAR1	-0.685313807	0.043206861	down	voltage-gated calcium channel activity	0.117595602
SPATA9	1.317730806	4.08E-12	up	CDKL2	-0.662987467	0.00979478	down	extracellular matrix structural constituent	0.117595602
MAGED4B	1.301382139	0.047485559	up	HP	-0.662157873	0.002270713	down	interstitial matrix	0.068800881
MEIS2	1.294673182	5.48E-08	up	ZNF334	-0.662091237	0.027437192	down	desmosome	0.12758322
MET-TL21C	1.290253279	0.00725593	up	RBPMS2	-0.657358546	0.006187048	down	postsynaptic density	0.12758322
HRK	1.280002213	5.00E-09	up	MMP9	-0.65591262	0.000469485	down	asymmetric synapse	0.12758322
ADORA3	1.279501247	1.38E-20	up	OSBPL6	-0.6358606	0.001538798	down	postsynaptic specialization	0.12758322
UBE2QL1	1.264160844	0.003886345	up	LEP	-0.633461196	0.018519773	down	neuron to neuron synapse	0.128335931
PTGDR2	1.254097094	1.35E-19	up	TPST1	-0.62704747	0.000250291	down		
CEBPE	1.246412903	1.75E-22	up	EFCAB1	-0.623230903	0.041421833	down		
SPNS3	1.245291404	4.22E-27	up	ALOX5AP	-0.621613066	2.68E-05	down		
SAG	1.233046217	0.003514198	up	KREMEN2	-0.615883351	0.018242649	down		

Gene	Log2Fold-Change	P-value	Regulated	Gene	Log2Fold-Change	P-value	Regulated	Description	P.adjust
CLDN1	1.187002174	0.012219211	up	CCL2	-0.615422332	0.042326641	down		
FGFR2	1.181084748	8.45E-09	up	ORM1	-0.61362554	0.014538859	down		
ADAMTS7	1.173908885	0.000845324	up	SERINC2	-0.609408506	0.011038271	down		
IDO1	1.148511104	9.40E-13	up	SH3RF2	-0.604195221	0.009394635	down		
HRH4	1.144467812	5.21E-14	up	RGS8	-0.593542291	0.031207079	down		

Table E10. Top 300 genes with highest correlation with blood eosinophil counts in patients with CRSwNP

Gene	Cor_results	Gene	Cor_results	Gene	Cor_results	Gene	Cor_results
OLIG2	0.730898435	RHOBTB3	0.54346479	ATP6V0A2	0.443397458	NUDT4	0.377893
SMPD3	0.724122289	ASRGL1	0.543029496	IL1RL1	0.441599103	HK3	0.377392
SPNS3	0.718959674	GATA1	0.542718546	KLHL13	0.441393086	MSRB3	0.376478
CLC	0.713449915	PNPLA6	0.542448551	OLFM2	0.440813444	ZNRF1	0.376066
SLC29A1	0.712495112	FAM124B	0.540526764	BAMBI	0.439660107	AUNIP	0.376004
PRSS33	0.707019143	TEC	0.540277658	CRACR2B	0.438445762	PAFAH2	0.374745
CEBPE	0.702512743	IDO1	0.539572767	HILPDA	0.437375592	CDK2AP1	0.373542
SIGLEC8	0.701835377	MINAR1	0.537786007	GRHL1	0.436950538	TBX1	0.373539
IL34	0.700094621	PMP22	0.536624823	HK2	0.43657315	UPP1	0.372223
ALOX15	0.698647968	OXER1	0.536572321	HRK	0.436505351	LSM14B	0.371101
TFF3	0.694286765	TNNT1	0.530966482	DOK2	0.435154948	NUDT17	0.371054
OLIG1	0.689389165	ACSF2	0.528796396	TMEM14C	0.435082531	ANXA1	0.370917
FRRS1	0.681518254	MEIS2	0.527590442	PLIN2	0.434700707	ARMH1	0.370909
IL5RA	0.676358589	SYCP2L	0.525965267	NR2F6	0.434394761	MGME1	0.369994
HSD3B7	0.673708775	CYP4F12	0.525351158	ANKRD55	0.431889053	SMAD5	0.366904
CAMK1	0.665641614	GRID1	0.523985682	NPFF	0.431765888	CNR1	0.365944
CACNG6	0.665457055	GIPR	0.521419295	DIXDC1	0.431142654	KCNMB3	0.365743
ACOT11	0.665226095	IQSEC2	0.520562327	PROCA1	0.430538014	KLHL6	0.363967
ADORA3	0.664829584	RIMKLA	0.518810783	RNASE3	0.430095481	CEP85	0.363582
LGALS12	0.662199591	KCTD15	0.518294139	PAX2	0.430015076	IER5	0.363362
PTGDR2	0.661512926	FBN1	0.515550125	FGFR2	0.429766124	UBE2QL1	0.363007
THBS4	0.648600037	PLEKHA7	0.511134672	PSTPIP2	0.429010372	SEPTIN11	0.361903
GPR82	0.641149315	ANKRD33B	0.508799677	FAAH	0.427935814	CCDC125	0.360685
CCL23	0.639995579	SCN4B	0.507827676	FBP1	0.423311828	SLC35D1	0.360507
SEMA7A	0.638451993	CSF1	0.507418989	LONRF2	0.422639499	ABCB10	0.360059
SPATA9	0.633272298	TEX30	0.506965688	BCAR1	0.420025506	GSTM4	0.360005
AJAP1	0.632873307	SAG	0.504944001	CD101	0.419543636	CD244	0.357513
SRGAP3	0.630402246	SLC16A14	0.504144632	ACACB	0.419530119	SWAP70	0.356058
HRH4	0.626710673	LFNG	0.502609218	GAPT	0.419200481	B9D1	0.355776
PIK3R6	0.626406434	CACFD1	0.499717149	CD200R1	0.418982486	TRERF1	0.355216
VSTM1	0.623068784	GFI1B	0.498934773	P2RY6	0.41869004	NOXO1	0.354776
P2RY14	0.622766228	LTC4S	0.495924526	CLINT1	0.416842203	AMPD3	0.353545
ABTB2	0.620319413	ALDH6A1	0.495759907	ARHGAP10	0.416113318	GOLGA8H	0.35336
CD9	0.620226113	PKP2	0.493424865	TENT5B	0.414766291	GPR137B	0.352978
HYAL3	0.620157755	PIP5K1B	0.493190517	FLVCR1	0.408670104	FES	0.352225
BACE2	0.610086755	BRI3BP	0.492413712	CHST13	0.408652984	ZNF597	0.351643
EPN2	0.60954485	CNKSR3	0.491381435	SPINT2	0.407485553	DHRS1	0.351641
PPP1R26	0.60904078	CCR3	0.490385166	GALNT6	0.405646059	CREB3L3	0.351024
EFNB2	0.608198542	NDFIP2	0.490315481	CTNS	0.404947272	MEX3B	0.350678

Gene	Cor_results	Gene	Cor_results	Gene	Cor_results	Gene	Cor_results
P2RX6	0.607720822	IGFBP6	0.488949793	UGT2B11	0.404354166	SERPINB2	0.349035
CYSLTR2	0.607322864	PLCD3	0.488339664	WEE1	0.404286904	VSIG10	0.348875
MFSD6L	0.604881605	TTC7B	0.487934214	ARSB	0.403373229	TMED3	0.348153
MYB	0.604767578	CACNA1D	0.486820068	GSTM2	0.402727187	CHKA	0.347967
PRSS41	0.60471866	SCGB3A1	0.484972803	ZSCAN29	0.401040041	F12	0.347901
CACNG8	0.604683961	ACSM3	0.48436717	HIC1	0.400738162	GPI	0.347564
ADGRE1	0.603779672	MGAT3	0.483248277	WNT5B	0.40062223	SNRNP25	0.347536
ZNRF3	0.602921465	CDK15	0.482625956	NRDE2	0.397817746	TNFRSF12A	0.347505
TNNI3	0.602664527	GPR176	0.477737403	C3AR1	0.397121062	MGAT4B	0.346231
DACH1	0.602339608	LYPD1	0.475673179	JAG1	0.396706002	CSRP1	0.34611
PLAAT5	0.596202024	ARL6IP6	0.473857698	SYNE1	0.396561691	CFD	0.345925
HES1	0.595504104	GPR34	0.473552228	PDLIM1	0.395289308	ENTPD5	0.344478
SLC7A8	0.592586944	CASP3	0.472074469	PAPSS1	0.394894899	WIPI1	0.343307
RAB44	0.590532429	EPAS1	0.471143165	PAQR7	0.394632856	GOLIM4	0.343278
CAT	0.590496036	LRRC17	0.470673709	AKR1C1	0.394509014	ID2	0.343141
KHDRBS3	0.589312531	MUC8	0.468992211	MARCKSL1	0.39370011	CAPNS2	0.343133
CYP7B1	0.587105237	MTFR1L	0.464267854	CLEC3B	0.392822266	ST14	0.341824
ZBTB42	0.586954154	SORD	0.463729899	SERF1B	0.39257485	SOCS2	0.341456
CD24	0.583625103	SIGLEC10	0.463250609	KLHL7	0.390325289	TSNAXIP1	0.341065
MYCT1	0.581975717	EPX	0.46079669	SRI	0.38812205	SMIM10L2A	0.340801
P2RY2	0.577473032	BIK	0.459879229	PRSS21	0.387517887	DENND2C	0.340576
ASB2	0.572168685	STAC	0.459780754	CHPT1	0.387361846	IL2RA	0.339808
RPS6KA2	0.56487739	SVOPL	0.458838829	KBTBD11	0.387042611	ARHGEF6	0.339201
FOXI1	0.562891813	EFCAB5	0.45805641	HES6	0.386980844	ATL1	0.339163
ADGRG5	0.562770659	TMEM38A	0.453643807	RNF144A	0.386845123	CENPU	0.338767
GFOD1	0.56269361	GPR132	0.453288403	SPNS2	0.386659643	ARMT1	0.33785
TRPC6	0.562120745	C9orf40	0.45321403	SNTB1	0.386465762	GALNT12	0.337418
TMEM273	0.560998795	VEGFA	0.452749212	ESYT1	0.386159417	ZDHHC2	0.337291
GADD45A	0.558873686	AOC1	0.451896013	SLC24A3	0.385013207	DAPK2	0.336777
CNR2	0.557429486	RNASE2	0.451704759	PPP2R5B	0.384252651	C16orf91	0.336588
PYROXD2	0.556467781	TMIGD3	0.450471733	PIM1	0.380905253	CCDC126	0.336559
CCDC170	0.555703525	KY	0.450007036	ZNF823	0.380453059	SLC4A8	0.336337
INPP1	0.551118457	CORO2A	0.447702068	LPCAT2	0.380365971	PTX3	0.33603
GADD45G	0.550082796	PROX1	0.447362416	ENPP2	0.379177266	DEPDC5	0.335602
VLDLR	0.549460621	PPARA	0.446873243	KSR1	0.379066365	PLD4	0.33551
EEF2K	0.54567285	TOX2	0.445661053	SCPEP1	0.377984756	PFKM	0.335392

Table E11. Genes associated with EOS based on IncNodePurity.

Gene	IncNodePurity	Gene	IncNodePurity	Gene	IncNodePurity	Gene	IncNodePurity
CLC	0.726336897	UPP1	0.032725603	CLEC3B	0.011768225	PIP5K1B	0.005354611
EFNB2	0.651024267	LTC4S	0.032092374	PRSS41	0.011733234	TOX2	0.005248372
SPNS3	0.526624607	DACH1	0.031291324	ENPP2	0.01159459	SYNE1	0.005240611
BCAR1	0.493550321	IDO1	0.031148552	CEP85	0.011390547	LONRF2	0.005128734
MYB	0.408789524	KHDRBS3	0.030697143	OXER1	0.011208686	LPCAT2	0.005121347
PRSS33	0.364990243	MYCT1	0.030126695	DIXDC1	0.011189563	EEF2K	0.005086297
FLVCR1	0.357770871	ADGRE1	0.028756902	CRACR2B	0.0105353	GALNT12	0.00504686
ADORA3	0.355348872	CNKSR3	0.028237746	KCNMB3	0.010433888	CCDC170	0.004965198
CCL23	0.291332983	HYAL3	0.027772253	KLHL13	0.010345739	CACNG8	0.004920521
CEBPE	0.286531353	HIC1	0.027138106	SCPEP1	0.010258448	ZNF597	0.004867089
TMEM14C	0.267587083	SRI	0.027120948	TMED3	0.010197398	GFI1B	0.004855183
SLC7A8	0.249522226	CD9	0.026719958	NPFF	0.01016502	DHRS1	0.004752223

Gene	IncNodePurity	Gene	IncNodePurity	Gene	IncNodePurity	Gene	IncNodePurity
SCN4B	0.236513602	CFD	0.026630463	PKP2	0.010086604	RNASE2	0.004720218
SMPD3	0.205212674	P2RY14	0.026480229	ABCB10	0.009952723	ARL6IP6	0.004649356
CACNG6	0.198887324	HES6	0.025278992	GSTM2	0.009788477	LRRC17	0.004511924
SIGLEC8	0.191880907	BAMBI	0.024964799	ZNRF3	0.009751261	SWAP70	0.004428139
THBS4	0.170806554	OLIG1	0.02494087	PAQR7	0.009732415	ST14	0.00440673
AJAP1	0.167965636	TSNAXIP1	0.024797573	GIPR	0.009338934	PDLIM1	0.004398221
ALOX15	0.165110115	BIK	0.02371665	P2RX6	0.009259452	P2RY6	0.004376543
B9D1	0.155202706	TNNT1	0.022614163	CAT	0.009207529	GOLIM4	0.004329325
IL5RA	0.15374328	GRID1	0.02258019	HK2	0.009164932	ENTPD5	0.00430519
TFF3	0.152304017	VLDLR	0.021640473	CDK15	0.008982042	MTFR1L	0.004300748
GADD45G	0.147243576	PYROXD2	0.021197288	UGT2B11	0.008962046	AMPD3	0.004210409
SLC29A1	0.144987612	SNTB1	0.020876535	RNF144A	0.008703543	CASP3	0.004116423
HSD3B7	0.140673378	TMEM273	0.019654185	TMIGD3	0.008692962	ACACB	0.004070906
GADD45A	0.12663817	MUC8	0.019320365	FES	0.008587118	NRDE2	0.003893522
SPATA9	0.125751605	CACFD1	0.019122672	PLCD3	0.008499513	PROCA1	0.003877402
CHPT1	0.120017356	CHST13	0.019085435	GAPT	0.008462988	WNT5B	0.003844174
INPP1	0.116959004	MFSD6L	0.018720318	TNFRSF12A	0.008299333	FAAH	0.003838765
FRRS1	0.115290775	MEIS2	0.018689967	ATL1	0.008198483	KCTD15	0.003786805
SRGAP3	0.109016968	PMP22	0.01847481	CSF1	0.008119941	EPAS1	0.003740569
CNR1	0.103186572	MGAT3	0.018116453	FAM124B	0.007998173	PAFAH2	0.003708906
EFCAB5	0.0998098	DOK2	0.018097081	SVOPL	0.007958512	NDFIP2	0.003707801
GATA1	0.099027699	NOXO1	0.017214449	SPNS2	0.007931726	BRI3BP	0.003684652
RNASE3	0.096475486	PROX1	0.017181185	CLINT1	0.007921541	UBE2QL1	0.003564969
MINAR1	0.086747211	TEX30	0.017027653	RAB44	0.00783381	PIM1	0.003543923
IL34	0.079684137	CD101	0.016857064	ANKRD33B	0.007775426	JAG1	0.003510057
CYP7B1	0.076635961	LYPD1	0.016339465	GPR137B	0.007705846	MGAT4B	0.003484621
TRPC6	0.075904633	ZNF823	0.015823555	SYCP2L	0.007550568	SMIM10L2A	0.003463269
IGFBP6	0.071475814	MGME1	0.015773631	ARMH1	0.007545405	LSM14B	0.003416749
SCGB3A1	0.070129146	C3AR1	0.0156363	SERPINB2	0.007523655	ESYT1	0.003349933
GPR82	0.068776282	PTX3	0.01556829	KY	0.007490872	CHKA	0.003235185
EPX	0.064649978	PNPLA6	0.015329495	ALDH6A1	0.007460132	CORO2A	0.003182021
P2RY2	0.06259099	SOCS2	0.01531233	SIGLEC10	0.007364967	ASRGL1	0.003076834
CAMK1	0.062147527	CREB3L3	0.015295438	MEX3B	0.007132042	ANXA1	0.002927871
NR2F6	0.062024749	STAC	0.0149834	PLD4	0.007087075	SPINT2	0.002898366
VSTM1	0.060217051	SNRNP25	0.014890216	ZSCAN29	0.007037526	C16orf91	0.002776992
ABTB2	0.059099401	AOC1	0.014789333	CCR3	0.00694402	PPARA	0.002721685
OLIG2	0.058714072	PRSS21	0.014773867	RPS6KA2	0.006932049	TTC7B	0.002637199
ACOT11	0.057318278	HES1	0.01471796	GOLGA8H	0.006931165	PLEKHA7	0.002635971
HRH4	0.054222905	ZDHHC2	0.014698286	ZNRF1	0.006852084	WIPI1	0.002475854
PPP2R5B	0.052347323	CACNA1D	0.014546703	DEPDC5	0.006836099	SEPTIN11	0.002449613
TNNI3	0.050513069	AUNIP	0.014400378	TMEM38A	0.006783117	VEGFA	0.002304748
PLAAT5	0.050025487	C9orf40	0.014238667	MSRB3	0.006692198	ATP6V0A2	0.002277832
IQSEC2	0.048256245	CCDC125	0.014111194	SLC4A8	0.006542731	IL2RA	0.002247477
PTGDR2	0.047418089	SLC24A3	0.014001559	ASB2	0.006502793	CD200R1	0.002245196
FOXI1	0.046313006	CDK2AP1	0.013916684	CYSLTR2	0.006474297	NUDT4	0.002193464
FBN1	0.044172667	MARCKSL1	0.013787469	ANKRD55	0.006469829	NUDT17	0.00208608
LGALS12	0.043557592	PAX2	0.013770401	ID2	0.006429215	HILPDA	0.002081808
FGFR2	0.043295913	SERF1B	0.013714873	CTNS	0.006144466	ARSB	0.002041093
CD24	0.042811348	GPR34	0.013682801	DAPK2	0.006133425	KBTBD11	0.001992719
SEMA7A	0.042149382	DENND2C	0.013375977	ACSF2	0.005948363	TEC	0.00199064
SLC16A14	0.041813312	CAPNS2	0.013341715	FBP1	0.005898034	SORD	0.001916186
GFOD1	0.039538721	TENT5B	0.013190927	PLIN2	0.00578496	PPP1R26	0.001734772
EPN2	0.03898665	ARMT1	0.013068375	ACSM3	0.005783046	CSRP1	0.001705107

Gene	IncNodePurity	Gene	IncNodePurity	Gene	IncNodePurity	Gene	IncNodePurity
ARHGAP10	0.038237117	CD244	0.012947184	PIK3R6	0.005768709	LFNG	0.001661597
RHOBTB3	0.037423141	CYP4F12	0.012897577	IER5	0.005697665	TRERF1	0.001654408
TBX1	0.037415797	GPI	0.012699519	ZBTB42	0.005685221	KLHL6	0.001510763
GSTM4	0.036463491	F12	0.01245985	PAPSS1	0.005569377	KLHL7	0.00146032
HRK	0.036194202	OLFM2	0.012426006	PSTPIP2	0.00552704	WEE1	0.001211703
CENPU	0.03571867	CCDC126	0.012347381	GRHL1	0.005498667	SMAD5	0.001147942
ADGRG5	0.033733852	HK3	0.012195567	AKR1C1	0.005470423	SLC35D1	0.000963986
BACE2	0.033475989	SAG	0.011960516	IL1RL1	0.005443456	CNR2	0.000963918
GPR176	0.032800143	VSIG10	0.011862931	ARHGEF6	0.005390276	KSR1	0.000886284
RIMKLA	0.032783298	GALNT6	0.011823796	PFKM	0.005360025	GPR132	0.000651687

Table E12. Top50 upregulated and downregulated DEGs in whole peripheral blood of patients with CRSwNP in Cluster 1 vs Cluster 2

Gene	Log2FoldChange	P-value	Regulated	Gene	Log2FoldChange	P-value	Regulated
STAC	3.142745611	1.44E-08	up	PHYHIP	-5.90366	0.001143	down
EPX	2.568520791	7.12E-10	up	KRT14	-2.56208	0.046549	down
CCL23	2.17324305	4.39E-10	up	MUC5AC	-1.85767	0.009901	down
CCDC144A	2.138014414	0.0107922	up	CST1	-1.80505	0.014357	down
C4BPA	2.116974052	3.81E-05	up	IGFBP5	-1.59798	0.017279	down
UGT2B11	2.040552084	6.74E-05	up	PIGR	-1.57639	0.006323	down
IL34	1.99095464	5.50E-19	up	SHISA7	-1.51795	2.21E-06	down
EIF3CL	1.973552651	5.82E-08	up	ERFE	-1.49777	0.000738	down
OLIG2	1.810465586	2.96E-17	up	FDCSP	-1.46432	0.033029	down
PRSS41	1.771294129	3.26E-14	up	IQSEC3	-1.40975	0.00177	down
COL12A1	1.746301802	0.01227161	up	SFRP2	-1.3625	7.44E-06	down
LONRF2	1.716188617	2.21E-09	up	ACHE	-1.35655	0.000326	down
CDK15	1.684240085	2.40E-08	up	ALAS2	-1.3386	0.000133	down
IL1RL1	1.682632029	3.36E-18	up	HBA2	-1.32693	3.38E-07	down
SIGLEC8	1.67613064	1.07E-16	up	CPE	-1.31159	0.00522	down
SMPD3	1.620086751	5.11E-19	up	CXCL17	-1.30576	0.048796	down
PLAAT5	1.59881555	2.45E-14	up	HBQ1	-1.30209	2.54E-07	down
ALOX15	1.597735717	8.75E-17	up	ASS1	-1.29427	0.003785	down
UBE2QL1	1.572423636	0.006538964	up	RUNDC3A	-1.23837	1.45E-07	down
SPATA9	1.557411323	1.67E-11	up	TBC1D3C	-1.22314	0.019706	down
IL5RA	1.535159566	6.56E-17	up	IGF2	-1.21783	0.000568	down
CACNG8	1.530662933	8.74E-14	up	RAB3IL1	-1.20385	9.85E-06	down
SYCP2L	1.528763779	0.000100486	up	ESPN	-1.20357	2.29E-05	down
PRSS33	1.527323279	1.06E-11	up	SORBS2	-1.20304	0.003072	down
HRH4	1.520628469	2.21E-15	up	SPARCL1	-1.19658	0.027376	down
CLC	1.49739186	2.38E-13	up	WFDC2	-1.19475	0.02406	down
MEIS2	1.48880409	9.50E-07	up	F3	-1.17334	0.010729	down
HRK	1.48595248	6.37E-08	up	OR2T8	-1.1573	0.006054	down
CACNG6	1.476560838	8.67E-10	up	SLC6A9	-1.13874	6.06E-05	down
VAMP7	1.44710107	8.07E-06	up	SELENBP1	-1.13501	8.70E-05	down
TRPC6	1.42815895	2.76E-06	up	HBA1	-1.11997	5.97E-05	down
PMP22	1.420127341	5.34E-09	up	PKP3	-1.11031	0.036319	down
CYP7B1	1.400579776	8.13E-10	up	AQP1	-1.10828	4.52E-06	down
FGFR2	1.385607821	2.51E-08	up	LOC107986860	-1.10479	0.016869	down
IL3RA	1.383826787	0.000618403	up	ACKR1	-1.08336	0.000251	down
SLC29A1	1.328105607	2.55E-14	up	PDZK1IP1	-1.08301	4.15E-05	down
IDO1	1.309796531	1.29E-11	up	GMPR	-1.08292	5.55E-06	down
GRID1	1.307672699	0.000539205	up	CCDC3	-1.07815	0.003287	down

Gene	Log2FoldChange	P-value	Regulated	Gene	Log2FoldChange	P-value	Regulated
MYCT1	1.301095521	1.65E-08	up	CA1	-1.07233	0.000816	down
PTGDR2	1.258315014	2.89E-12	up	THEM5	-1.05826	0.002223	down
RAB44	1.252507862	1.74E-20	up	CNN1	-1.05599	0.031277	down
CA8	1.239181207	1.49E-06	up	CHAC1	-1.04753	0.005876	down
TFF3	1.237337731	0.000149197	up	RNASE1	-1.0412	0.002114	down
OR2I1P	1.215689189	0.016421734	up	GCAT	-1.036	5.51E-05	down
EFNB2	1.19793576	5.13E-07	up	SLC25A39	-1.03099	1.78E-06	down
ADORA3	1.189242784	2.35E-10	up	WNK2	-1.02645	0.000296	down
RNASE3	1.17953411	3.29E-05	up	IGFBP2	-1.02554	0.007431	down
CREB3L3	1.171003472	0.000436827	up	EPB42	-1.01502	0.000132	down
ACOT11	1.165146319	2.23E-12	up	KLF1	-1.01377	0.000109	down
FRRS1	1.156198747	1.44E-14	up	H2AC17	-1.01032	0.017198	down

Table E13. Top50 upregulated and downregulated DEGs in whole peripheral blood of patients with CRSwNP in Cluster 1 vs Cluster 3

Gene	Log2FoldChange	P-value	Regulated	Gene	Log2FoldChange	P-value	Regulated
STAC	2.595292526	1.96E-09	up	TUBB8B	1.635362079	-3.558443504	down
RASD2	2.09232039	0.030687817	up	FOLR1	2.456635054	-3.079079775	down
UGT2B11	1.943061059	2.84E-05	up	DSC3	1.026104336	-2.434388321	down
EPX	1.89965055	1.92E-06	up	C6orf58	3.195692183	-2.290665061	down
CCL23	1.851671398	8.22E-10	up	PRSS50	1.746964048	-1.967886724	down
FERMT1	1.758090591	3.79E-05	up	ADH1C	1.680852361	-1.866218858	down
METTL21C	1.757366085	0.001302924	up	EDNRB	2.643941778	-1.813040049	down
OLIG2	1.712302332	1.44E-14	up	CST1	6.929663656	-1.760052446	down
CDK15	1.684259902	4.65E-09	up	PKP1	1.095379907	-1.682907477	down
ALDH3B2	1.663330028	5.44E-05	up	STATH	67.71666283	-1.672657504	down
UBE2QL1	1.620767479	0.001077696	up	MUC5AC	10.1698647	-1.656879104	down
TEX52	1.545397232	0.011074945	up	ODAM	2.20616924	-1.641716413	down
TNNI3	1.543823893	0.005316521	up	LOC105373989	2.494964708	-1.575542754	down
MRAP	1.53641989	0.013771665	up	OLAH	12.49863529	-1.565902736	down
IL34	1.523125268	1.12E-12	up	CD177	706.1851931	-1.522368654	down
PRSS33	1.506540915	3.17E-11	up	TP53TG3D	1.769996793	-1.504902669	down
SMPD3	1.497396768	3.60E-16	up	TRIM29	2.41874866	-1.471433851	down
PRSS41	1.490539442	6.88E-13	up	IGFBP5	10.86146282	-1.465403972	down
SIGLEC8	1.480280036	5.72E-13	up	TMPRSS11E	1.454965239	-1.455252044	down
CACNG6	1.479200881	7.38E-12	up	TBC1D3H	2.930083909	-1.430508771	down
NPPA	1.467371697	0.010412569	up	ORM1	383.3258517	-1.428361439	down
PCDH17	1.461402576	0.005719445	up	TMEM92	12.69147908	-1.409427343	down
FREM1	1.435811284	0.007620566	up	PGA5	2.771283713	-1.399958374	down
TFF3	1.428757593	6.00E-06	up	FOXB1	1.792237079	-1.388331572	down
ALOX15	1.425248148	3.53E-13	up	SCRG1	3.485188258	-1.378618594	down
PMP22	1.36469597	3.70E-11	up	GSDMC	3.715268606	-1.336591827	down
LOC107986217	1.363292211	0.003687216	up	PRL	1.580593396	-1.310636992	down
TLCD5	1.341386632	0.001008453	up	MPV17L	4.68715281	-1.295889959	down
RNASE3	1.327045614	8.70E-07	up	PRUNE2	53.51980456	-1.292871445	down
ATP6V1C2	1.316765662	0.005768902	up	SLC2A14	84.53490762	-1.288129188	down
CLC	1.316082164	1.28E-11	up	MMP9	4892.10052	-1.273714352	down
BOLA2B	1.314180285	0.001932502	up	GNG5P2	4.667775758	-1.272758313	down
AJAP1	1.30460181	3.94E-07	up	ASS1	4.701653873	-1.265606535	down
FANCD2OS	1.301875603	0.019783109	up	SHROOM2	3.457609887	-1.236801691	down
SLC29A1	1.300175328	3.86E-15	up	ALDH3A1	2.358193753	-1.218534548	down
HRK	1.295688277	6.39E-07	up	INHBB	31.01908841	-1.195693394	down

Gene	Log2FoldChange	P-value	Regulated	Gene	Log2FoldChange	P-value	Regulated
SPATA9	1.29402749	2.33E-11	up	CBS	28.95946829	-1.19375273	down
SAG	1.292622054	0.004216049	up	BMX	194.6180235	-1.191889257	down
IL5RA	1.292075159	9.85E-14	up	ANOS1	5.019150809	-1.188276665	down
CYP7B1	1.28855638	1.80E-09	up	EFCAB1	5.908114674	-1.174953627	down
TRPC6	1.284129507	1.98E-07	up	GALNT14	159.3038037	-1.174469266	down
CACNG8	1.267077167	1.66E-10	up	ADAMTS2	11.22129065	-1.155226751	down
UROC1	1.266073676	0.007013263	up	MADCAM1	36.46162192	-1.150150602	down
PLAAT5	1.260322095	8.91E-09	up	NFASC	1.897004049	-1.148475234	down
CERKL	1.259297372	0.00891778	up	UPK1A	1.603713028	-1.14071089	down
SMTNL1	1.253949453	0.028610111	up	CDO1	6.180236991	-1.127175131	down
CCDC39	1.245221964	0.011316063	up	SULT1A2	58.73957581	-1.115637734	down
MUC8	1.242291511	9.85E-11	up	C2orf66	2.011494906	-1.097313621	down
PROX1	1.240775533	0.002680285	up	NTRK3	1.948051882	-1.096312164	down
FAM166A	1.233115289	0.009282548	up	OTX1	127.5641728	-1.087593469	down

Table E14. Top50 upregulated and downregulated DEGs in whole peripheral blood of patients with CRSwNP in Cluster 3 vs Cluster 2.

Gene	Log2FoldChange	P-value	Regulated	Gene	Log2FoldChange	P-value	Regulated
FOLR1	2.863661944	0.002403823	up	PHYHIP	4.748293723	-4.821599129	down
NXF3	2.160582823	0.000275889	up	SLX1B	2.318265586	-2.633851553	down
C4BPA	1.980440134	0.000100074	up	FAM166A	4.889407671	-1.717919299	down
OLAH	1.693428057	8.88E-05	up	PKP3	3.786875164	-1.640509392	down
GALNT8	1.647754725	0.000576402	up	LAD1	2.66942583	-1.584472918	down
GSDMC	1.640290768	0.00010253	up	UPK2	2.523146248	-1.535350111	down
IL3RA	1.624016187	0.0002358	up	HAP1	2.346391864	-1.53103046	down
CNTNAP3B	1.444222789	0.00062135	up	TLX2	2.190938756	-1.523082139	down
VNN1	1.426381121	3.00E-10	up	TEX52	2.063590225	-1.521202084	down
SCRG1	1.40692931	0.00186135	up	GLT8D2	2.129523557	-1.517998466	down
PTGFR	1.335813599	0.008077726	up	SLC7A4	2.002630061	-1.497855291	down
ATP2C2	1.332430563	0.000151944	up	C22orf23	4.008895834	-1.435335996	down
PRUNE2	1.266809076	0.000117696	up	LOC107986217	6.246792631	-1.41542767	down
C10orf82	1.261753788	0.007091917	up	DNAAF3	3.758156987	-1.370895667	down
FAM228A	1.260003033	0.000323428	up	AANAT	3.903406662	-1.366539651	down
CD300LD	1.24527056	0.000618814	up	CLDN22	2.167116419	-1.355941317	down
OR6K3	1.240289763	0.01379962	up	ERFE	12.03702792	-1.306863773	down
CSMD1	1.203316381	0.028440041	up	ACHE	15.10358809	-1.293697691	down
SLC22A14	1.202181764	8.03E-05	up	LOC107985556	3.966113397	-1.286423139	down
RUNDC3B	1.197297586	0.010260962	up	SPRN	5.649057244	-1.283249555	down
LURAP1L	1.141500231	0.009528435	up	RAP1GAP	56.60950532	-1.271917625	down
PLSCR4	1.126457759	0.01920301	up	EPHA10	2.290387934	-1.269839478	down
FGF13	1.10568596	0.000218966	up	VSTM2B	12.66599073	-1.267000423	down
RYR3	1.086126306	0.007148359	up	DBH	2.837453854	-1.24298393	down
OOSP3	1.077270484	0.000972673	up	ALAS2	17336.37758	-1.241409404	down
TMTC1	1.060906722	0.001640216	up	SPDYE2B	2.367813919	-1.235888433	down
TRIM9	1.051067803	4.45E-09	up	FIBCD1	4.095561423	-1.234982659	down
ZNF608	1.045981738	7.20E-08	up	HBA2	820536.6982	-1.234553818	down
TBC1D3E	1.045297045	0.000219723	up	MICOS10-NBL1	3.179404225	-1.226354532	down
GALNT14	1.042489362	6.73E-07	up	ALX3	2.878909563	-1.225741388	down
ALDH1A2	1.016254222	0.00077313	up	SELENBP1	1835.878363	-1.184676149	down
KL	1.012958769	2.24E-05	up	LOC107986860	4.329065354	-1.183153017	down
NAIP	0.989360349	4.30E-12	up	ESPN	552.0752348	-1.167216334	down
DNER	0.987782549	0.046644942	up	RPL3L	10.19751191	-1.158676469	down
MAB21L3	0.985573964	1.11E-05	up	TRARG1	3.788675906	-1.140882438	down

Gene	Log2FoldChange	P-value	Regulated	Gene	Log2FoldChange	P-value	Regulated
EREG	0.985339026	0.000517338	up	PCDHGB6	6.999832462	-1.138069647	down
CNTNAP3	0.983427408	1.15E-05	up	MAFA	5.490807889	-1.137061886	down
SLC26A8	0.981870219	1.61E-08	up	CCDC74A	3.92532056	-1.133320644	down
INHBB	0.980896168	0.000135169	up	IFI27	81.3436905	-1.132573576	down
VAMP7	0.97890521	0.001189697	up	CABP7	8.302535706	-1.125089556	down
DSC2	0.968986224	1.56E-09	up	CFAP157	12.59172673	-1.124160389	down
XKR3	0.968391267	0.020577744	up	NACAD	6.302608512	-1.123197362	down
CTTNBP2	0.967299095	0.005740506	up	SPATA21	95.05599611	-1.121307204	down
NIPAL1	0.965042033	0.011702809	up	CGREF1	2.216160385	-1.12105494	down
NECTIN2	0.960692887	8.40E-05	up	KRT1	364.0342998	-1.119431703	down
CNTNAP3C	0.955794451	0.004487803	up	OR2T8	5.153469912	-1.113072085	down
FBN2	0.948824706	7.63E-10	up	LIM2	15.74965787	-1.110793401	down
CASP5	0.944427151	2.60E-06	up	TEDC2	5.988199712	-1.102467089	down
CXCL6	0.943502731	0.000189398	up	KIF7	9.297188308	-1.093351711	down
NMNAT2	0.931819194	0.004788654	up	KRT74	3.015603833	-1.087378959	down

Table E15. Top50 upregulated and downregulated DEGs in nasal polyp tissues of patients in Cluster 1 versus those in Cluster 2.

Gene	Log2FoldChange	P-value	Regulated	Gene	Log2FoldChange	P-value	Regulated
CLCA1	5.192050322	2.16E-08	up	BRINP3	-5.953472426	0.001144138	down
SBSN	4.723562655	0.000132574	up	DMP1	-5.235103054	0.043685725	down
CCL18	4.698087826	2.17E-09	up	IBSP	-5.124716563	0.015484573	down
GPR42	4.606411167	2.16E-08	up	MRGPRX3	-4.563388231	0.000358234	down
SPRR2E	4.384205284	0.012239853	up	NXPH2	-4.207495484	2.37E-05	down
IGHG4	4.307083903	1.34E-06	up	MEPE	-4.204548356	0.027225199	down
IGHE	4.15626559	9.45E-06	up	LDHC	-3.896473365	0.00016454	down
RBP4	4.050176542	3.10E-06	up	RSPO2	-3.816308482	0.000993739	down
IGHV3-43	3.982846621	1.18E-07	up	C22orf42	-3.675968599	0.002464812	down
PGA3	3.973964003	0.000493821	up	PCDHA6	-3.655023193	6.55E-09	down
PRB4	3.880929695	1.78E-05	up	SLC22A8	-3.626233551	0.000214614	down
FFAR3	3.861163935	1.72E-08	up	SYT5	-3.396302016	0.000112771	down
IGHEP1	3.795910538	1.58E-06	up	NPY	-3.377266672	0.002763749	down
SPRR2D	3.75709893	0.016267245	up	SPADH	-3.33070209	0.00755911	down
IGLVI-70	3.750024464	2.10E-06	up	MDGA2	-3.204862849	0.00184351	down
MYOC	3.669040626	0.000100092	up	LOC105377188	-3.075184732	0.020118284	down
LINC02802	3.580480865	0.001368738	up	NPAS4	-3.049166759	1.79E-10	down
LOC107985200	3.580480865	0.001368738	up	TEX55	-2.957590697	0.000136362	down
PRB3	3.575604007	0.000900051	up	ARPP21	-2.826444629	1.33E-05	down
IL13	3.568260509	1.37E-05	up	LINC02461	-2.822596083	4.48E-05	down
CST4	3.558545048	0.000264642	up	LOC124907878	-2.809036028	0.001956603	down
ITLN2	3.516252422	8.84E-05	up	CGA	-2.721989883	0.042094495	down
ITLN1	3.431420482	0.000475693	up	OPRK1	-2.714747662	0.001509568	down
IGHV4-39	3.400506515	2.44E-09	up	LINC01695	-2.708835893	0.001846445	down
RPL18P9	3.353104199	9.17E-05	up	IL20	-2.694440754	0.038203059	down
CAPN14	3.260710228	3.69E-08	up	KCNB2	-2.644766928	5.49E-05	down
VGF	3.180294699	0.005941269	up	PLAC4	-2.607329307	1.20E-07	down
PCAT2	3.137570815	3.28E-08	up	MAS1	-2.558932127	0.004553436	down
LINC01303	3.136938293	6.91E-07	up	LINC03025	-2.510503545	0.0076839	down
IL5	3.1076877	2.49E-05	up	DKK4	-2.50518436	4.80E-05	down
GNG13	3.093819548	6.23E-06	up	SLC17A8	-2.499573788	0.000135697	down
HTR3E	3.087501528	0.000370875	up	TNMD	-2.493957506	0.00090382	down
CEBPE	3.082402704	0.000143623	up	B3GALT1	-2.476756383	1.17E-05	down
SH2D6	3.077179983	3.66E-06	up	CEACAM7	-2.455107361	5.32E-05	down

Gene	Log2FoldChange	P-value	Regulated	Gene	Log2FoldChange	P-value	Regulated
LINC02072	3.061956632	9.18E-07	up	DES	-2.450868538	0.002455069	down
LINC02073	3.061956632	9.18E-07	up	LINC02257	-2.448332715	0.005176468	down
TERB2	3.051220304	0.004348284	up	CADM3	-2.440570217	8.93E-06	down
SAG	3.016000938	2.66E-06	up	GRIK1	-2.439380154	1.64E-06	down
COL6A5	2.992734368	0.006150386	up	PDZRN4	-2.41216871	2.13E-05	down
LOC100422190	2.991278009	0.00058585	up	LOC124904294	-2.403431924	0.00142054	down
TAC1	2.98954052	0.019214086	up	NELL1	-2.359077577	0.000974467	down
IGKV1-27	2.964750653	1.15E-05	up	PPDPFL	-2.317803674	0.001185835	down
CHAT	2.941764743	0.000393742	up	XKR4	-2.294071619	0.000608639	down
KCNJ16	2.932810092	3.14E-05	up	MYH6	-2.291032237	0.009065893	down
KRT1	2.92603089	4.02E-05	up	NOX5	-2.288162068	0.004620803	down
VSTM1	2.885208207	0.000771071	up	LINC00112	-2.283789244	0.012663002	down
LIPN	2.883926463	1.05E-06	up	KCNIP1	-2.273680009	4.99E-07	down
LOC105377267	2.877651769	0.006786049	up	CDH10	-2.260533992	0.000265759	down
RHOXF1P1	2.876544041	0.000170221	up	B4GALNT2	-2.221498453	0.009659726	down
RPS27AP11	2.872290446	0.003188692	up	TMT1B	-2.220652811	0.001833492	down

Table E16. Top50 upregulated and downregulated DEGs in nasal polyp tissues of patients in Cluster 1 versus those in Cluster 3.

Gene	Log2FoldChange	P-value	Regulated	Gene	Log2FoldChange	P-value	Regulated
HTR3C	6.983116991	3.08E-13	up	BRINP3	-4.804391745	0.002967054	down
CLCA1	6.916175989	4.39E-12	up	ACOD1	-4.467765897	0.003153759	down
FETUB	6.142093235	9.56E-07	up	RSPO2	-4.136460402	0.000477363	down
IGHE	6.053160797	2.46E-13	up	LGALS17A	-3.870541328	0.00033729	down
UGT2B11	6.001238701	1.12E-13	up	PON1	-3.617650744	0.002173897	down
CCL18	5.868440955	4.98E-17	up	NXPH2	-3.582928365	1.14E-07	down
COL6A5	5.754880007	1.73E-10	up	NHLH2	-3.538378225	0.000138863	down
LOC105377267	5.4267936	2.73E-11	up	NR0B1	-3.451074429	7.89E-05	down
OLIG2	5.277944301	5.67E-07	up	NPY	-3.417896428	0.000277487	down
HRH4	5.114368053	9.86E-14	up	KCNB2	-3.343569832	7.52E-07	down
VSTM1	4.998447834	1.78E-10	up	GRM5	-3.340435334	0.002432446	down
LOC100422190	4.876320888	7.50E-08	up	OR2M4	-3.331382166	0.003798005	down
LEFTY2	4.711825477	3.56E-09	up	LOC100129844	-3.277188582	0.002937706	down
PTGDR2	4.70402332	1.09E-11	up	AOX3P	-3.271616409	0.000439282	down
OLIG1	4.67433599	2.06E-09	up	FGF13-AS1	-3.246991327	0.01357579	down
AHSG	4.611368752	2.15E-06	up	MDGA2	-3.220096728	0.000578304	down
HTR3E	4.569121237	1.48E-05	up	LINC02461	-3.210830681	2.55E-06	down
CHAT	4.529814199	8.52E-08	up	GRIK1	-3.17815223	2.40E-10	down
KCNJ16	4.497824007	2.08E-15	up	ANXA10	-3.173152192	0.004413244	down
IGHG4	4.478765684	5.79E-07	up	SCN1A	-3.144098695	0.002773338	down
LOC100422022	4.450566135	0.000183783	up	MRGPRX3	-3.115422461	0.003379417	down
SH2D6	4.432562296	3.45E-08	up	PCDHA6	-3.114227995	8.51E-05	down
PRB3	4.425418043	0.000125162	up	FSTL5	-3.043290066	0.005592306	down
RHOXF1P1	4.40234658	3.56E-08	up	TNN	-3.006828472	2.73E-05	down
GFI1B	4.360848036	7.85E-10	up	OPRK1	-2.991857204	5.49E-05	down
PNPLA1	4.334364769	6.63E-14	up	MYH6	-2.931315996	0.001164496	down
IGHEP1	4.312863692	1.77E-08	up	CXCL9	-2.901069401	0.000476041	down
RAB44	4.261048017	6.13E-18	up	PPDPFL	-2.888054653	5.15E-05	down
LOC101930276	4.246988606	0.001284544	up	SPADH	-2.884756803	0.000339759	down
TERB2	4.217825456	0.000114212	up	RNU6-403P	-2.865139757	0.024477624	down
OR7E24	4.202974422	5.37E-05	up	DBX1	-2.856388335	0.00570572	down
SLC5A7	4.19950068	2.90E-07	up	CXCL11	-2.819854301	0.000476464	down
XKR3	4.195892268	3.49E-05	up	IGFL1	-2.798314625	0.045187108	down

Gene	Log2FoldChange	P-value	Regulated	Gene	Log2FoldChange	P-value	Regulated
LINC01043	4.153458721	4.65E-05	up	TMEM163	-2.78300046	2.19E-11	down
UGT2B28	4.145492998	1.32E-06	up	LINC01285	-2.778618883	0.001677433	down
CPLX2	4.130352398	0.00011345	up	KLHDC7B	-2.757923192	1.01E-05	down
ANKRD63	4.129550383	1.17E-07	up	PAPPA2	-2.753798659	2.03E-09	down
CCR3	4.084448247	5.58E-15	up	GABRA2	-2.74136088	0.022245544	down
LINC02072	4.074490319	1.60E-14	up	MYBPH	-2.733314984	0.006568781	down
LINC02073	4.074490319	1.60E-14	up	MAB21L2	-2.724286834	0.021198546	down
GPR42	4.054484689	4.00E-05	up	GAL	-2.722982012	5.58E-06	down
FFAR3	4.053487546	5.07E-08	up	SBK2	-2.702101123	0.034817095	down
GATA1	4.03244205	6.60E-13	up	ACTC1	-2.693981309	0.013746807	down
SPATA8	4.018175843	5.38E-06	up	IFI44L	-2.688323475	4.49E-07	down
PADI4	4.002452072	3.75E-10	up	NPFFR2	-2.685458145	0.000301174	down
ITLN1	3.997580918	0.000192921	up	CXCL10	-2.672527321	0.000684289	down
CEBPE	3.971015432	1.94E-07	up	SLC26A3	-2.651570632	0.023523658	down
IL13	3.966471181	1.50E-05	up	SERTM2	-2.62240422	0.016015057	down
SIRLNT	3.950778166	5.90E-09	up	CD300E	-2.621073176	0.00010411	down
SIGLEC8	3.948952197	2.58E-16	up	CASP5	-2.597964199	0.000787851	down

Table E17. Top50 upregulated and downregulated DEGs in nasal polyp tissues of patients in Cluster 3 versus those in Cluster 2.

Gene	Log2FoldChange	P-value	Regulated	Gene	Log2FoldChange	P-value	Regulated
IGHV1-69-2	7.593147981	1.43E-06	up	FETUB	-6.532411159	0.025980104	down
SDAD1-AS1	4.404482606	0.001298552	up	IBSP	-6.436017148	0.013223486	down
CCL7	3.977923156	0.009106294	up	CST1	-5.846202661	9.21E-10	down
LOC105373347	3.946341554	0.046208751	up	DMP1	-5.671194241	0.025797714	down
TRAJ3	3.665909839	9.47E-05	up	MEPE	-4.482718469	0.034686858	down
IGFL1	3.52459509	0.019906193	up	OR2A4	-4.44108857	2.15E-05	down
RPS3AP29	3.311619437	0.00999052	up	SLC22A8	-4.369631631	9.64E-05	down
SBK2	3.270788609	0.008727669	up	LOC100996379	-4.040958812	0.004254383	down
LOC105377043	3.134964601	0.001717229	up	ACNATP	-3.853505976	0.000500446	down
TBC1D3B	3.114575928	0.015468595	up	IRS4	-3.426493728	0.00058598	down
TBC1D3G	3.114575928	0.015468595	up	DPYSL5	-3.393576549	0.000391909	down
ACOD1	3.028253612	0.025393675	up	ANKRD63	-3.284183513	0.000916737	down
LINC02802	2.953555662	0.000650151	up	SRP72P2	-3.279412649	0.035433443	down
LOC107985200	2.953555662	0.000650151	up	UGT2B11	-3.252440615	0.034945324	down
KRT8P49	2.948357885	0.018278362	up	HTR3E	-3.187125069	0.035885971	down
CIR1P1	2.861979463	0.022588236	up	STMN2	-3.104385051	6.10E-05	down
IGHV3-52	2.828084739	0.007324473	up	LINC02347	-2.954278641	0.023145431	down
CSAG3	2.813185814	0.030730049	up	LINC01115	-2.935984192	0.010293638	down
TREML3P	2.773988785	0.010239288	up	LENEP	-2.92558911	0.040358897	down
GCSIR	2.756806272	0.013402626	up	LOC102724560	-2.761269786	0.012545542	down
CD300E	2.702551538	8.01E-05	up	NPIPP1	-2.737797134	0.021385968	down
LINC02178	2.677070505	0.013537002	up	C17orf98	-2.712945999	0.023900401	down
PGA3	2.607555154	0.014572988	up	LMOD2	-2.67745947	0.030344462	down
CD300LD	2.601941023	0.047989706	up	SIRLNT	-2.645862235	0.007980553	down
RPL36AP26	2.56890071	0.042555501	up	LOC124907878	-2.629346854	0.002141469	down
KCNA4	2.504417596	0.02324781	up	LOC105377267	-2.614113651	0.033600868	down
RFPL4A	2.473667917	0.012475091	up	HSD17B13	-2.609264615	0.000480436	down
RPL10P13	2.459825293	0.036458476	up	SPACA3	-2.569221314	0.013530275	down
SCEL	2.397823902	0.005070207	up	RNA5SP122	-2.561139178	0.043681319	down
LGALS17A	2.364902503	0.006043267	up	PTGDR2	-2.555659723	0.003360082	down
MAB21L2	2.364748462	0.016872565	up	UGT2B28	-2.552330699	0.003081847	down
LILRA5	2.336305142	7.90E-05	up	LOC646112	-2.540529893	0.009240187	down
FSTL5	2.262084224	0.009848299	up	HRH4	-2.460367113	0.000480093	down

Gene	Log2FoldChange	P-value	Regulated	Gene	Log2FoldChange	P-value	Regulated
LOC101928143	2.255509555	0.009636389	up	PRB3	-2.448009828	0.00381876	down
CXCL9	2.230770935	0.004915262	up	LDHC	-2.445434623	0.004887904	down
SMCR5	2.22434288	0.038250701	up	LINC00656	-2.420584351	0.037186443	down
SLC8A2	2.212848481	0.002368005	up	HSD3B2	-2.399460426	0.006175544	down
IL31RA	2.20493211	0.000613932	up	OLIG1	-2.388259679	0.020089376	down
PARM1-AS1	2.203639858	0.010791884	up	SLC30A8	-2.358682284	0.001371808	down
CASP5	2.184153431	0.001119499	up	VSTM1	-2.297265382	0.019672861	down
RNY3P16	2.126462019	0.023442742	up	GPR166P	-2.279245524	0.036785518	down
KRT13	2.0448439	0.008461928	up	OBP2A	-2.253591232	0.027802231	down
RHCG	2.027641859	0.000274492	up	ADGRD2	-2.234757678	0.017222513	down
GBP5	2.008101389	0.001840436	up	C1orf167	-2.230574109	0.0237802	down
IL4I1	2.002707311	0.000443368	up	MIR7152	-2.207779811	0.04763487	down
S100A12	1.988325718	0.001384276	up	SH2D7	-2.201540817	0.002901312	down
MYH7	1.979958854	0.008920282	up	PNPLA1	-2.166333621	0.00014736	down
LINC01093	1.963352206	0.009900638	up	TTR	-2.152895848	0.005044089	down
DUOXA2	1.961874158	0.00574576	up	EVPLL	-2.138141009	0.013209543	down
IDO1	1.939473464	0.011379868	up	LEFTY2	-2.135146959	0.02273326	down

Table E18. Machine learning-derived gene signatures and coefficients among distinct CRSwNP clusters

Gene	Log2FoldChange	P-value
ALOX15	130.573	Cluster 1
DERL1	12.101	Cluster 1
FBP1	46.512	Cluster 1
FEXO7	1.611	Cluster 1
PDIA4	28.829	Cluster 1
PLEKHA2	16.478	Cluster 1
CIZ1	13.925	Cluster 2
DEGS1	-32.907	Cluster 2
DPM2	98.279	Cluster 2
HBA2	0.002	Cluster 2
HLA-DRB1	-1.462	Cluster 2
KRT23	-15.128	Cluster 2
LPCAT2	-1.452	Cluster 2
SHARPIN	38.620	Cluster 2
SPON2	6.217	Cluster 2
SRXN1	-12.349	Cluster 2
TCF7	17.033	Cluster 2
UBE2D1	-4.105	Cluster 2
ESYT2	-23.166	Cluster 3
HBG2	0.481	Cluster 3
HLA-DRB1	1.962	Cluster 3
HLA-DRB5	1.489	Cluster 3
KCNJ15	43.698	Cluster 3
MAN2A2	34.824	Cluster 3
OSCAR	2.349	Cluster 3
PF4	22.154	Cluster 3
PPBP	4.752	Cluster 3
PTGDS	-13.042	Cluster 3
RNF187	-3.855	Cluster 3

Gene	Log2FoldChange	P-value
S100A12	0.151	Cluster 3
SHARPIN	-82.039	Cluster 3
SLC25A39	-0.578	Cluster 3
SLPI	0.870	Cluster 3
SRA1	27.012	Cluster 3
TMEM91	5.946	Cluster 3
YBX3	-3.186	Cluster 3

Table E19. Top50 upregulated and downregulated DEGs in whole peripheral blood of patients with CRSwNP in pred-cluster 1 versus those in pred-cluster 2 from independent validation cohort

Gene	Log2FoldChange	P-value	Regulated	Gene	Log2FoldChange	P-value	Regulated
CCL23	2.592103399	0.002261577	up	RIMBP2	-4.882524994	0.011693583	down
STAC	2.27288805	0.002904993	up	TREML4	-3.516990349	0.032731452	down
ARHGEF10	2.183814911	0.000698304	up	OR6K3	-2.189060523	0.001301032	down
SIK1	2.085323257	0.010007072	up	BTNL3	-2.130046243	0.040259389	down
SIGLEC8	2.029994338	2.48E-06	up	LCN2	-2.12856532	0.006326721	down
THBS4	2.012675118	8.62E-09	up	TMEM52B	-2.126927492	0.013785574	down
IDO1	1.938809937	1.16E-08	up	CAMP	-2.096190513	0.001835371	down
GPR82	1.90242836	3.98E-11	up	LMOD1	-2.064324667	0.0031584	down
TRPC6	1.900906024	2.83E-05	up	CD177	-2.04838893	0.000771783	down
OLIG2	1.886551432	5.92E-06	up	LTF	-2.004814722	0.01427235	down
RCVRN	1.833074926	0.000966329	up	ORM1	-1.99176288	0.000991183	down
CACNG6	1.790338806	0.000222865	up	POSTN	-1.973937755	0.005344421	down
CYP4F12	1.782905899	1.26E-09	up	TUBB2A	-1.903513919	0.011057538	down
FAT1	1.778846254	0.016213696	up	HBG1	-1.88109619	0.0016062	down
CDK15	1.698846346	0.00302141	up	ATP6V1C2	-1.750782768	0.02758618	down
ALOX15	1.664883088	1.95E-05	up	AQP10	-1.694542718	3.97E-05	down
FGFR2	1.661586194	0.001378642	up	ACHE	-1.686911923	0.02136845	down
SEMG1	1.659819621	1.13E-05	up	KRT1	-1.676921402	0.011755025	down
FGF2	1.649995411	0.026241371	up	SLC5A11	-1.667913888	0.027284234	down
PRSS33	1.621012662	0.001148389	up	SLC2A4	-1.638702416	0.040225747	down
TMTC1	1.548721058	0.012584301	up	RAB3IL1	-1.621945439	0.001078742	down
CNKSR3	1.530795357	0.000423866	up	SHISA7	-1.608550613	0.006856434	down
SLC29A1	1.530049806	7.96E-07	up	HBM	-1.596720239	0.000246358	down
IL5RA	1.529158995	4.45E-06	up	MYL9	-1.592849118	0.005494704	down
ABTB2	1.510100128	8.91E-07	up	ALAS2	-1.577541481	0.024218475	down
SMPD3	1.50843889	5.08E-06	up	HBD	-1.537303076	0.004590716	down
LINGO2	1.492463281	0.003917343	up	FAM3D	-1.489169372	0.006646779	down
ADORA3	1.48468946	2.26E-07	up	SELENBP1	-1.486888016	0.007183128	down
SLC16A14	1.482434938	4.34E-05	up	DUSP13	-1.462761654	0.011473049	down
IL34	1.454515598	0.000469754	up	AHSP	-1.444205469	0.00367501	down
MEIS2	1.454266835	0.00564492	up	VWCE	-1.441046285	0.005211262	down
FRRS1	1.453813765	1.11E-08	up	ZNF215	-1.433746836	0.040616479	down
C20orf204	1.451049173	0.004036989	up	ATOH8	-1.431958619	0.012912684	down
CLC	1.433834591	0.000790542	up	KLK1	-1.422463823	0.013084405	down
AREG	1.433577425	0.030007764	up	NKAPL	-1.400112914	0.003331208	down
ACOT11	1.430201576	4.07E-06	up	SEC14L5	-1.397991026	0.000100198	down
TEX29	1.416645468	0.009831041	up	PLPPR3	-1.354996137	0.041031278	down
FAM118A	1.405311654	9.36E-07	up	SMIM24	-1.335775443	0.008684142	down
PMP22	1.372019391	0.001272187	up	ADAMTSL2	-1.333626754	0.029766067	down
PCDHGC3	1.34435159	0.011609998	up	SLC4A1	-1.322954479	0.015695973	down

Gene	Log2FoldChange	P-value	Regulated	Gene	Log2FoldChange	P-value	Regulated
SORCS3	1.341418748	0.036005351	up	TRIM58	-1.31783714	0.019802201	down
HRK	1.333012319	0.001063929	up	SGIP1	-1.315295669	0.045968816	down
TMIGD3	1.320260714	0.000169393	up	MCMDC2	-1.309510948	0.032232044	down
SPATA9	1.299313255	0.003519222	up	SEC14L4	-1.306632172	0.015327488	down
P2RY14	1.295077806	5.45E-08	up	CA1	-1.273061787	0.046389165	down
SPNS3	1.294214267	3.29E-06	up	HBA2	-1.25220866	0.032974201	down
NPIPA7	1.290437217	0.004634102	up	EMID1	-1.249321098	0.007191176	down
ADAMDEC1	1.283388198	0.005781229	up	KLHDC8A	-1.248297587	0.011605506	down
CYSLTR2	1.270468618	1.42E-08	up	SMIM1	-1.247938243	9.60E-05	down
GTPBP6	1.269828308	0.045308334	up	KEL	-1.237384718	0.011103458	down

Table E20. Top50 upregulated and downregulated DEGs in whole peripheral blood of patients with CRSwNP in pred-cluster 1 versus those in pred-cluster 3 from independent validation cohort.

Gene	Log2FoldChange	P-value	Regulated	Gene	Log2FoldChange	P-value	Regulated
DIRAS2	3.663176473	8.85E-05	up	RFPL4A	-4.791572752	0.00022235	down
BPIFB4	3.226576253	0.010747678	up	RFPL4AL1	-3.736648841	0.00310048	down
CSDC2	2.758228989	0.040844702	up	OR7D2	-3.530332417	0.008936219	down
FOXI1	2.523781056	0.000702723	up	RIMBP2	-3.514154006	0.001000119	down
CCL23	2.512706473	2.40E-06	up	GJD4	-3.496007029	0.000206055	down
PKD1L3	2.479183728	0.010937644	up	C3orf70	-3.493991804	8.53E-05	down
FIGN	2.419955863	0.015687096	up	BCL2L10	-2.959142119	0.008900086	down
HTR1B	2.125021937	0.015208903	up	RNF17	-2.909071652	0.040456516	down
EPX	2.013770773	0.004938426	up	ROR2	-2.80578053	3.77E-06	down
PRSS33	1.995960377	1.35E-07	up	SLC7A10	-2.666443756	0.005603994	down
GPR176	1.995496461	0.001035146	up	SHISA3	-2.578348546	0.009987936	down
TFF3	1.965022444	8.92E-06	up	KCNJ10	-2.535338658	0.032202143	down
RPS6KA6	1.960634385	0.003464927	up	LVRN	-2.426906927	0.031425855	down
SIGLEC8	1.932483382	2.62E-07	up	BMPER	-2.328681826	0.021785652	down
CALN1	1.912981879	0.042753122	up	SCG2	-2.274668953	0.007472849	down
IFNE	1.86617983	0.012455528	up	CPA5	-2.26976281	0.000436492	down
INHBA	1.862217644	0.009555229	up	HFM1	-2.245435405	0.035402583	down
IL34	1.811502956	6.93E-07	up	SVEP1	-2.232370173	0.015093335	down
PCDH17	1.806851199	0.007005049	up	CD177	-2.203543537	0.000130027	down
CACNG6	1.790415743	3.55E-08	up	MAP7D2	-2.146618759	0.008012087	down
PMP22	1.786022232	1.86E-07	up	BVES	-2.109849149	0.046276045	down
DEFA1	1.767710558	0.027274409	up	TBC1D3E	-2.104995205	2.61E-05	down
SPTBN4	1.760797843	0.002008548	up	THSD4	-2.096632023	0.011921441	down
CYP21A2	1.746540512	0.008356076	up	TP53TG3D	-2.046665883	0.027404221	down
OLIG2	1.734851776	1.74E-08	up	FAM3D	-1.957728075	1.24E-05	down
FGFR2	1.720068456	7.93E-06	up	F8A2	-1.941081156	0.008902495	down
IL5RA	1.718739021	1.65E-10	up	LRRN2	-1.906428879	0.009620153	down
CLC	1.71716491	1.05E-09	up	C1orf167	-1.906380328	0.010811774	down
CTSG	1.701755835	0.020814876	up	PTGFR	-1.871664933	0.027489256	down
TRPC6	1.684994586	7.99E-06	up	SULT1A2	-1.829342628	1.29E-05	down
PGBD5	1.671246419	0.011002652	up	DUSP13	-1.744754094	0.000387982	down
UGT2B11	1.665827395	0.034975747	up	ORM2	-1.701360026	0.018564393	down
IDO1	1.649286476	3.15E-06	up	PGPEP1L	-1.679518372	0.049350763	down
SLC16A14	1.639481434	1.33E-06	up	GNG10	-1.677972426	0.033360836	down
PGA5	1.631823703	0.040266807	up	GPR42	-1.673150067	0.018528753	down
CEBPE	1.625334592	5.97E-11	up	PEG3	-1.671663793	0.031193695	down
THBS4	1.624023427	1.29E-07	up	BICDL2	-1.649570742	0.000102481	down

Gene	Log2FoldChange	P-value	Regulated	Gene	Log2FoldChange	P-value	Regulated
PCDHGA12	1.617175835	0.027412924	up	SLC13A3	-1.559256926	0.004125483	down
ALOX15	1.591597715	1.29E-08	up	ORM1	-1.548793871	0.001328196	down
SMPD3	1.571931348	7.42E-09	up	FGF13	-1.513075925	0.024444348	down
ACTG2	1.568437425	0.029129603	up	RGPD1	-1.482882909	0.009125065	down
GPR82	1.566625015	1.59E-11	up	NKAPL	-1.450932409	0.000805112	down
FERMT1	1.562982642	0.015710493	up	DAAM2	-1.431207528	0.032026305	down
BAMBI	1.558979341	0.001659805	up	NPIPB8	-1.368266675	0.008896064	down
PRSS41	1.554112717	1.60E-05	up	PAQR5	-1.356826017	0.014869062	down
SLC29A1	1.544942631	1.52E-11	up	MIXL1	-1.354966612	0.004927481	down
ADORA3	1.536740144	1.02E-08	up	AP3S2	-1.328760421	0.030791715	down
PROX1	1.506013497	0.011019224	up	TMEM178B	-1.323100441	0.022556386	down
CDK15	1.50374923	0.000346323	up	ARG1	-1.322482121	0.007670641	down
HRK	1.477571762	1.01E-05	up	OR6K3	-1.294009699	0.049007429	down

Table E21. Top50 upregulated and downregulated DEGs in whole peripheral blood of patients with CRSwNP in pred-cluster 3 versus those in pred-cluster 2 from independent validation cohort

Gene	Log2FoldChange	P-value	Regulated	Gene	Log2FoldChange	P-value	Regulated
TBC1D3G	2.46629324	0.034328499	up	DEFA1	-2.400332347	0.006583107	down
ALDH1A3	2.294161231	0.004855844	up	ALAS2	-2.224094638	3.74E-06	down
RCVRN	2.19755402	0.000220391	up	ITLN1	-2.20556456	1.53E-07	down
TDRD1	2.155719257	0.006049088	up	OCLN	-2.167681532	0.007369694	down
LCN8	2.080492465	0.039956255	up	OLFM4	-2.160422759	0.001594226	down
PNMA6A	2.051174721	0.003864675	up	TUBB2A	-2.134869666	0.000717234	down
CLEC2A	2.031097177	0.014494129	up	LCN2	-2.075897967	0.000551864	down
DAAM2	2.005389259	0.002633668	up	ACHE	-2.067644359	0.000270822	down
TBC1D3E	1.588470423	0.001399662	up	KLC3	-1.972863382	9.46E-06	down
IFI44L	1.565738394	0.004908949	up	KRT1	-1.953260759	0.000138089	down
NPIPB8	1.559760831	0.006333674	up	PCOLCE2	-1.896622287	0.041151639	down
CLDN10	1.501631639	0.026212826	up	LTF	-1.865107758	0.002921062	down
AK8	1.452770237	0.005778191	up	HBZ	-1.848383665	0.002202014	down
TUSC3	1.435334893	0.049389509	up	CA1	-1.789112651	0.000598147	down
RSAD2	1.423933771	0.012908731	up	MMP8	-1.784952676	0.005575307	down
TEX29	1.380395138	0.005772192	up	ESPN	-1.774754408	9.70E-05	down
HTR6	1.344291381	0.035208216	up	HBA2	-1.773361954	9.28E-05	down
CRYGN	1.33994854	0.01336362	up	SELENBP1	-1.760639874	0.000142999	down
P4HA2	1.330623529	0.017561818	up	RAB3IL1	-1.754686505	8.70E-05	down
IFI44	1.330544707	0.004714621	up	OR2L13	-1.731689023	0.007148537	down
INHBB	1.313681702	0.002471393	up	HBG1	-1.727311461	0.001265861	down
AP3S2	1.286574103	0.031540759	up	OLR1	-1.713821062	0.008438399	down
PLSCR2	1.226306895	0.033971486	up	COL17A1	-1.705703542	0.021698953	down
STAC	1.218192361	0.044447437	up	C17orf99	-1.686843852	0.000856998	down
OSBPL6	1.189726621	0.008894186	up	CEACAM8	-1.667651226	0.014422443	down
KIRREL3	1.185364993	0.032134386	up	CTSE	-1.666721252	0.003061304	down
FAM118A	1.161739959	0.000735256	up	AHSP	-1.654925824	7.56E-05	down
LAMP3	1.141880082	0.007669705	up	CEACAM6	-1.642258054	0.015077636	down
TSKS	1.135877882	0.004952666	up	SLC4A1	-1.637255166	0.000188514	down
LIF	1.134246427	0.030839071	up	SHISA7	-1.62429467	0.010452731	down
PPP4R4	1.125081378	0.024285925	up	HBA1	-1.618288209	0.000490635	down
A3GALT2	1.123568761	0.042822504	up	HBQ1	-1.610424534	8.00E-06	down
ARMH2	1.117275905	1.08E-05	up	TRIM58	-1.605995362	0.000262676	down
ETV7	1.109503265	0.032747059	up	RHD	-1.60097804	1.77E-06	down
MYO10	1.103672538	0.001843492	up	CAMP	-1.593840502	0.00081944	down
CFB	1.089540115	0.022651669	up	BCAM	-1.593113298	0.006848869	down

Gene	Log2FoldChange	P-value	Regulated	Gene	Log2FoldChange	P-value	Regulated
CREG2	1.083087216	0.025041107	up	SPTB	-1.592628142	0.000162657	down
ANKRD22	1.065315723	0.000660351	up	THEM5	-1.576796764	0.004730868	down
OAS3	1.047000405	0.024154074	up	KEL	-1.567446329	0.00041184	down
AK4	1.041818402	0.000938501	up	SLC35D3	-1.539138201	0.020694266	down
BICDL2	1.039018181	0.019577734	up	BPI	-1.532641832	0.001860994	down
EYS	1.037031887	0.015409804	up	OR2W3	-1.520992462	0.001875196	down
RUFY4	1.036851635	0.004023665	up	SLC38A5	-1.514211076	1.65E-06	down
IFIT1	1.027050937	0.028881412	up	SEC14L4	-1.510128872	0.007630884	down
ANKRD34B	1.022846194	0.000242249	up	EPB42	-1.504977933	0.00040947	down
FFAR3	1.017925492	0.030299042	up	KLHDC8A	-1.504844281	0.001886357	down
SERPING1	1.015277892	0.038936884	up	YBX3	-1.501783581	4.10E-05	down
SPACA6	1.014886372	0.000569382	up	PAGE2B	-1.494383616	9.72E-05	down
SEMG1	0.998097566	0.017445237	up	SNCA	-1.484552009	0.000298844	down
RIPK4	0.986844327	0.01274488	up	GMPR	-1.462838839	5.18E-05	down

Table E22. Analyze software lists and versions.

Analysis	Software	Version
Quality control and quantitative	fastp	0.20.1
	fastqc	v0.11.9
	hisat2	2.1.0
	samtools	1.9
Differentiation analysis	DESeq2	1.40.2
	Differentiation analysis	1.0.12
	ggplot2	3.4.4
	VennDiagram	1.7.3
Enrichment analysis	clusterProfiler	3.4.4
Correlation analysis	corrplot	0.92
Machine learning	glmnet	4.1-8
	caret	6.0-94
	pROC	1.18.5
	multiROC	1.1.1
	randomforrest	4.7-1.1
	Hmisc	5.1-1
	genefilter	1.82.1
Dataset analysis	GEOquery	2.68.0